

Technical Report

Title: *Geochemical and SEM/EDS Analysis of DGR-1 and DGR-2 Core*

Document ID: TR-08-02


Authors: Activation Laboratories Ltd.,
Ancaster, Ontario

Revision: 0

Date: April 16, 2009

DGR Site Characterization Document
Intera Engineering Project 06-219



Intera Engineering DGR Site Characterization Document		
Title:	Geochemical and SEM/EDS Analysis of DGR-1 and DGR-2 Core	
Document ID:	TR-08-02	
Revision Number:	0	Date: April 16, 2009
Author(s):	Aniceta Skowron and Eric Hoffman, Actlabs, Ancaster, Ontario. Edited by Richard Jackson	
Technical Review:	Kenneth Raven; Monique Hobbs, Branko Semec (NWMO)	
QA Review:	John Avis	
Approved by:	 Kenneth Raven	

Document Revision History		
Revision	Effective Date	Description of Changes
0	April 16, 2009	Initial Issue

TABLE OF CONTENTS

1	INTRODUCTION	1
2	BACKGROUND.....	1
3	METHODS.....	3
	3.1 Geochemistry	3
	3.2 SEM/EDS	3
4	RESULTS.....	3
	4.1 Geochemistry	3
	4.2 SEM/EDS	3
5	DATA QUALITY AND USE	8
6	CONCLUSIONS	9
7	REFERENCES	9

LIST OF TABLES

Table 1	Depths, Formations, Descriptions & Analyses of DGR-1 Core Samples.....	1
Table 2	Depths, Formations, Descriptions & Analyses of DGR-2 Core Samples.....	2
Table 3	DGR-1 Elemental Geochemistry	4
Table 4	DGR-2 Elemental Geochemistry	6
Table 5	Summary of SEM/EDS Observations of DGR-1 and DGR-2 Samples.....	8

LIST OF APPENDICES

- APPENDIX A: ActLabs Report on SEM/EDS and XRD Analyses of DGR-1 Core
APPENDIX B: ActLabs Report on SEM/EDS Analyses of DGR-2 Core

1 Introduction

Intera Engineering Ltd. has been contracted by Ontario Power Generation (OPG) to implement the Geoscientific Site Characterization Plan (GSCP) for the Bruce site located at Tiverton, Ontario. The purpose of this site characterization work is to assess the suitability of the Bruce site to construct a Deep Geologic Repository (DGR) to store low-level and intermediate-level radioactive waste. The GSCP is described by Intera Engineering Ltd., (2006).

As part of the GSCP, Intera Engineering Ltd. retained Activation Laboratories (ActLabs) of Ancaster, Ontario to undertake geochemical testing of cores collected from boreholes DGR-1 and DGR-2. This report summarizes the results of the geochemical, scanning electron microscopy (SEM) and energy dispersive spectral (EDS) analysis of DGR-1 and DGR-2 core samples to quantify the major minerals present in the cores and to identify the pore fabric and composition.

Work described in this Technical Report was undertaken in accordance with Test Plan TP-07-01 – Laboratory Testing of DGR-1 and DGR-2 Solid Core for Geochemistry & Mineralogy (Intera Engineering Ltd., 2007b), which was prepared following the general requirements of the DGR Project Quality Plan (Intera Engineering Ltd., 2007a).

2 Background

Core samples of 76 mm diameter were collected during diamond coring of boreholes DGR-1 and DGR-2 at the Bruce site from January until August, 2007. All core samples were vacuum sealed within nitrogen flushed polyethylene and aluminium foil/polyethylene bags following core retrieval and the general preservation and handling requirements of TP-06-10 (Intera Engineering Ltd., 2007c). Thirty-three preserved core samples from boreholes DGR-1 (Table 1) and DGR-2 (Table 2) were shipped to ActLabs (following procedure DGR P4).

Table 1 **Depths, Formations, Descriptions & Analyses of DGR-1 Core Samples**

<i>Intera Sample ID</i>	<i>Formation</i>	<i>Core Sample Description</i>	<i>Analyses</i>
DGR1-049.16	Amherstburg	Light brown-grey, fine-grained dolostone	Geoch
DGR1-097.08	Bois Blanc	Grey-brown cherty dolostone	Geoch
DGR1-130.03	Bass Islands	Grey, very fine-grained dolostone	Geoch
DGR1-156.63	Bass Islands	Grey-brown fine-grained dolostone	Geoch
DGR1-231.49	Salina E Unit	Grey-tan brecciated dolostone with shale matrix	Geoch
DGR1-267.78	Salina B Unit	Dark green-grey dolomitic shale & gypsum veins	Geoch
DGR1-322.19	Salina A2 Unit	Massive light grey-blue anhydrite	Geoch
DGR1-361.76	Salina A1 Unit	Grey laminated argillaceous dolostone	Geoch
DGR1-399.85	Gasport	Grey dolomitic limestone	Geoch
DGR1-419.99	Cabot Head	Red-maroon massive shale	Geoch
DGR1-446.25	Manitoulin	Interlaminated green-grey shale and dolostone	Geoch
DGR1-455.45	Queenston	Red-maroon massive shale	Geoch
DGR1-456.01	Queenston	Red-maroon massive shale with orange vein	Geoch/SEM/EDS/ XRD
DGR1-460.77	Queenston	Grey-green and red-maroon shale	Geoch

Table 1 lists the Intera sample identifier with depth (m), geologic formation, sample description based on core inspection in the field, and the analyses performed on the 14 DGR-1 samples selected for geochemical/SEM/EDS testing. The bulk rock and fracture infilling (vein) of sample DGR1-456.01 were analysed separately by SEM/EDS and also for XRD. Table 2 lists similar information for the 19 DGR-2 samples. One sample – DGR2-687.42 – was sent for petrographic analysis but was not analysed by XRD or for litho-geochemistry and SEM/EDS analyses.

Table 2 Depths, Formations, Descriptions & Analyses of DGR-2 Core Samples

<i>Intera Sample ID</i>	<i>Formation</i>	<i>Core Sample Description</i>	<i>Analyses</i>
DGR2-451.33	Queenston	Grey-green and red-maroon massive shale	Geoch
DGR2-482.45	Queenston	Interbedded green shale and grey limestone	Geoch/SEM/EDS
DGR2-508.93	Queenston	Red-maroon and grey-green shale	Geoch
DGR2-535.56	Georgian Bay	Grey-green shale with minor limestone	Geoch/SEM/EDS
DGR2-550.28	Georgian Bay	Interbedded grey-green shale and limestone	Geoch
DGR2-570.73	Georgian Bay	Interbedded grey-green shale with minor limestone	Geoch/SEM/EDS
DGR2-590.10	Georgian Bay	Dark grey-green shale	Geoch
DGR2-606.62	Georgian Bay	Dark grey-green argillaceous limestone with halite fracture infilling	Geoch/SEM/EDS
DGR2-606.96	Georgian Bay	Dark grey-green shale, some limestone	Geoch/SEM/EDS
DGR2-626.29	Blue Mountain	Dark grey massive shale	Geoch
DGR2-644.49	Blue Mountain	Dark grey-black massive shale	Geoch/SEM/EDS
DGR2-659.31	Collingwood Member, Cobourg	Interbedded grey shale and argillaceous limestone	Geoch/SEM/EDS
DGR2-669.27	Cobourg	Grey argillaceous limestone	Geoch
DGR2-677.93	Cobourg	Mottled grey argillaceous limestone	Geoch
DGR2-695.51	Sherman Fall	Grey argillaceous limestone	Geoch
DGR2-704.87	Sherman Fall	Grey fossiliferous argillaceous limestone	Geoch/SEM/EDS
DGR2-745.97	Kirkfield	Grey argillaceous limestone	Geoch
DGR2-816.85	Gull River	Grey fine-grained dolomitic limestone	Geoch
DGR2-844.95	Cambrian	Tan-grey dolostone with minor sandstone	Geoch

The core samples were inspected by Actlabs and Dr. Eva Schandl on receipt at Actlabs. If the cores were laminated with shale intervals in the case of carbonate rocks or were principally shale, then the shale was retained by Actlabs and analysed for clay-mineral identification (Intera Engineering Ltd, 2009a). Thin sections were prepared from the bulk rock and results recorded by photomicrographs (i.e., TR-07-12, Intera Engineering Ltd., 2009b). In addition, Actlabs analyzed the whole rock by XRD to determine mineral concentrations (Intera Engineering Ltd., 2008a).

This report presents the geochemical analysis of the 33 cores in terms of 10 oxides, other parameters and 45 elements, as well as providing the SEM/EDS results for nine selected core samples from the Queenston Formation shale down to the Sherman Fall Formation argillaceous limestone.

3 Methods

3.1 Geochemistry

The DGR-1 and DGR-2 cores were subject to a 'lithochemical' analysis that included measurement of 10 oxides and 45 trace elements. Method detection limits (MDL) and sample preparation are included in TP-07-01 (Intera Engineering Ltd., 2007b). The core samples were prepared by fusion and then analysed by ICP. The oxides are analysed by ICP-optical emission spectrometry (ICP-OES), while the trace elements are analysed by ICP-mass spectrometry (ICP-MS). The precision of ICP measurements varies with the MDL: at the MDL, it is $\pm 100\%$; at 10x MDL, it is $\pm 15\text{-}20\%$; and at 100x MDL, it is $\pm 5\%$.

Infrared analysis was used to characterise organic carbon and sulphur directly using an Eltra C,S analyzer with a resistance furnace heated to 400°C, Instrumental neutron activation analysis (INAA) is used for total chloride and coulometry for carbon dioxide.

Because ^4He , ^{40}Ar and other radionuclides and the in-situ neutron fluxes for ^{129}I and ^{36}Cl in-growth are being measured (see GSCP, p.38), a number of geogenic elements have also been measured to determine the background radioactivity, e.g., Li, U, Th, Ra, Rb, K and Gd. With the exception of Li, these were analysed using a lithium borate flux in a fusion process that is followed by measurement using inductively coupled plasma spectrometry (ICP). Li was analysed by a total acid digestion process followed by ICP analysis.

3.2 SEM/EDS

Selected core samples were freshly cleaved, coated with thin film of gold and mounted for the examination. Phillips 515 scanning electron microscope equipped with energy dispersive spectrometer was used.

4 Results

4.1 Geochemistry

Tables 3 and 4 present the elemental analyses of DGR-1 and DGR-2 cores, respectively. Tables 3 and 4 list the oxide and other parameters (Cl, C-total, C-organic, loss on ignition, CO_2 , S-total and SO_4) analyses in percent (%) and the elemental analyses in parts per million (ppm).

4.2 SEM/EDS

Table 5 presents the results of the SEM/EDS analysis of the one DGR-1 core sample and the eight DGR-2 core samples. Appendix A is the complete Actlabs SEM/EDS and XRD analysis report for the DGR-1 core sample. Appendix B contains the complete Actlabs report for the SEM/EDS analyses of DGR-2 core samples.

NaCl appeared as cube-like crystallites with the majority of the EDS spectra showing high Cl and appreciable Na content. The ratio of Cl to Na peak intensities in the EDS spectra was similar to that observed for the NaCl vein present in DGR1-456.01 sample. Thin layers covering large areas of the surfaces of cleaved samples, for example see Appendix B Figure 20, were rich in Cl and had a glassy, somewhat crusty appearance. Such layers, which seemed fairly abundant, were probably more brittle than the surrounding matrix as their glassy appearance would suggest. The concentration of Na appeared to be lower in the layers than it was for the cube-like crystallites, but this might be an artefact of the experimental procedure.

Table 3 - DGR-1 Elemental Geochemistry

Sample Number	DGR1-049.06	DGR1-097.08	DGR1-130.03	DGR1-156.63	DGR1-231.49	DGR1-267.78	DGR1-322.19	DGR1-361.76
Oxides (%)								
Al ₂ O ₃	0.35	0.83	1.16	0.08	3.66	9.2	0.08	1.45
CaO	43.49	27.99	27.73	29.97	27.26	13.38	40.86	49.64
Fe ₂ O ₃	0.22	0.4	0.33	0.07	1.65	3.75	0.03	0.57
K ₂ O	0.05	0.33	0.66	0.05	0.98	2.37	< 0.01	0.47
MgO	9.48	4	20.02	21.98	16.12	9.21	0.36	2.61
MnO ₂	0.006	0.008	0.008	0.006	0.025	0.044	< 0.001	0.01
Na ₂ O	0.01	0.04	0.13	0.1	0.31	0.95	0.08	0.17
P ₂ O ₅	0.01	0.01	0.02	< 0.01	< 0.01	0.08	< 0.01	0.02
SiO ₂	1.46	39.2	5.52	0.33	14.58	36.51	1.49	4.31
TiO ₂	0.008	0.038	0.042	< 0.001	0.18	0.45	< 0.001	0.048
Other Parameters (%)								
Cl (INAA)	0.05	0.04	0.04	0.05	0.13	0.63	0.04	0.12
C-total	12.6	7.58	12.1	13	8.38	3.99	1.43	11.6
C-organic	< 0.05	0.14	< 0.05	< 0.05	< 0.05	< 0.05	< 0.05	< 0.05
Loss on Ignition	44.66	26.14	43.34	46.85	33.2	23.02	4.59	40.46
CO ₂	44.6	26.2	43	46.8	28.9	13.2	4.08	39.9
S-total	0.09	0.13	0.06	< 0.01	3.69	2.66	23.2	0.54
SO ₄ -total	0.4	0.6	0.3	< 0.3	10.3	6.8	69.8	2.7
Fusion-ICP (ppm)								
Ag	< 0.5	< 0.5	< 0.5	< 0.5	< 0.5	< 0.5	< 0.5	< 0.5
As	< 5	< 5	15	< 5	9	9	< 5	< 5
Ba	9	23	25	< 3	108	666	19	31
Be	< 1	< 1	< 1	< 1	< 1	2	< 1	< 1
Bi	0.5	< 0.1	0.1	< 0.1	0.9	0.4	0.7	0.1
Ce	2.74	11	9.08	1.55	22.3	51	0.37	6.53
Co	< 1	< 1	< 1	< 1	3	9	< 1	< 1
Cr	< 20	< 20	< 20	< 20	< 20	50	< 20	< 20
Cs	0.2	0.4	10	< 10	1.3	2.7	< 0.1	0.6
Cu	10	20	10	< 10	120	30	20	20
Dy	0.26	1.02	0.61	0.12	1.36	3.05	0.03	0.44
Er	0.16	0.55	0.34	0.07	0.76	1.74	0.02	0.24
Eu	0.06	0.254	0.163	0.028	0.364	0.846	0.006	0.119
Ga	< 1	1	1	< 1	5	13	< 1	2
Gd	0.22	1.11	0.63	0.11	1.47	3.22	0.03	0.47
Ge	< 0.5	< 0.5	< 0.5	< 0.5	< 0.5	1	< 0.5	< 0.5
Hf	< 0.1	0.5	0.4	< 0.1	1.1	2.7	< 0.1	0.3
Ho	0.05	0.2	0.12	0.02	0.26	0.59	< 0.01	0.08
In	< 0.1	< 0.1	< 0.1	< 0.1	< 0.1	< 0.1	< 0.1	< 0.1
La	2.26	10.9	4.32	0.79	11	25.8	0.2	3.38
Li	5	16	42	6	67	94	2	20
Lu	0.017	0.067	0.044	0.007	0.106	0.246	0.003	0.036
Mo	< 2	< 2	< 2	< 2	3	< 2	< 2	< 2
Nb	< 0.2	1	0.9	< 0.2	4	8.8	< 0.2	1
Nd	1.33	7.5	3.9	0.64	9.5	21.6	0.16	2.96
Ni	< 20	< 20	< 20	< 20	20	40	< 20	< 20
Pb	< 5	< 5	6	< 5	20	13	< 5	< 5
Pr	0.34	1.95	1.03	0.17	2.54	5.88	0.04	0.77
Rb	3	9	11	< 1	33	92	< 1	16
Sb	< 0.2	< 0.2	< 0.2	< 0.2	< 0.2	1.2	0.8	< 0.2
Sc	< 1	1	2	< 1	3	8	< 1	1
Sm	0.24	1.25	0.73	0.1	1.75	3.82	0.03	0.55
Sn	< 1	< 1	< 1	< 1	< 1	2	< 1	< 1
Ta	0.02	0.07	0.07	< 0.01	0.28	0.66	0.01	0.08
Tb	0.04	0.02	0.11	0.02	0.24	0.54	< 0.01	0.08
Th	0.3	0.09	1.11	0.08	2.81	6.54	0.07	0.96
Tl	0.07	0.06	0.06	< 0.05	0.15	0.24	< 0.05	0.08
Tm	0.022	0.077	0.049	0.01	0.11	0.259	< 0.005	0.036
U	3.03	4.41	2.49	1.43	2.15	1.77	0.48	1.58
V	11	10	14	< 5	27	63	< 5	14
W	0.9	< 0.5	< 0.5	< 0.5	< 0.5	2.8	< 0.5	< 0.5
Y	3.1	7.7	3.4	0.8	8.3	17.6	< 0.5	2.5
Yb	0.13	0.47	0.31	0.06	0.71	1.64	0.02	0.23
Zn	< 30	< 30	< 30	< 30	< 30	40	< 30	< 30
Zr	5	19	20	< 4	44	103	< 4	10

Table 3 cont. - DGR-1 Elemental Geochemistry

Sample Number	DGR1-399.85	DGR1-419.99	DGR1-446.25	DGR1-455.45	DGR1-456.01	DGR1-460.77
Oxides (%)						
Al ₂ O ₃	0.35	9.61	15.42	11.72	11.36	9.89
CaO	50.29	14.1	4	16.98	17.02	22.95
Fe ₂ O ₃	0.58	3.91	8.21	5.48	5.24	3.64
K ₂ O	0.21	3.21	5.05	3.69	3.57	3.09
MgO	2.77	9.13	4.28	3.74	3.89	3.64
MnO ₂	0.038	0.099	0.081	0.075	0.076	0.08
Na ₂ O	0.29	0.4	0.54	0.41	1.08	0.36
P ₂ O ₅	0.03	0.14	0.31	0.16	0.19	0.13
SiO ₂	2.07	33.58	49.31	36.44	35.68	31.42
TiO ₂	0.006	0.486	0.78	0.554	0.541	0.467
Other Parameters (%)						
Cl (INAA)	0.1	0.61	0.81	0.63	1.38	0.51
C-total	11.8	5.7	1.57	4.27	4.34	5.59
C-organic	0.22	< 0.05	< 0.05	< 0.05	0.1	< 0.05
Loss on Ignition	42.04	23.96	11.07	19.22	20.6	22.98
CO ₂	42.5	19.9	4.87	14.7	14.9	19.7
S-total	0.04	0.44	0.03	0.02	0.04	0.05
SO ₄ -total	< 0.3	0.5	< 0.3	< 0.3	< 0.3	< 0.3
Fusion-ICP (ppm)						
Ag	< 0.5	< 0.5	< 0.5	< 0.5	< 0.5	< 0.5
As	< 5	11	6	6	5	< 5
Ba	17	232	409	261	257	221
Be	< 1	< 1	2	2	2	2
Bi	< 0.1	1.5	0.6	0.6	0.5	0.3
Ce	6.75	52.5	83.7	64	61	54.7
Co	< 1	24	12	11	10	9
Cr	< 20	40	60	60	60	50
Cs	0.4	4.3	7.8	5.4	5.3	4.6
Cu	20	40	10	10	10	10
Dy	0.7	3.6	7.07	3.95	3.75	3.56
Er	0.41	2.1	3.69	2.32	2.18	1.96
Eu	0.158	0.923	1.95	1.04	1.03	0.953
Ga	< 1	15	24	20	19	17
Gd	0.73	3.6	8.17	4.07	3.9	3.73
Ge	< 0.5	1	2	1.6	1.6	1.3
Hf	0.4	3	4.6	2.9	2.8	2.3
Ho	0.14	0.71	1.29	0.77	0.74	0.67
In	< 0.1	< 0.1	< 0.1	< 0.1	< 0.1	< 0.1
La	5.32	26.3	40.7	33	31.1	27.9
Li	7	60	76	58	57	52
Lu	0.049	0.311	0.514	0.337	0.322	0.277
Mo	< 2	< 2	< 2	< 2	< 2	< 2
Nb	0.8	8.6	13.9	10	9.7	8.5
Nd	3.66	22.4	39.8	28.9	27.2	24.9
Ni	< 20	40	40	40	30	30
Pb	< 5	13	8	6	6	< 5
Pr	0.94	6.02	10.2	7.56	7.23	6.54
Rb	7	99	175	130	128	110
Sb	< 0.2	0.2	0.2	3.1	1.2	3.5
Sc	2	10	16	12	12	10
Sm	0.68	4.26	8.83	5.14	4.91	4.62
Sn	< 1	2	3	5	2	2
Ta	0.05	0.69	1.11	0.84	0.76	0.66
Tb	0.12	0.62	1.33	0.7	0.67	0.62
Th	0.76	7.69	13.2	9.11	8.58	7.31
Tl	< 0.05	0.32	0.46	0.42	0.28	0.33
Tm	0.058	0.32	0.532	0.351	0.328	0.291
U	0.87	2.36	2.32	2.23	2.21	1.81
V	< 5	78	116	97	95	82
W	< 0.5	< 0.5	0.7	1.2	1	0.9
Y	6.6	19.8	37.6	22.3	22.3	20.8
Yb	0.35	2.08	3.41	2.27	2.14	1.86
Zn	< 30	50	80	60	60	50
Zr	< 4	104	168	96	96	80

Table 4 - DGR-2 Elemental Geochemistry

Sample Number	DGR2-451.33	DGR2-482.45	DGR2-508.93	DGR2-535.56	DGR2-550.28	DGR2-570.73	DGR2-590.1	DGR2-606.62	DGR2-606.96
Oxides (%)									
Al ₂ O ₃	9.47	13.26	11.48	16.31	15.19	15.61	15.38	15.62	16.28
CaO	22.83	11.77	14.75	2.97	4.29	3.48	3.35	2.84	2.76
Fe ₂ O ₃	3.67	5.04	5.18	7.09	6.59	7.01	6.77	6.62	6.96
K ₂ O	3.04	4.27	3.5	5.13	4.9	4.92	4.57	4.67	4.94
MgO	4.37	5.16	5.1	4.09	3.6	3.74	3.41	3.34	3.16
MnO ₂	0.081	0.08	0.105	0.087	0.101	0.1	0.089	0.074	0.075
Na ₂ O	0.38	0.39	0.49	0.57	0.44	0.44	0.77	0.56	0.54
P ₂ O ₅	0.12	0.18	0.16	0.31	0.24	0.29	0.28	0.23	0.28
SiO ₂	29.96	42.09	39.74	51.25	53.54	51.53	53.94	55.47	55.57
TiO ₂	0.444	0.645	0.605	0.826	0.868	0.846	0.88	0.874	0.896
Other Parameters (%)									
Cl (INAA)	0.45	0.58	0.57	0.62	0.56	0.6	0.61	0.57	0.57
C-total	5.79	3.53	4.2	0.98	1.29	1.19	1.27	6.47	1.18
C-organic	0.08	0.16	<0.05	0.06	<0.05	0.37	<0.05	0.33	<0.05
Loss on Ignition	24.43	17.53	19.5	9.97	10.31	10.27	10.23	10.23	9.47
CO ₂	20.7	11.6	14	2.7	3.63	3.1	2.85	23.8	2.37
S-total	0.05	0.11	0.05	0.11	0.18	0.43	0.86	0.61	1.06
SO ₄ -total	< 0.3	0.4	<0.3	<0.3	0.4	0.4	0.6	1.8	0.8
Fusion-ICP (ppm)									
As	< 5	< 5	6	19	25	18	19	11	13
Ba	220	300	242	353	345	353	375	352	368
Be	< 1	2	2	3	3	3	3	3	3
Bi	0.2	0.9	2	4.3	6.9	8.3	6.1	5.7	5.8
Ce	51.5	63.6	60.8	81.9	79.5	80.8	82.3	93.8	86.4
Co	7	26	12	23	23	25	21	16	23
Cr	40	60	70	90	90	90	90	70	100
Cs	4.3	5.6	4.7	8.2	7.1	7.7	7.4	2.9	6.1
Cu	50	90	40	50	50	30	50	40	80
Dy	3.27	3.75	4.06	5.13	5.2	5.35	5.43	8.1	6.52
Er	1.79	2.26	2.31	2.99	3.09	3.02	3.12	3.8	3.34
Eu	0.881	1.04	1.08	1.34	1.39	1.48	1.42	2.44	1.9
Ga	13	18	17	25	23	24	23	10	20
Gd	3.65	4.28	4.52	5.79	5.98	6	5.82	9.41	7.5
Ge	1	1.2	1.5	2.1	2	2.1	2	1.8	2.1
Hf	2.3	2.6	3.8	3.7	4.1	3.9	4.6	3.1	3.8
Ho	0.61	0.75	0.78	0.98	1.02	1.01	1.03	1.41	1.18
In	< 0.1	< 0.1	< 0.1	< 0.1	< 0.1	< 0.1	< 0.1	< 0.1	< 0.1
La	25.7	32.1	29.9	40.7	40.3	40.9	41.3	39.3	39.1
Li	37	62	50	67	61	69	64	33	55
Lu	0.264	0.321	0.334	0.436	0.433	0.444	0.441	0.406	0.401
Mo	< 2	< 2	2	< 2	2	< 2	2	2	3
Nb	7.5	10.7	10.9	15	15.3	15.2	15.3	8.3	13
Nd	22.7	26.7	25.9	34.8	33.6	35.5	34.9	43.8	38.3
Ni	40	30	40	50	50	50	40	50	60
Pb	13	8	17	13	17	25	34	39	45
Pr	6.13	7.39	7.26	9.64	9.39	9.83	9.71	11.2	10.2
Rb	98	122	115	173	150	160	152	67	128
Sb	2.3	< 0.2	2	6.6	5	4.1	10.2	0.8	1.7
Sc	10	14	14	17	17	18	16	15	18
Sm	4.16	4.93	4.91	6.56	6.37	6.62	6.61	9.47	7.74
Sn	2	2	2	3	3	4	3	3	7
Ta	0.59	0.82	0.91	1.21	1.21	1.19	1.24	1.35	1.22
Tb	0.57	0.66	0.71	0.89	0.93	0.94	0.96	1.52	1.2
Th	7.12	8.53	8.73	12	11.5	11.8	11.9	6.36	10.1
Tl	0.3	0.49	0.36	0.59	0.55	0.62	0.49	0.18	0.36
Tm	0.276	0.331	0.339	0.456	0.453	0.45	0.475	0.514	0.472
U	1.67	2.36	2.48	3.19	3.29	3.26	3.64	2.03	3.1
V	70	106	102	139	130	135	129	137	141
W	0.7	3.7	2.7	2.6	2.7	2.6	2.5	1.1	1.7
Y	18.5	20.5	22	27.6	28.9	29.3	29.9	29.1	28.4
Yb	1.79	2.11	2.16	2.98	2.91	2.96	3.08	3	2.94
Zn	90	70	70	100	110	100	100	80	100
Zr	82	104	150	135	154	142	165	158	146



Table 4 cont.- DGR-2 Elemental Geochemistry

Sample Number	DGR2-626.29	DGR2-644.49	DGR2-659.31	DGR2-669.27	DGR2-677.93	DGR2-695.51	DGR2-704.87	DGR2-745.97	DGR2-816.85	DGR2-844.95
Oxides (%)										
Al ₂ O ₃	16.49	15.76	2.32	3.31	1.25	1.01	3.86	2.83	0.32	0.45
CaO	2.79	4.14	46.6	42.9	49.67	48.56	41.48	44.3	37.42	29.11
Fe ₂ O ₃	6.95	6.49	0.89	1.01	0.68	0.74	1.4	0.91	0.38	0.64
K ₂ O	4.8	4.62	0.92	1.42	0.55	0.39	1.64	1.19	0.15	0.39
MgO	3.15	2.87	2.08	2.19	2.04	3.34	1.91	1.54	12.92	19.39
MnO ₂	0.075	0.07	0.048	0.036	0.04	0.051	0.033	0.025	0.045	0.123
Na ₂ O	0.5	0.48	0.12	0.16	0.09	0.1	0.16	0.15	0.12	0.16
P ₂ O ₅	0.27	0.34	0.11	0.11	0.05	0.05	0.09	0.19	< 0.01	0.02
SiO ₂	54.83	53.13	8.37	11.98	5.03	4.17	14	11.81	2.46	7.04
TiO ₂	0.872	0.845	0.119	0.165	0.056	0.039	0.147	0.11	0.009	0.013
Other Parameters (%)										
Cl (INAA)	0.51	0.45	0.1	0.14	0.08	0.08	0.18	0.11	0.24	0.26
C-total	1.79	2.09	10.7	10.1	11.3	11.4	9.4	10	11.8	11.4
C-organic	0.9	0.78	< 0.05	0.11	0.07	0.6	0.11	< 0.05	< 0.05	0.08
Loss on Ignition	9.92	10.43	38.46	36.1	40.15	41.23	34.43	35.93	44.64	43.59
CO ₂	1.98	2.94	38.2	35.3	40.7	41.5	33.7	35.4	44.7	43.7
S-total	1.23	1.23	0.14	0.14	0.14	0.16	0.37	0.21	0.06	0.04
SO ₄ -total	0.9	1.4	0.4	0.5	0.4	0.4	1.2	0.7	< 0.3	< 0.3
Fusion-ICP (ppm)										
As	5	6	< 5	< 5	< 5	< 5	< 5	< 5	< 5	< 5
Ba	358	353	52	81	33	25	64	53	13	35
Be	3	3	< 1	< 1	< 1	< 1	< 1	< 1	< 1	< 1
Bi	0.2	< 0.1	< 0.1	< 0.1	< 0.1	< 0.1	< 0.1	< 0.1	< 0.1	< 0.1
Ce	84.4	87.6	17.9	18.6	12.5	8.2	18.4	17.1	2.33	24.4
Co	20	18	< 1	< 1	< 1	< 1	3	< 1	< 1	< 1
Cr	80	80	< 20	< 20	< 20	< 20	40	< 20	< 20	< 20
Cs	7.8	7.2	1.4	2	0.7	0.6	2.4	1.8	0.1	< 0.1
Cu	50	50	10	10	10	10	10	10	90	20
Dy	5.61	5.86	1.24	1.19	0.73	0.43	0.91	0.8	0.12	1.67
Er	3.24	3.38	0.73	0.74	0.37	0.25	0.47	0.47	0.06	0.93
Eu	1.58	1.57	0.34	0.329	0.224	0.125	0.29	0.255	0.052	0.379
Ga	25	24	3	4	2	1	5	3	< 1	< 1
Gd	6.48	6.38	1.39	1.43	0.8	0.53	1.04	0.93	0.12	1.48
Ge	1.6	1.2	< 0.5	< 0.5	< 0.5	< 0.5	< 0.5	< 0.5	< 0.5	< 0.5
Hf	3.8	3.9	0.7	0.9	0.3	0.4	0.9	1	0.3	0.3
Ho	1.09	1.11	0.24	0.24	0.13	0.08	0.16	0.15	0.02	0.33
In	< 0.1	< 0.1	< 0.1	< 0.1	< 0.1	< 0.1	< 0.1	< 0.1	< 0.1	< 0.1
La	41.6	44.7	10.9	11	6.29	3.88	9.16	8.45	1.23	10.2
Li	59	52	11	16	7	7	21	24	3	5
Lu	0.444	0.477	0.093	0.09	0.045	0.032	0.066	0.065	0.012	0.129
Mo	< 2	< 2	< 2	< 2	< 2	< 2	< 2	< 2	< 2	< 2
Nb	14.3	13.2	2.6	3.6	1.5	0.9	2.6	2.2	0.2	0.2
Nd	37.4	37.7	8.41	8.14	5.46	3.14	7.3	6.7	1	9.84
Ni	50	40	< 20	< 20	< 20	< 20	30	< 20	90	< 20
Pb	19	17	< 5	< 5	< 5	6	8	< 5	14	6
Pr	10.3	10.5	2.2	2.15	1.41	0.85	2.01	1.8	0.26	2.72
Rb	154	145	24	33	12	11	43	28	3	4
Sb	< 0.2	< 0.2	< 0.2	1.1	0.2	1.6	< 0.2	7	3.8	0.6
Sc	18	17	2	3	1	1	3	2	< 1	< 1
Sm	7.33	7.17	1.48	1.53	0.95	0.59	1.28	1.12	0.21	1.93
Sn	6	4	< 1	< 1	< 1	< 1	< 1	< 1	2	< 1
Ta	1.1	1.09	0.18	0.26	0.1	0.06	0.19	0.16	< 0.01	< 0.01
Tb	1.01	1.04	0.23	0.22	0.13	0.08	0.17	0.15	0.02	0.27
Th	11.7	11.5	2.13	3.12	1.24	1.32	3.17	2.8	0.78	1.2
Tl	0.77	0.72	0.08	0.09	< 0.05	< 0.05	0.08	0.06	< 0.05	< 0.05
Tm	0.479	0.489	0.106	0.11	0.051	0.036	0.073	0.072	0.009	0.129
U	3.66	3.84	1.54	1.51	0.84	0.34	0.61	0.61	0.6	1.17
V	141	139	19	26	10	7	18	14	< 5	11
W	1.9	1.9	< 0.5	< 0.5	< 0.5	< 0.5	< 0.5	< 0.5	< 0.5	< 0.5
Y	31.7	33.7	7.8	7.7	4.1	2.3	4.7	4.5	0.7	9.3
Yb	3.05	3.18	0.67	0.68	0.3	0.23	0.45	0.47	0.06	0.82
Zn	90	100	< 30	< 30	< 30	< 30	< 30	< 30	30	< 30
Zr	142	140	25	33	13	14	31	37	13	10

Table 5 Summary of SEM/EDS Observations of DGR-1 and DGR-2 Samples

<i>Intera Sample ID</i>	<i>Formation</i>	<i>SEM/EDS Observations</i>
DGR1-456.01 – Bulk rock	Queenston	Presence of small grains of well-faceted crystallites (likely halite) Predominate Si, Ca and O, small amounts of Na and Cl.
DGR1-456.01 – Vein	Queenston	Predominately Na and Cl (halite) with minor calcite and quartz
DGR2-482.45	Queenston	General matrix – low Cl concentration. Regions of high Cl concentration. Morphology of the high Cl regions: spots and glassy looking layers.
DGR2-535.56	Georgian Bay	General matrix – low Cl concentration. Regions of high Cl concentration. Morphology of the high Cl regions: spots and glassy looking layers.
DGR2-570.73	Georgian Bay	Islands and layers of glassy phases with high Cl content and relatively low Na content. Glassy layers are thin, and are probably more brittle than the surrounding matrix since they predominate on cleaved surfaces Framboidal FeS present. Matrix has flake-like morphology, K and Fe present in the matrix.
DGR2-606.62	Georgian Bay	Regions of high and low density of cube-like particles Cube-like particles have high Cl concentration and Na is also present – these are probably NaCl crystallites
DGR2-606.96	Georgian Bay	Region of high Ca, S and O consistent with Gypsum Framboidal FeS present Matrix with flake-like morphology
DGR2-644.49	Blue Mountain	Framboidal FeS present. Matrix with flake-like morphology, K and F present. Cube-like particles with high Cl concentration, Na also present – these are probably NaCl crystallites.
DGR2-659.31	Collingwood Member, Cobourg	Matrix with faceted morphology, K and F present. Regions of high Ca concentration.
DGR2-704.87	Sherman Fall	Matrix with flake-like morphology, K and F present. Cube-like particles with high Ca concentration. Islands with semi-glassy appearance and high Na and Cl concentration.

5 Data Quality and Use

Because this is preliminary information from the first cores from the DGR project, caution is warranted in interpreting the results with respect to the geochemical conditions represented. However, that notwithstanding, the data presented in this Technical Report are suitable for providing the framework for development of Phase 1 descriptive geosphere models of the Bruce DGR site.

It is possible that the abundance and importance of the glassy NaCl layers was overestimated in the SEM study due to the fact that the layers were indeed more brittle than the surrounding matrix and cleaving the samples for the examination was preferentially exposing them.

6 Conclusions

Thirty-three cores from the DGR-1 and DGR-2 boreholes were analysed for their elemental geochemistry, including organic carbon, total sulphate and loss on ignition, and for 45 trace elements. NaCl appeared as cube-like crystallites in the scanning electron micrographs, presumably halite, with the majority of the EDS spectra showing high Cl and appreciable Na content. A particular feature of the SEM/EDS analysis was the presence of another, possibly related mineral, with high Cl concentration and glassy appearance.

7 References

Intera Engineering Ltd., 2009a. Technical Report: XRD Mineralogical Analysis of DGR-1 and DGR-2 Core, TR-08-01, Revision 0, April 16, Ottawa.

Intera Engineering Ltd., 2009b. Technical Report: Petrography of DGR-1 and DGR-2 Core, TR-07-12, Revision 0, April 16, Ottawa.

Intera Engineering Ltd., 2007a. Project Quality Plan, DGR Site Characterization, Revision 3, January 17, Ottawa

Intera Engineering Ltd., 2007b. Test Plan for Laboratory Testing of DGR-1 and DGR-2 Solid Core for Geochemistry and Mineralogy, TP-07-01, Revision 1, March 25, Ottawa.

Intera Engineering Ltd., 2007c. Test Plan for DGR-1 & DGR-2 Core Sampling and Distribution. TP-06-10, Revision 4, May 14, Ottawa.

Intera Engineering Ltd., 2006. Geoscientific Site Characterization Plan, OPG's Deep Geologic Repository for Low and Intermediate Level Waste, Report INTERA 05-220-1, OPG 00216-REP-03902-00002-R00, April, Ottawa.

APPENDIX A

ActLabs Report on SEM/EDS and XRD Analyses of DGR-1 Core

Activation Laboratories Ltd.
1336 Sandhill Drive, Ancaster
Ontario, Canada L9G 4V5

Mineralogy of DGR1-456.01
X-Ray Diffraction and Scanning Electron Microscopy Study

W.O. # A07-1311
Invoice # A07-1311
No. of pages: 6

Client: Intera Engineering Ltd
11 Venus Crescent, Heidelberg
ON N0B 1Y0

Contact person: Dr. Richard Jackson

Tel: 519-699-4657
Email: rjackson@intera.com

Date Received: April 11, 2007

Date Reported: July 6, 2007

INTRODUCTION

A series of 14 core samples were submitted for mineralogical evaluation. The main objective was to determine and quantify the minerals present in the samples, with special emphasis on determination and quantification of clay minerals, and to evaluate the morphology/texture of the samples to determine intrinsic porosity and possible presence and morphology of halite.

This report outlines the study of one of the samples from the series – identified as DGR-1 456.01, ActLabs ID A07-1311-2. The aim of this part of the study was to identify the minerals so that appropriate standards could be obtained for the subsequent quantitative analysis of the remaining samples.

The sample exhibited a distinct vein, several millimeters thick, which was examined separately from the bulk material.

EXPERIMENTAL

Analytical techniques

X-ray diffraction was performed using Phillips PW 1050 powder diffractometer equipped with Cu X-ray source and operated at 40 kV and 30 mA.

Scanning electron microscopy was performed using Phillips 515 instrument equipped with energy dispersive X-ray spectrometer (SEM/EDS).

Sample preparation for mineral identification

The material from the vein was drilled out and separated from the bulk material. The vein material was used for the mineral identification only, as there was not enough sample to perform clay separation and/or identification. The remaining bulk material was used for both mineral identification and clay speciation. For the mineral identification the bulk core sample were finely ground in a ceramic mortar.

Sample preparation for clay speciation

The bulk core sample was crushed in a ceramic mortar, soaked in purified water for 5 hours, sonicated and the clay fraction was decanted after sedimentation. The sample produced substantial amount of clay fraction, no less than 40 % by weight.

To prepare the oriented sample, a part of the decanted suspension containing the clay fraction was filtered through a 0.4 μm filter. The collected material was re-dispersed in a small amount of purified water; the suspension was placed on a glass slide and allowed to dry at room temperature.

After the dry oriented film had been examined, the sample was placed in a desiccator with ethylene glycol, evacuated for 15 minutes, left to saturate overnight and examined immediately after taking out of the desiccator.

Subsequently, the sample was heated at 400 °C and at 550 °C for 1.5 hour and examined after each treatment.

Sample preparation for scanning electron microscopy

A freshly broken fragment of the bulk core was used for the electron microscopic examination. Additionally, a freshly broken fragment of the vein was examined after coating it with gold.

RESULTS

Mineral identification

Spectrum 1 shows the diffraction pattern from the bulk sample; the identified minerals are listed in Table I.

Spectra 2 & 3 show the diffraction patterns from the vein material; the identified minerals are listed in Table II.

Table I. Minerals identified in the bulk portion of the sample DGR1-456.01

Client sample ID / ActLabs Sample ID	Minerals identified in bulk material	Comments
DGR1-456.01	Calcite, CaCO ₃	Medium/large amount
A07-1311-2	Quartz, SiO ₂	Medium amount
	Halite, NaCl	Small amount
	Dolomite, CaMg(CO ₃) ₂	Small amount
	Hematite, Fe ₂ O ₃	Small / trace amount
	Illite, KAl ₂ Si ₃ AlO ₁₀ (OH) ₂	Medium amount
	Chlorite, (Mg,Fe) ₅ (Al,Si) ₅ O ₁₀ (OH) ₈	Medium amount

Table II. Minerals identified in the vein portion of the sample DGR1-456.01

Client sample ID / ActLabs Sample ID	Minerals identified in Vein material	Comments
DGR1-456.01	Halite, NaCl	Predominant
A07-1311-2	Calcite, CaCO ₃	Medium amount
	Dolomite, CaMg(CO ₃) ₂	Small / trace amount
	Quartz, SiO ₂	Small / trace amount
	Illite, KAl ₂ Si ₃ AlO ₁₀ (OH) ₂	Trace amount
	Chlorite, (Mg,Fe) ₅ (Al,Si) ₅ O ₁₀ (OH) ₈	Trace amount

Clay speciation

Spectrum 4 shows the diffraction patterns from the oriented clay fraction after the diagnostic treatments. The Spectrum 5 shows the diffraction pattern from the random powder of clay fraction. As the spectra indicate, Quartz, Calcite and Dolomite were present in the clay fraction.

Table III summarizes the clay minerals identified in the bulk portion of the sample.

Table III. Clay minerals identified in the sample.

Treatment	Peak position	Peak position	Peak position
Air dried oriented	~7 Å	~10 Å	~14 Å
Ethylene glycol	No change	No change	No change
Heated ≈ 400° C,	No change	No change	No change
Heated ≈ 550° C,	Destroyed	No change	Increased in intensity
Random powder d(060)	1.54 Å	1.50 Å	1.54 Å
Result	Chlorite	Illite	Chlorite

Scanning Electron Microscopy

Vein material

The EDS and microscopic examination of the freshly cleaved vein indicated presence of crystalline material containing sodium and chlorine. Figures 1-3 show the general and magnified views of the vein, and the corresponding EDS spectrum is consistent with high abundance of Halite in the vein.



Figure 1. General view of the vein layer embedded in the core.

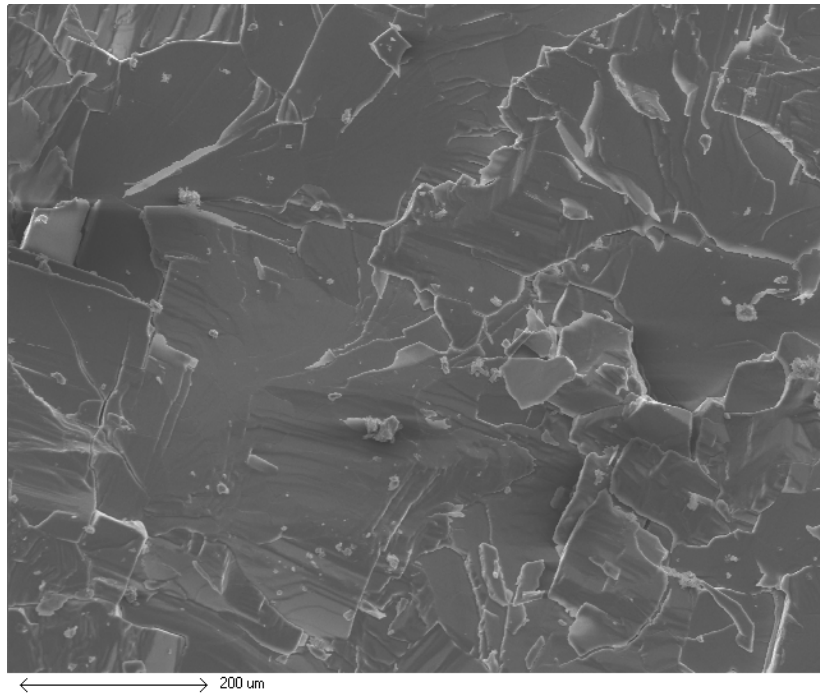


Figure 2. Surface features of the vein showing large crystalline cleavage planes.

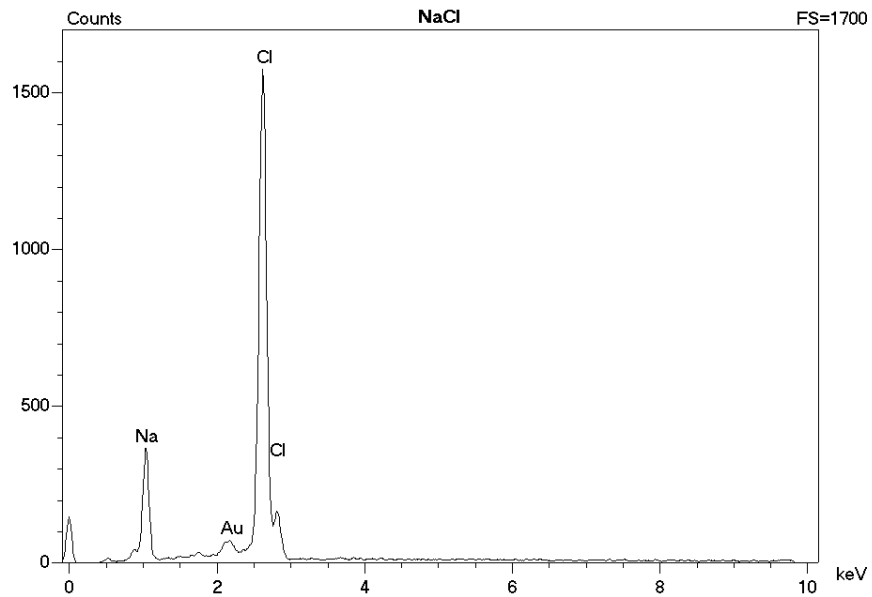


Figure 3. EDS spectrum from the region shown in Figure 2 indicating that the vein is predominantly composed of Halite. (Gold is present due to the applied surface coating).

Bulk material

The examination of regions of the bulk material far away from the vein indicated presence of small grains of well faceted crystallites and presence of varied amount of sodium and chlorine. The micrographs and the corresponding EDS spectra from two regions are shown below.

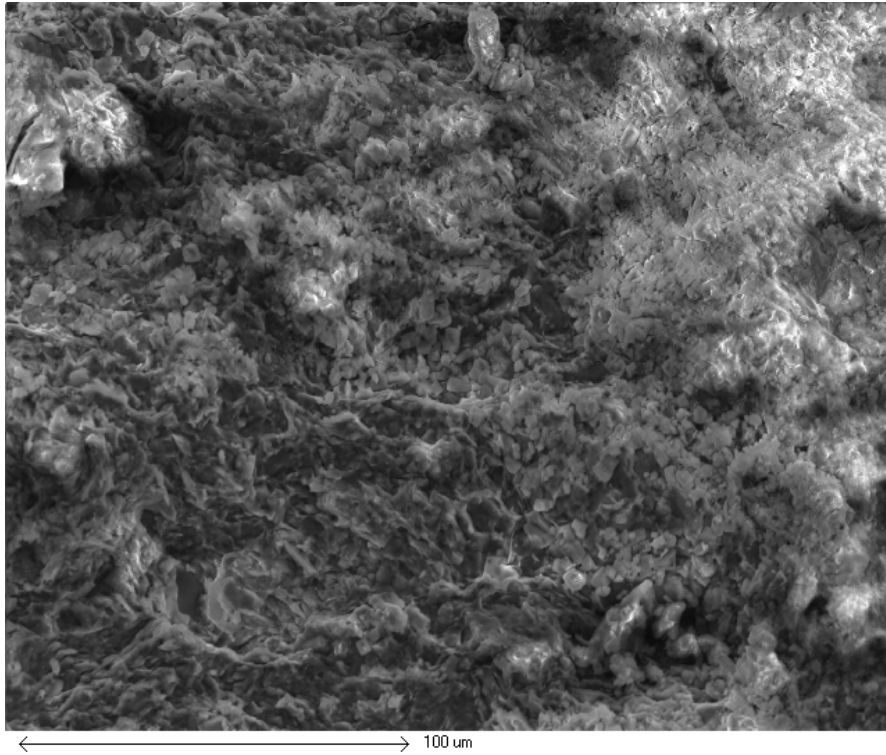


Figure 4. Surface features of a region from the bulk of the sample far away from the vein.

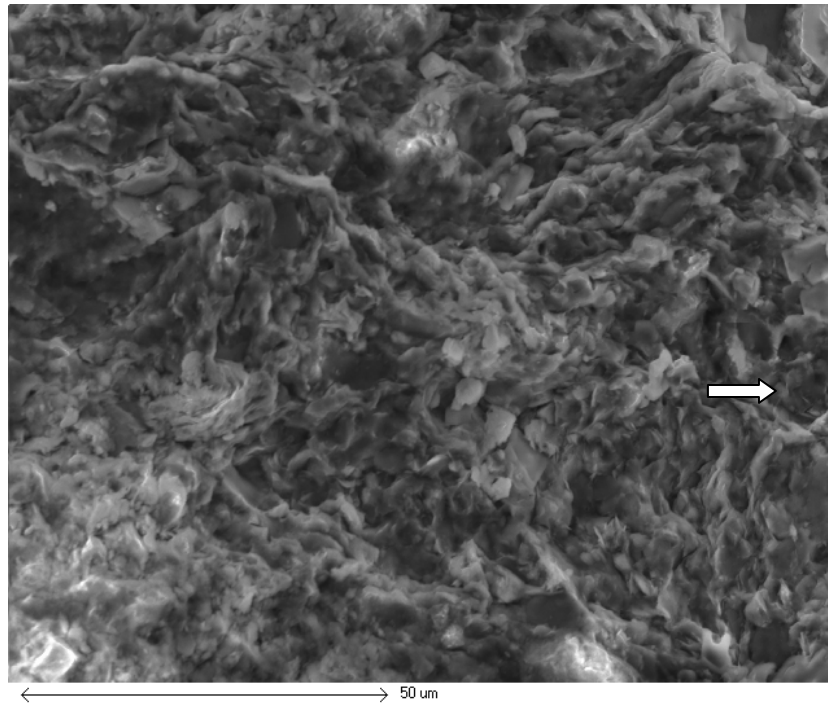


Figure 5. Magnification of the same area showing the presence of small, well faceted grains.

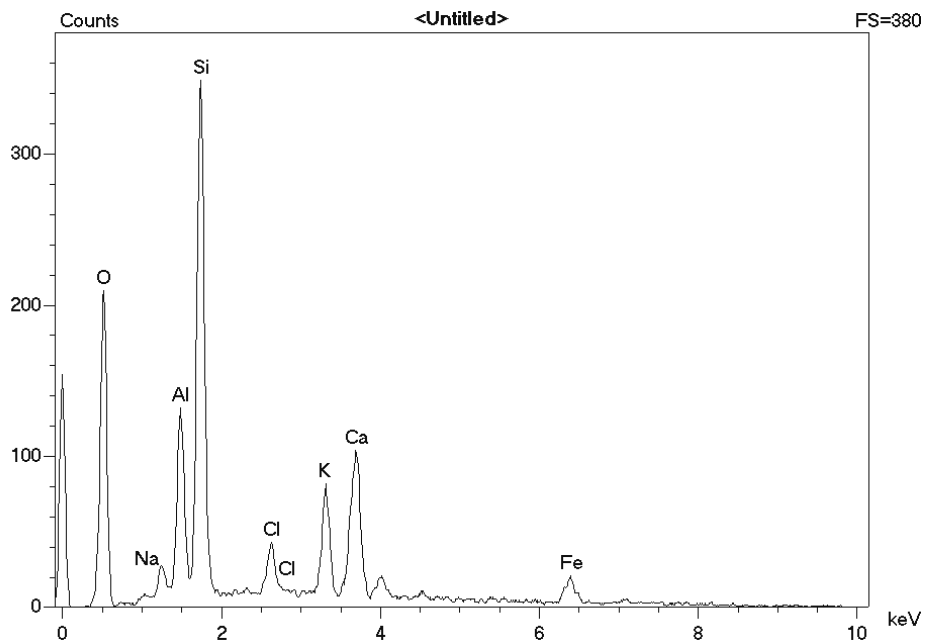


Figure 6. EDS spectrum from the area indicated by the arrow in Figure 5. Small amount of sodium and chlorine is evident.

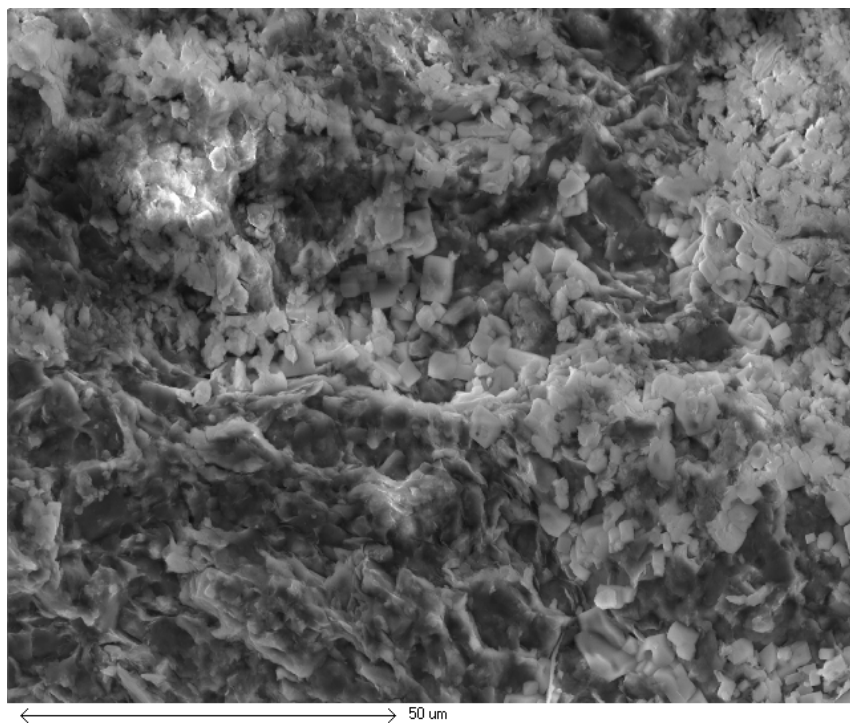


Figure 7. Another region of the bulk sample where small crystallites were found.

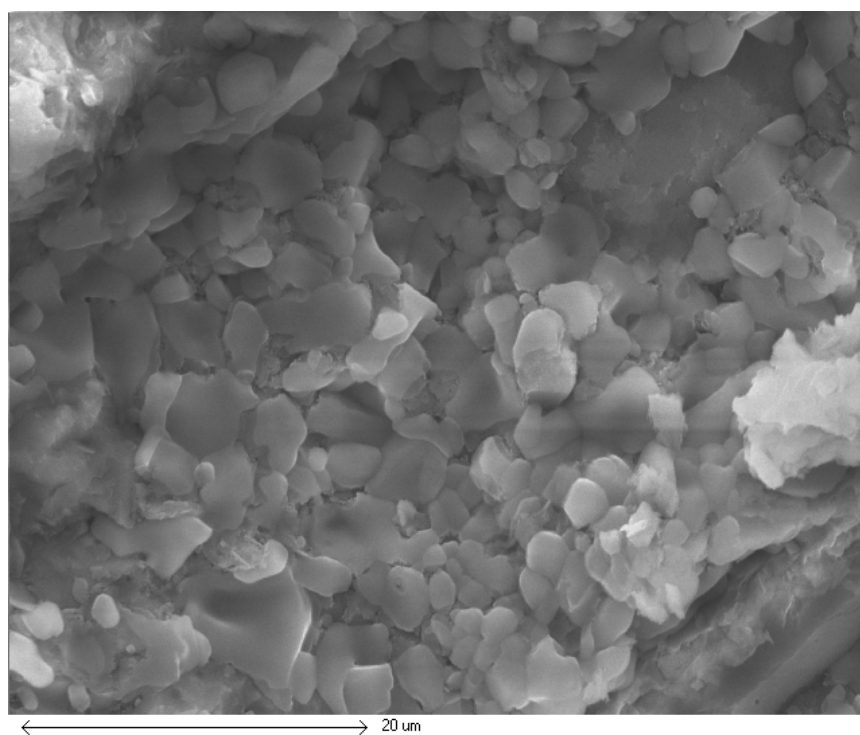


Figure 8. Magnification of the region shown in Figure 7.

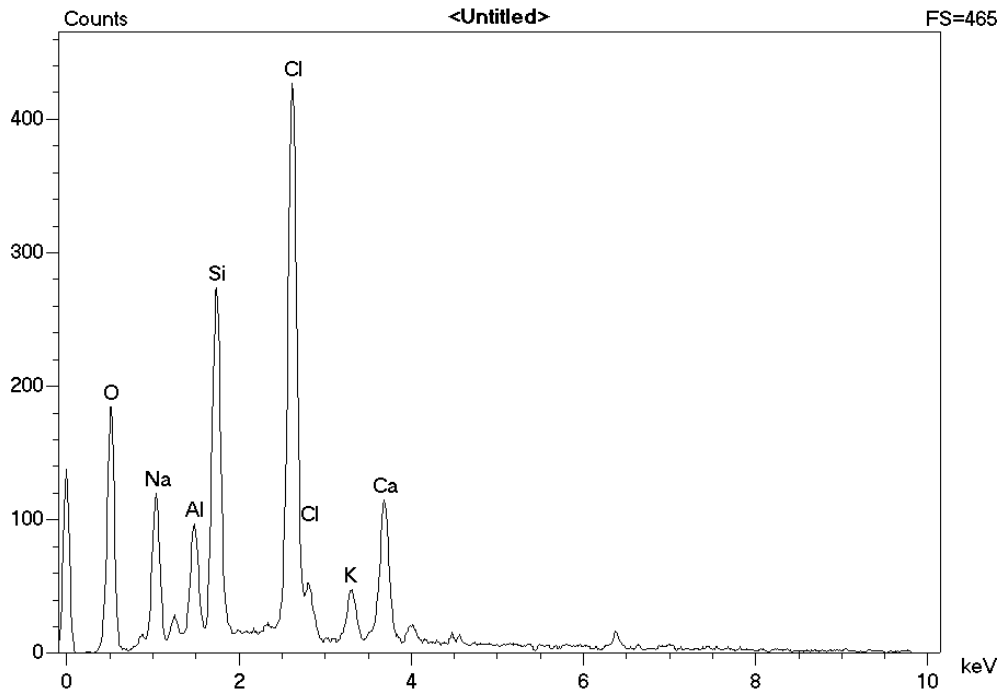


Figure 9. EDS spectrum corresponding to the region shown in Figure 8. Large amount of sodium and chlorine is evident, indicating that some of the crystallites are likely to be Halite.

CONCLUSIONS

The bulk of the core DGR1-456.01 contains Quartz, Calcite, Dolomite, Halite, Illite and Chlorite. The clay fraction constitutes at least 40% of the sample. Quantitative analysis will follow.

The vein present in the core contains mostly Halite with small amount of Calcite, Dolomite and Quartz.

Please do not hesitate to contact us if you have any questions.

Reported by:

Reviewed by:

Aniceta Skowron, Ph.D.
Senior Scientist
Activation Laboratories

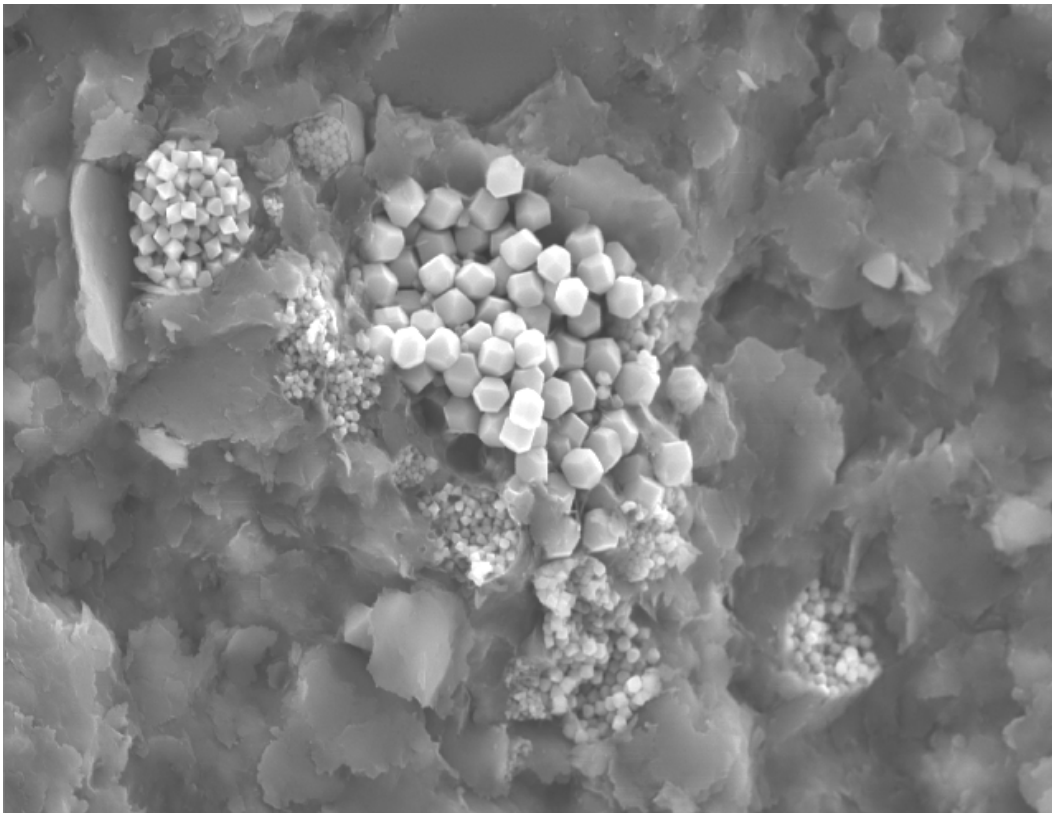
Eric Hoffman, Ph.D.
General Manager
Activation Laboratories

APPENDIX B

ActLabs Report on SEM/EDS Analyses of DGR-2 Core

**Activation Laboratories Ltd.
1336 Sandhill Drive, Ancaster
Ontario, Canada L9G 4V5**

SEM/EDS Examination of DGR-2 Cores



← 20 um →

for

Intera Engineering Ltd.

SEM/EDS Examination of DGR-2 Cores

W.O. # A07-0626, A07-0652, A07-0765
A07-1194, A07-1247, A07-1311

And

W.O. # A07-2009, A07-2082, A07-2338, A07-2536

No. of pages 52

FOR:

Intera Engineering Ltd
11 Venus Crescent, Heidelberg
ON N0B 1Y0

Richard Jackson
Tel: 519-699-4657
Email: rjackson@intera.com

February 21, 2007

INTRODUCTION

Eight core samples, identified as follows, were submitted for examination using Scanning Electron Microscopy and Energy Dispersive Spectroscopy (SEM/EDS) to determine general morphology and elemental composition of the samples.

Client sample ID	ActLabs sample ID
DGR2-482.45	A07-2082-1
DGR2-535.56	A07-2082-3
DGR2-570.73	A07-2082-5
DGR2-606.62	A07-2082-7
DGR2-606.96	A07-2082-8
DGR2-644.49	A07-2082-10
DGR2-659.31	A07-2338-2
DGR2-704.87	A07-2338-1

EXPERIMENTAL

Sample preparation

Selected core samples were freshly cleaved, coated with thin film of gold and mounted for the examination. Phillips 515 scanning electron microscope equipped with energy dispersive spectrometer was used.

RESULTS

The SEM/EDS observations are summarized in the Table 2 followed by SEM micrographs and EDS spectra, shown in Figures 1-77.

Table 2. Summary of SEM/EDS observations.

Sample ID	Observations
DGR2 – 482.45 (A07-2082-1)	<ul style="list-style-type: none"> • General matrix – low Cl concentration • Regions of high Cl concentration • Morphology of the high Cl regions: spots and glassy looking layers
DGR2 – 535.56 (A07-2082-3)	<ul style="list-style-type: none"> • General matrix – low Cl concentration • Regions of high Cl concentration • Morphology of the high Cl regions: spots and glassy looking layers
DGR2-570.73 (A07-2082-5)	<ul style="list-style-type: none"> • Islands and layers of glassy phases with high Cl content and relatively low Na content • Glassy layers are thin, and are probably more brittle than the surrounding matrix since they predominate on cleaved surfaces • Framboidal FeS present • Matrix has flake-like morphology, K and Fe present in the matrix
DGR2-606.62 (A07-2082-7)	<ul style="list-style-type: none"> • Regions of high and low density of cube-like particles • Cube-like particles have high Cl concentration and Na is also present – these are probably NaCl crystallites
DGR2-606.96 (A07-2082-8)	<ul style="list-style-type: none"> • Region of high Ca, S and O consistent with Gypsum • Framboidal FeS present • Matrix with flake-like morphology
DGR2-644.49 (A07-2082-10)	<ul style="list-style-type: none"> • Framboidal FeS present • Matrix with flake-like morphology, K and F present • Cube-like particles with high Cl concentration, Na also present – these are probably NaCl crystallites
DGR2-659.31 (A07-2338-2)	<ul style="list-style-type: none"> • Matrix with faceted morphology, K and F present • Regions of high Ca concentration
DGR2-704.87 (A07-2338-1)	<ul style="list-style-type: none"> • Matrix with flake-like morphology, K and F present • Cube-like particles with high Ca concentration • Islands with semi-glassy appearance and high Na and Cl concentration

Sample DGR2-482.45 (A07-2082-1)

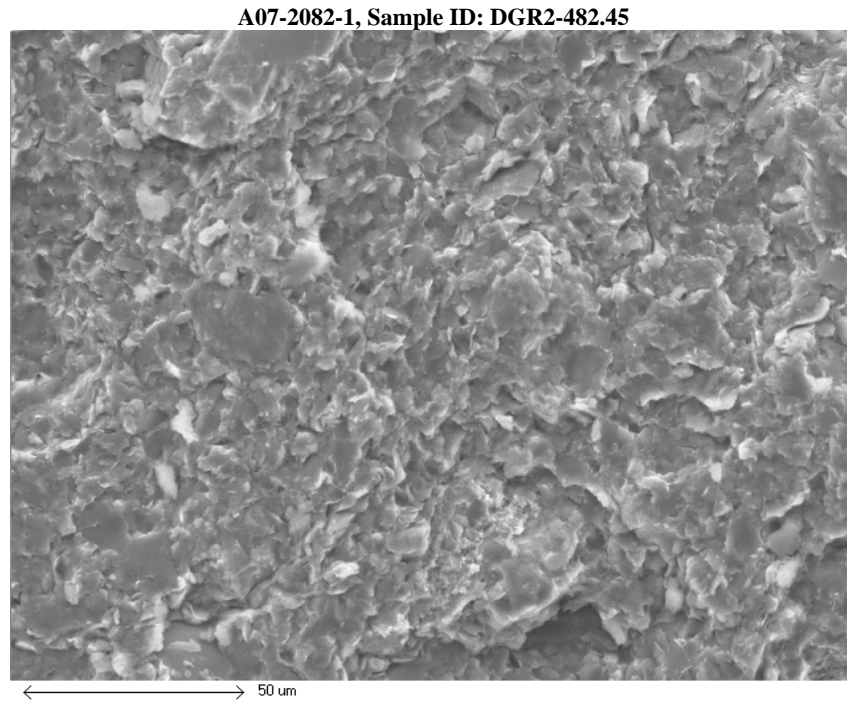


Figure 1. A typical view of the matrix of freshly cleaved core DGR2-482.45. The corresponding elemental composition is shown in Figure 2, SEM x600,

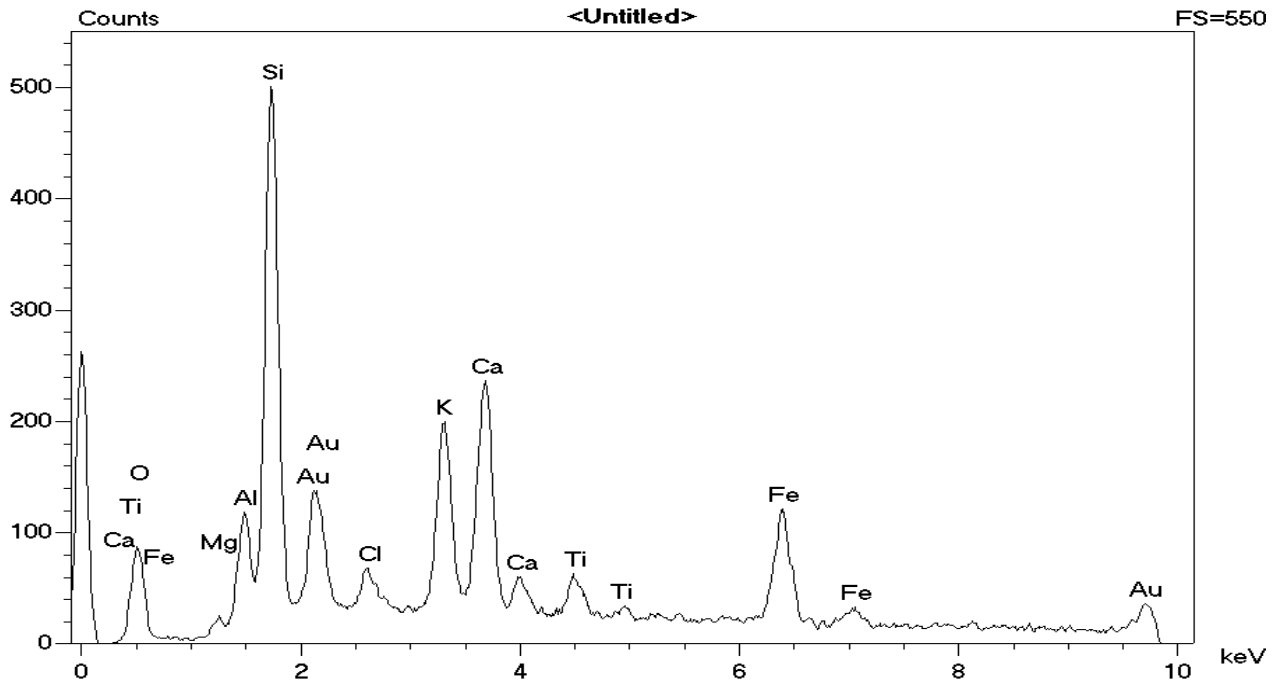


Figure 2, Elemental composition of the typical matrix of core DGR2-482.45 above. Gold originates from sputtered coating.

A07-2082-1, Sample ID: DGR2-482.45

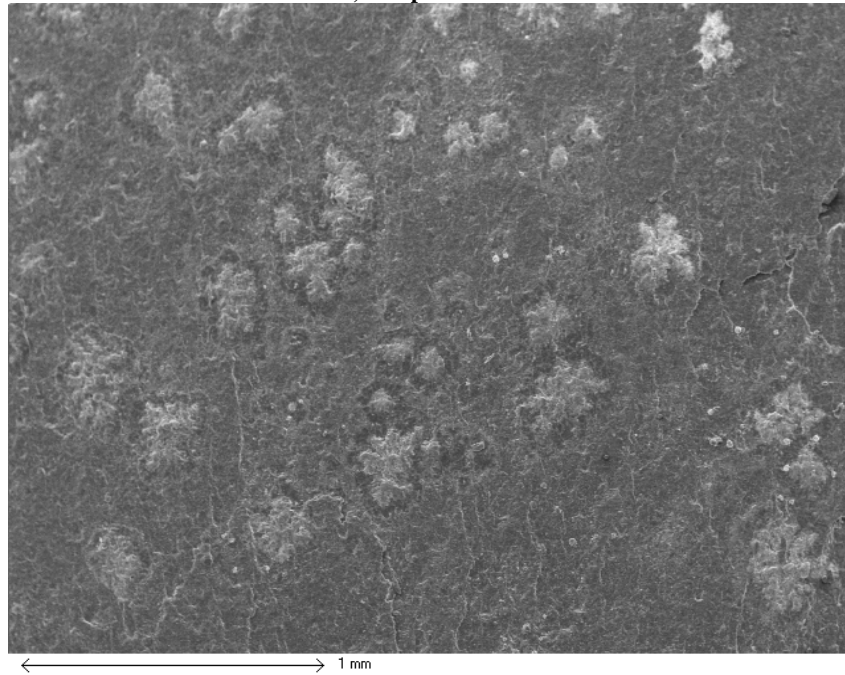


Figure 3, Regions of high Cl content on the freshly leaved surface of the core. The regions have the form of islands in the matrix of low Cl concentration, SEM x41.

A07-2082-1, Sample ID: DGR2-482.45

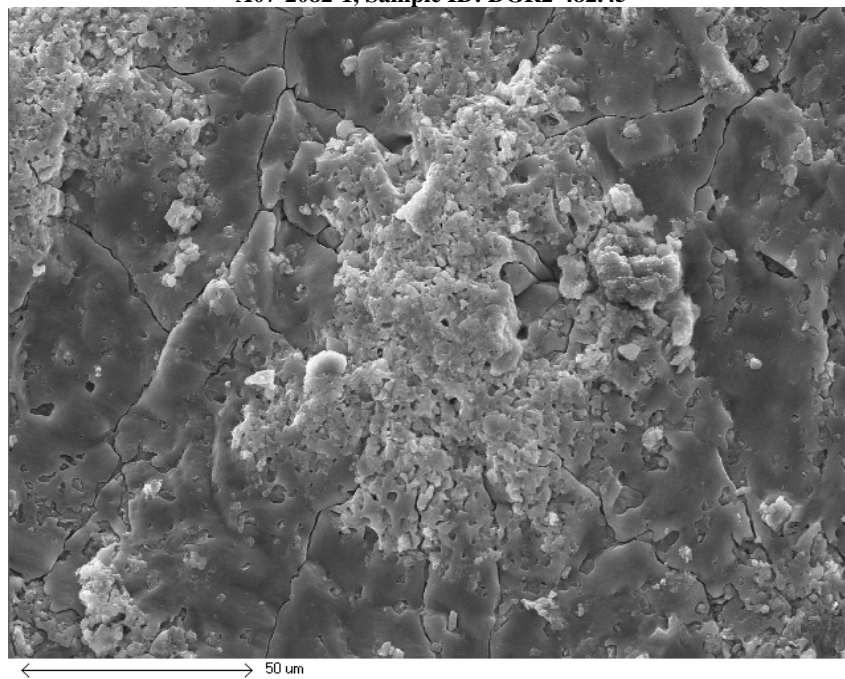


Figure 4, Detail of an island with high Cl concentration, shown in Figure3, SEMx 625.

A07-2082-1, Sample ID: DGR2-482.45

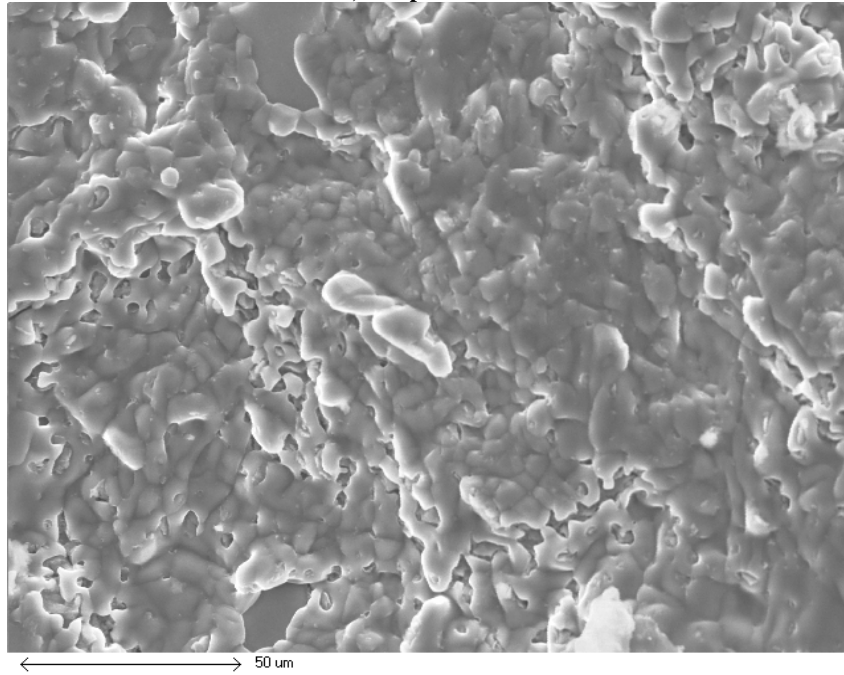


Figure 5, Region with high Cl concentration which covers a large area of the freshly cleaved fracture surface of the core, SEMx 600.

A07-2082-1, Sample ID: DGR2-482.45

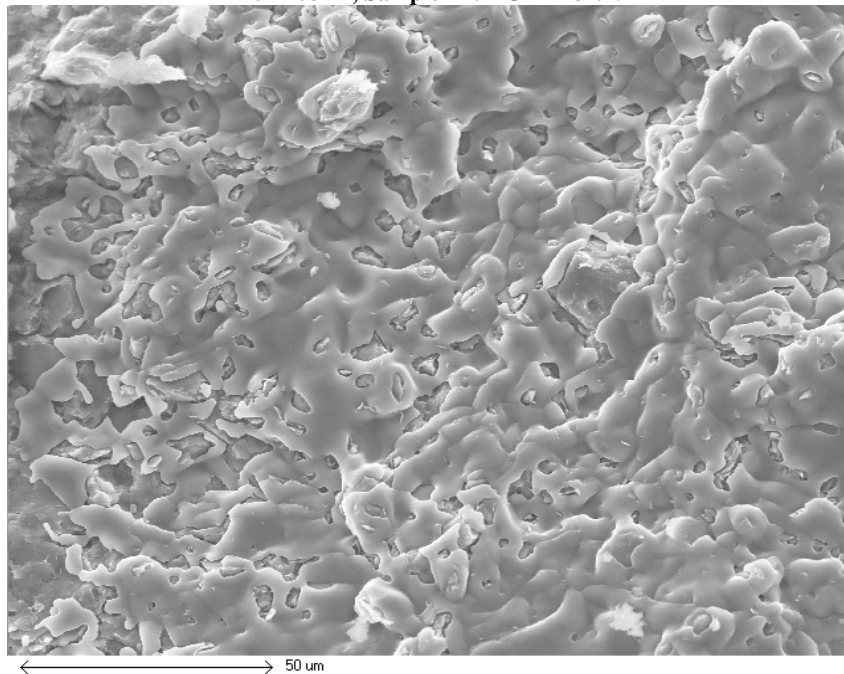


Figure 6, Another region of high Cl concentration covering a large area of the freshly cleaved fracture surface of the core, SEMx680.

A07-2082-1, Sample ID: DGR2-482.45

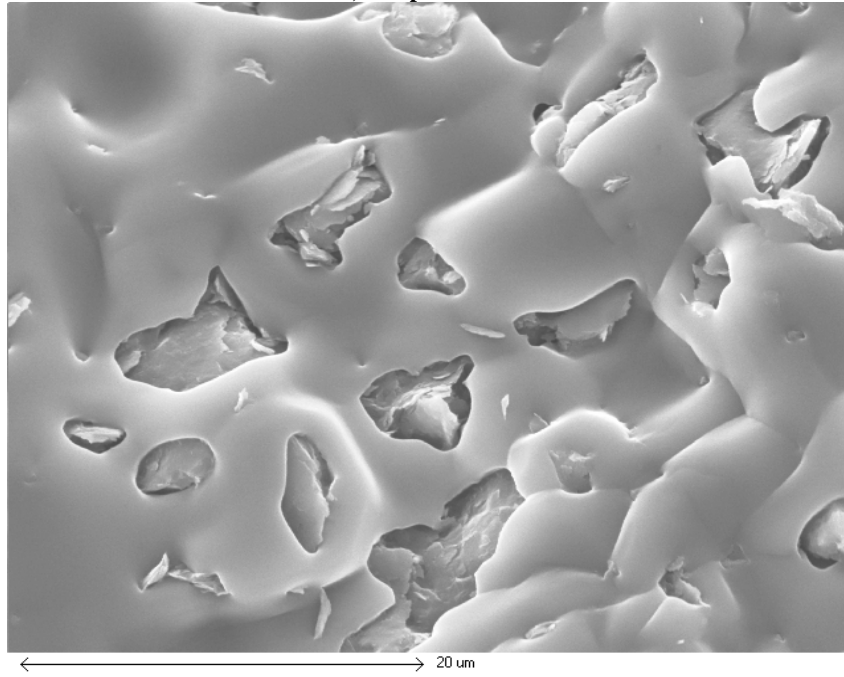


Figure 7, High magnification of the high Cl region shown in Figures 5 and 6, SEMx2720.

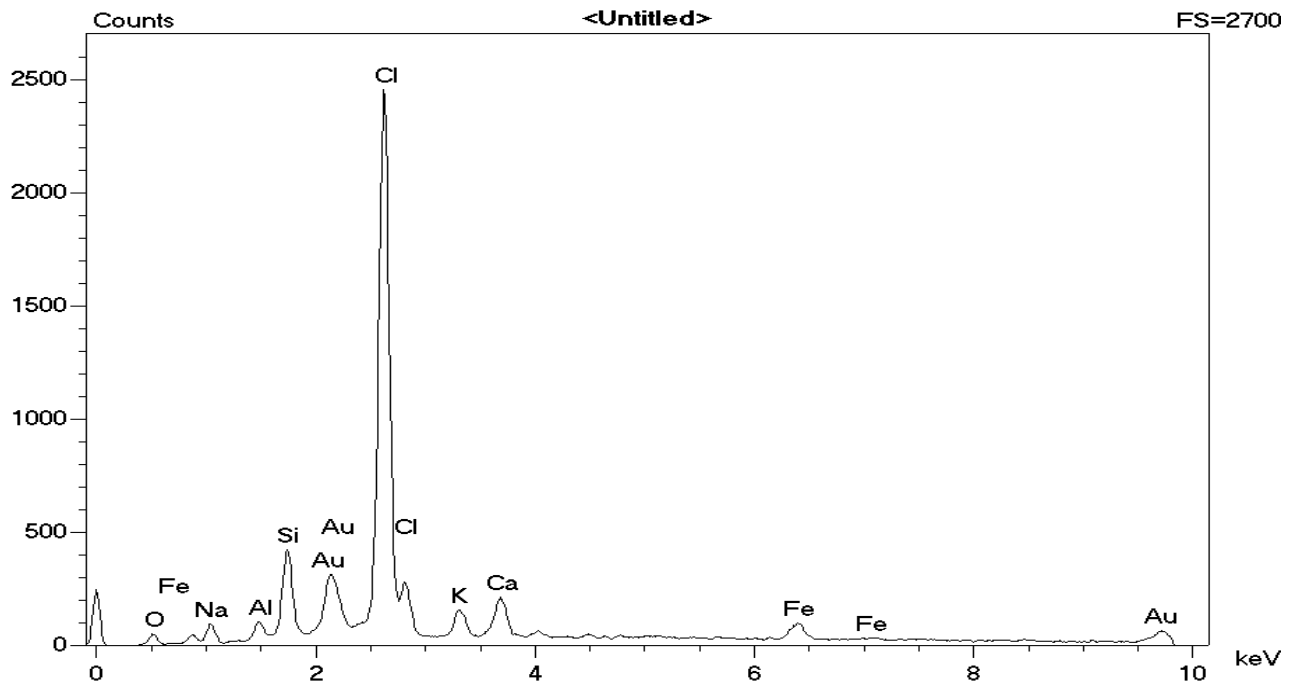


Figure 8, Elemental makeup of the high Cl concentration region. Gold originates from sputtered coating.

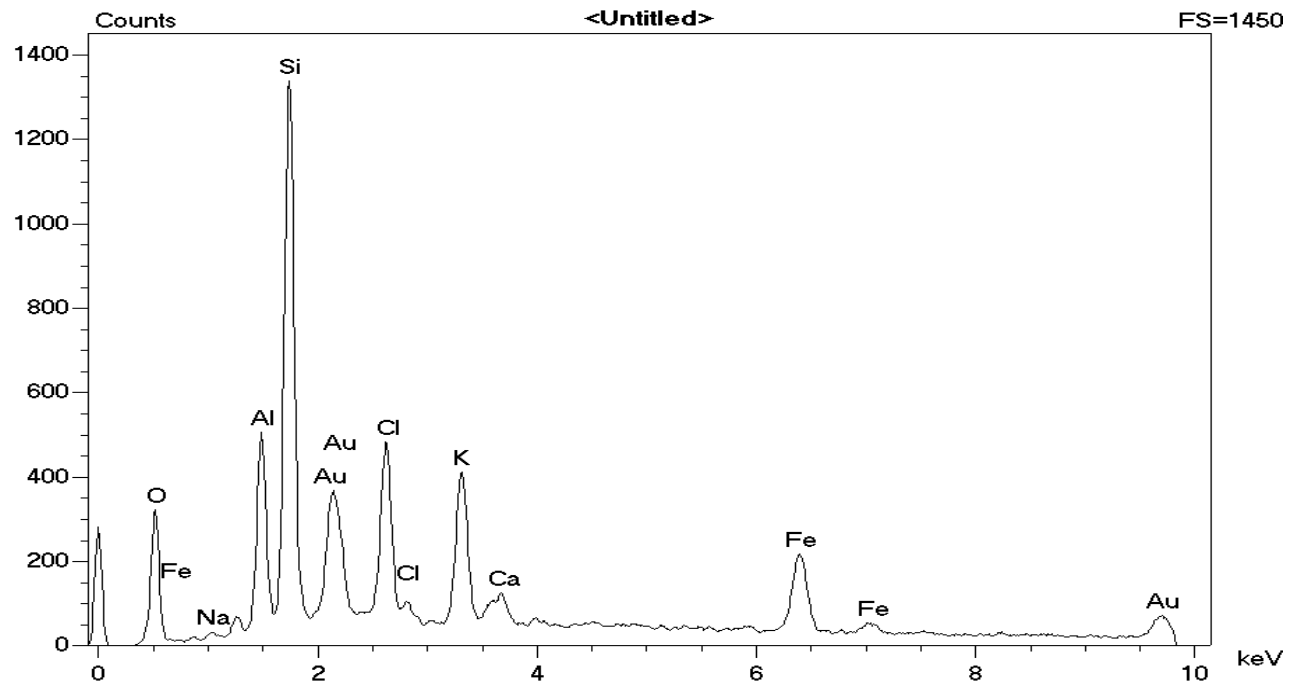


Figure 9, Elemental makeup of the matrix “island” indicates the presence of aluminosilicates and moderate Cl concentration.

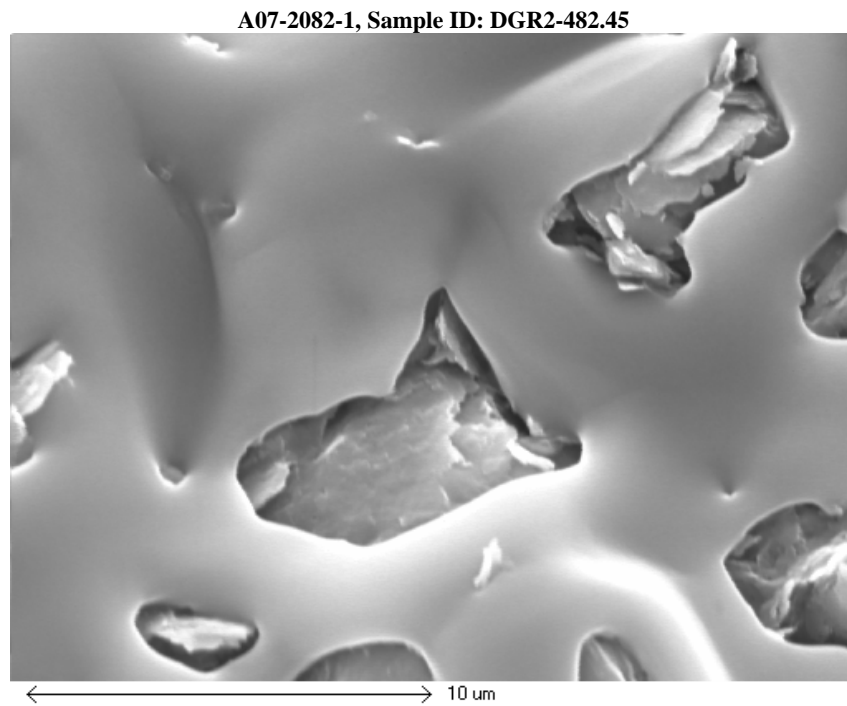


Figure 10. A region for which the elemental maps shown below were obtained, SEMx5450.

A07-2082-1, Sample ID: DGR2-482.45

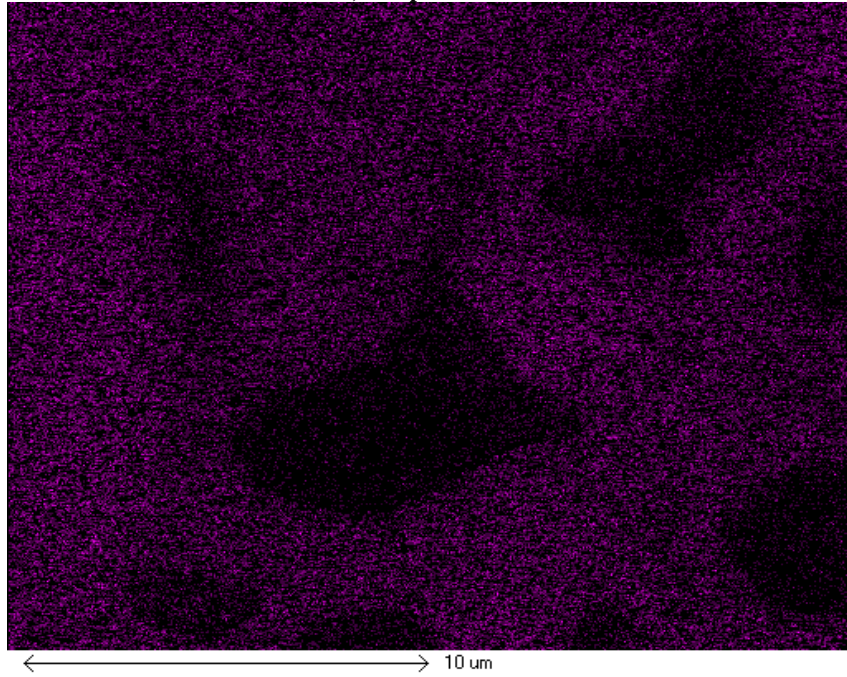


Figure 11, Chlorine map of the region shown in Figure 10.

A07-2082-1, Sample ID: DGR2-482.45

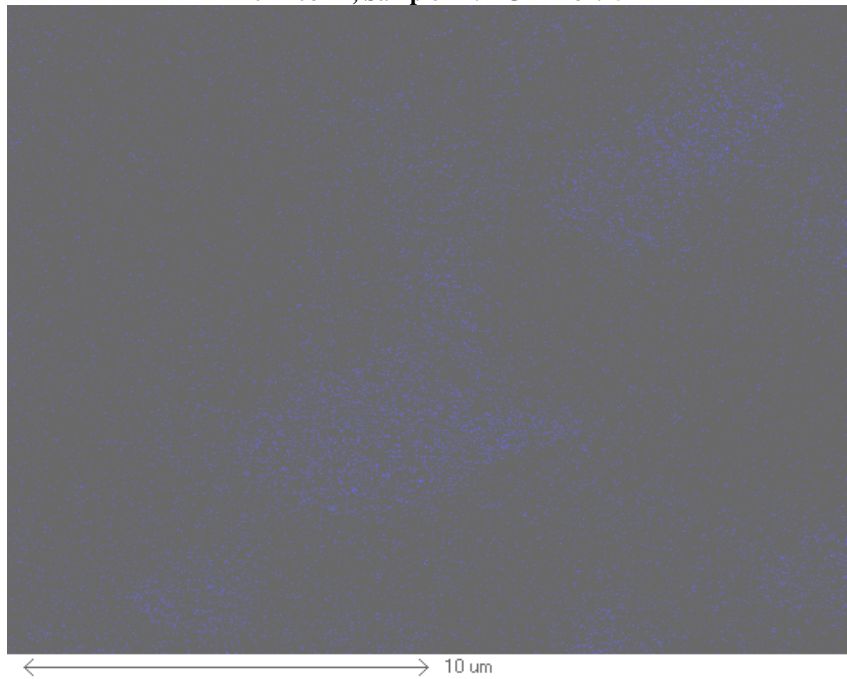


Figure 12, Silicon map of the region shown in Figure 10.

A07-2082-1, Sample ID: DGR2-482.45

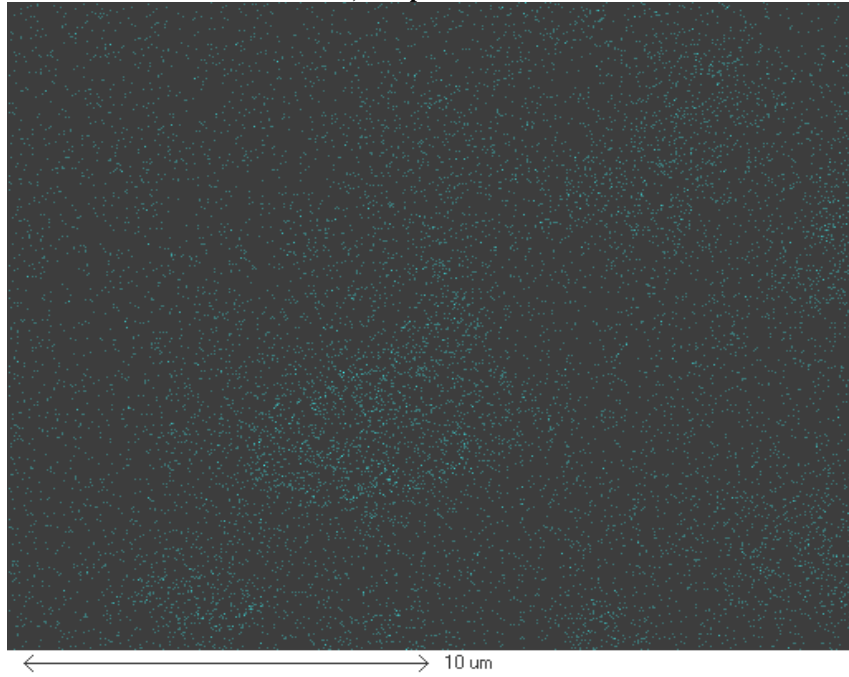


Figure 13, Potassium map of the region shown in Figure 10.

A07-2082-1, Sample ID: DGR2-482.45

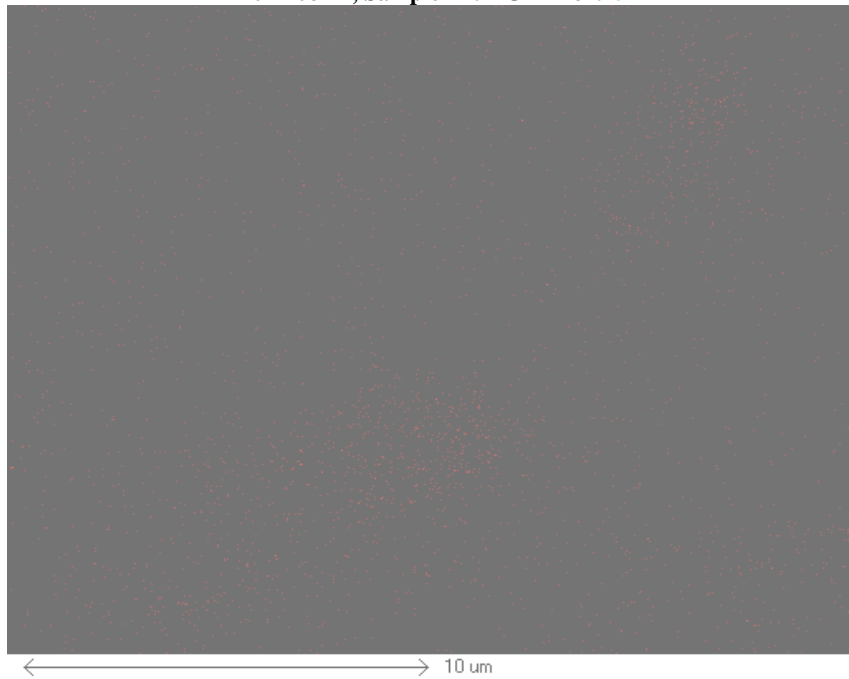


Figure 14, Oxygen map of the region shown in Figure 10.

A07-2082-1, Sample ID: DGR2-482.45

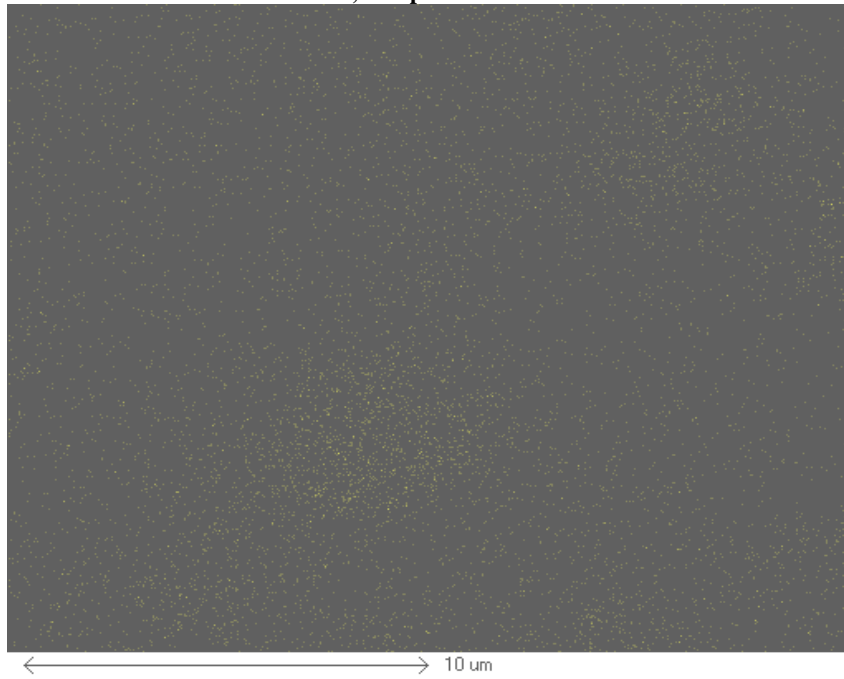


Figure 15, Aluminum map of the region shown in Figure 10.

A07-2082-1, Sample ID: DGR2-482.45

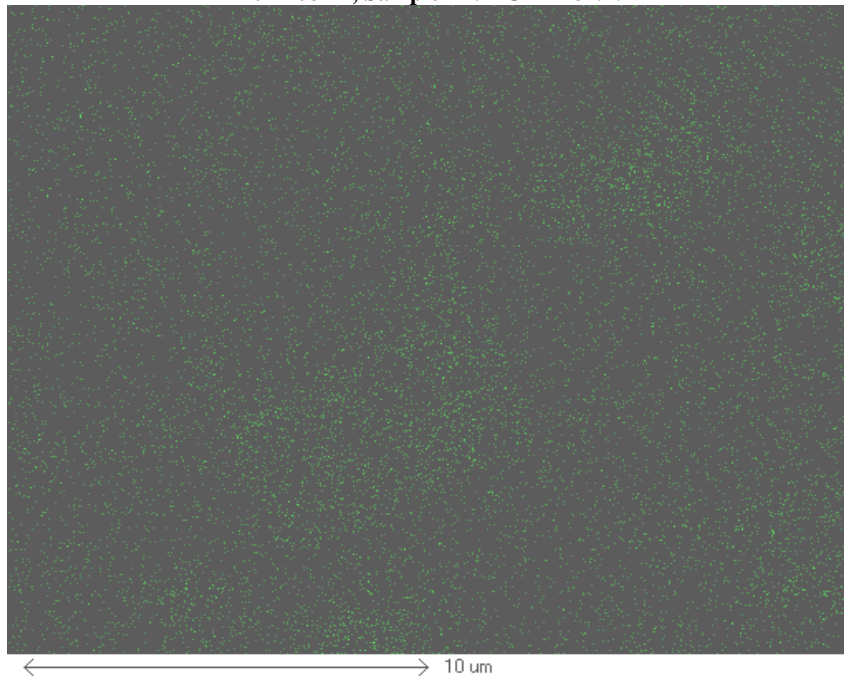


Figure 16, Iron map of the region shown in Figure 10.

Sample DGR2-535.56 (A07-2082-3)

A07-2082-3, Sample ID: DGR2-535.56

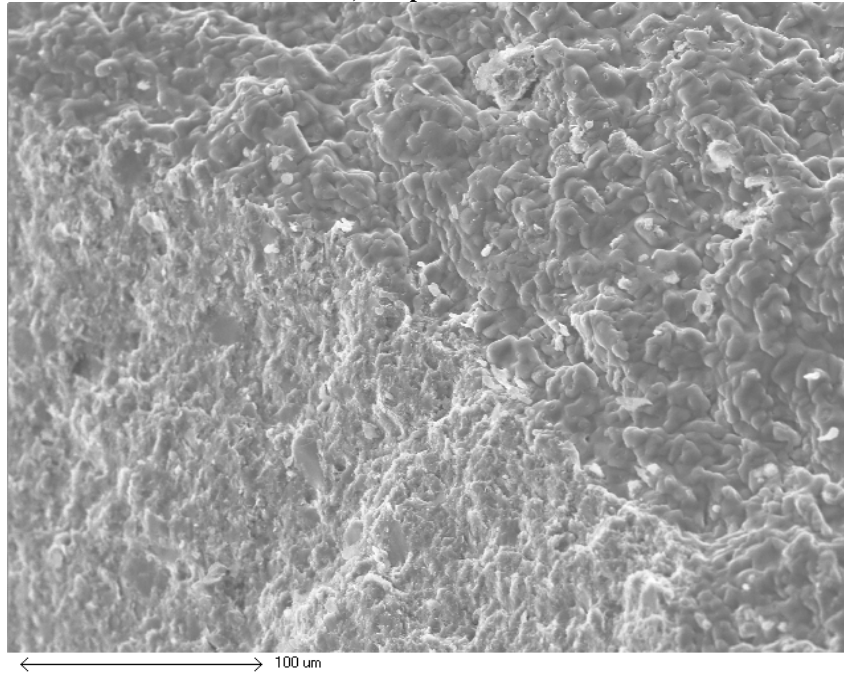


Figure 17, Fracture surface showing two kinds of regions, a high Cl concentration region at the right side-upper corner, and a low Cl concentration matrix at the left side bottom corner, SEMx326.

A07-2082-3, Sample ID: DGR2-535.56

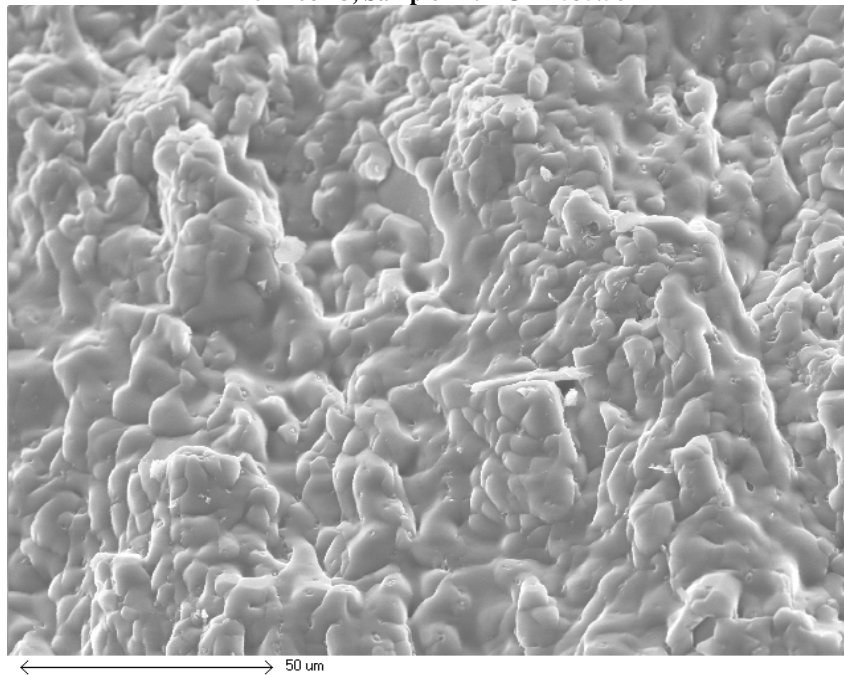


Figure 18, Detail of the high Cl concentration region, SEMx680.

A07-2082-3, Sample ID: DGR2-535.56

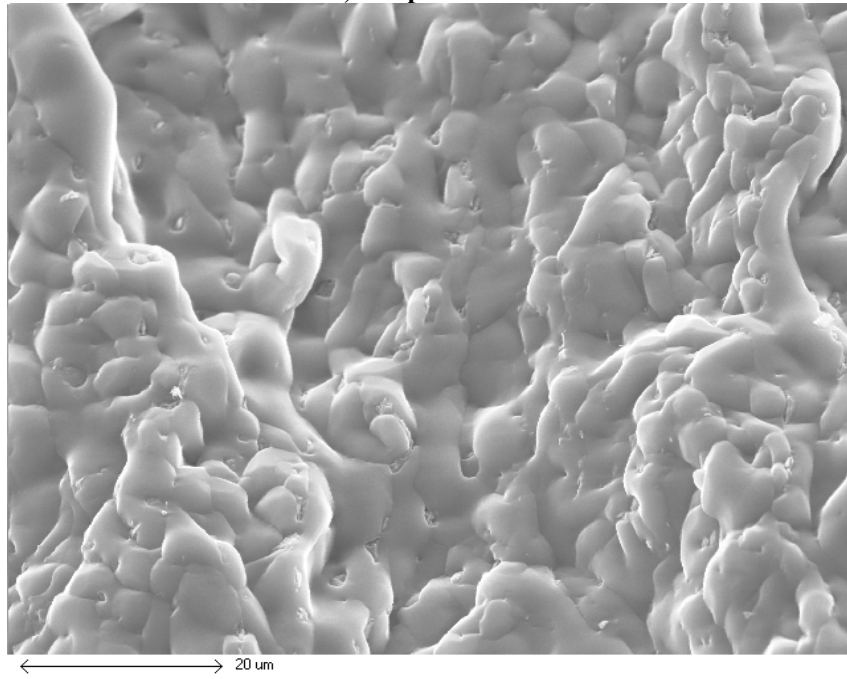


Figure 19, Detail of the high Cl concentration region, SEMx1360.

A07-2082-3, Sample ID: DGR2-535.56

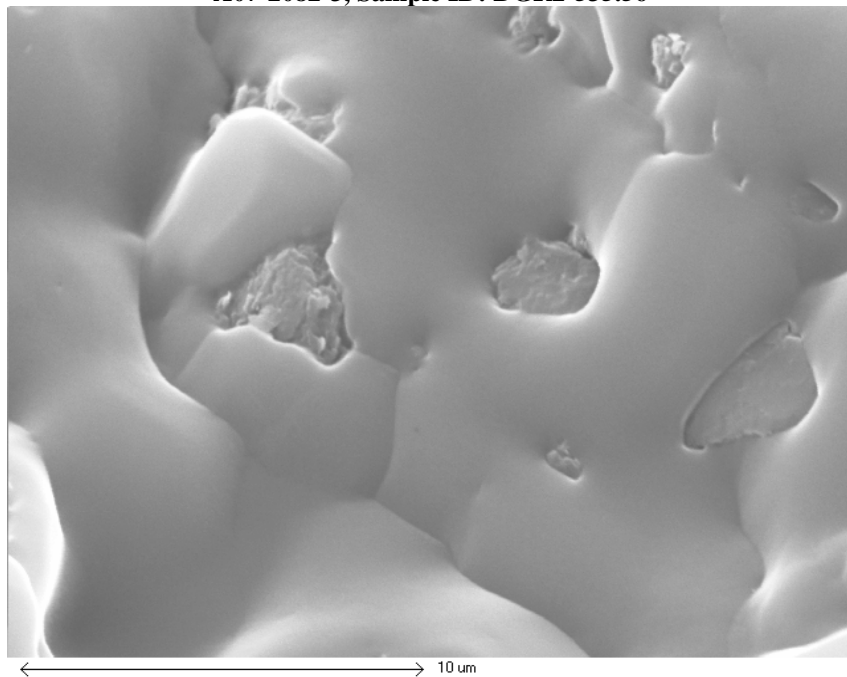


Figure 20, Detail of the high Cl concentration region, SEMx5450.

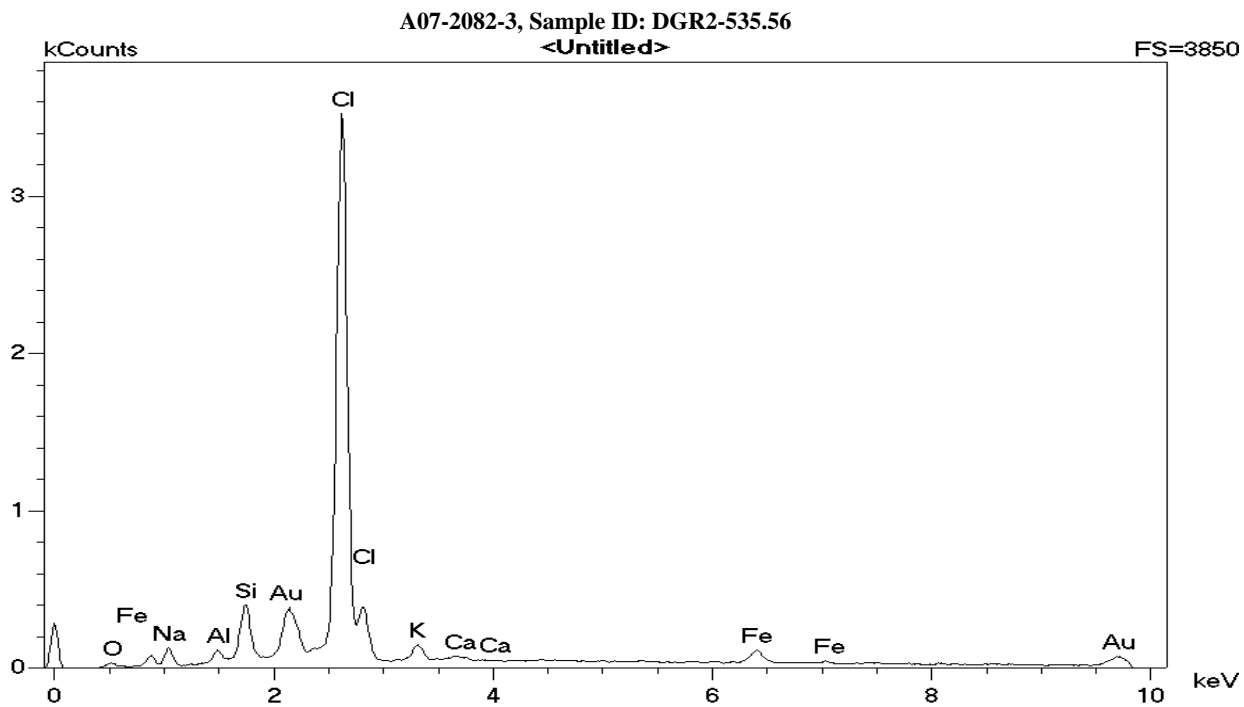


Figure 21, Elemental makeup of the high Cl concentration region. Gold originates from sputtered coating.

A07-2082-3, Sample ID: DGR2-535.56

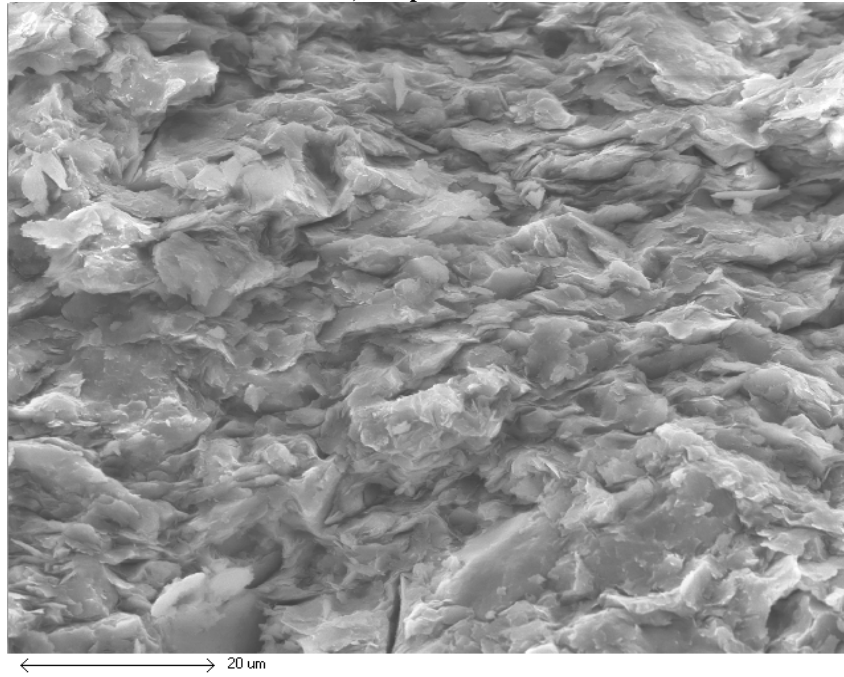


Figure 22, Morphology of the general matrix with low Cl concentration, SEMx1310.

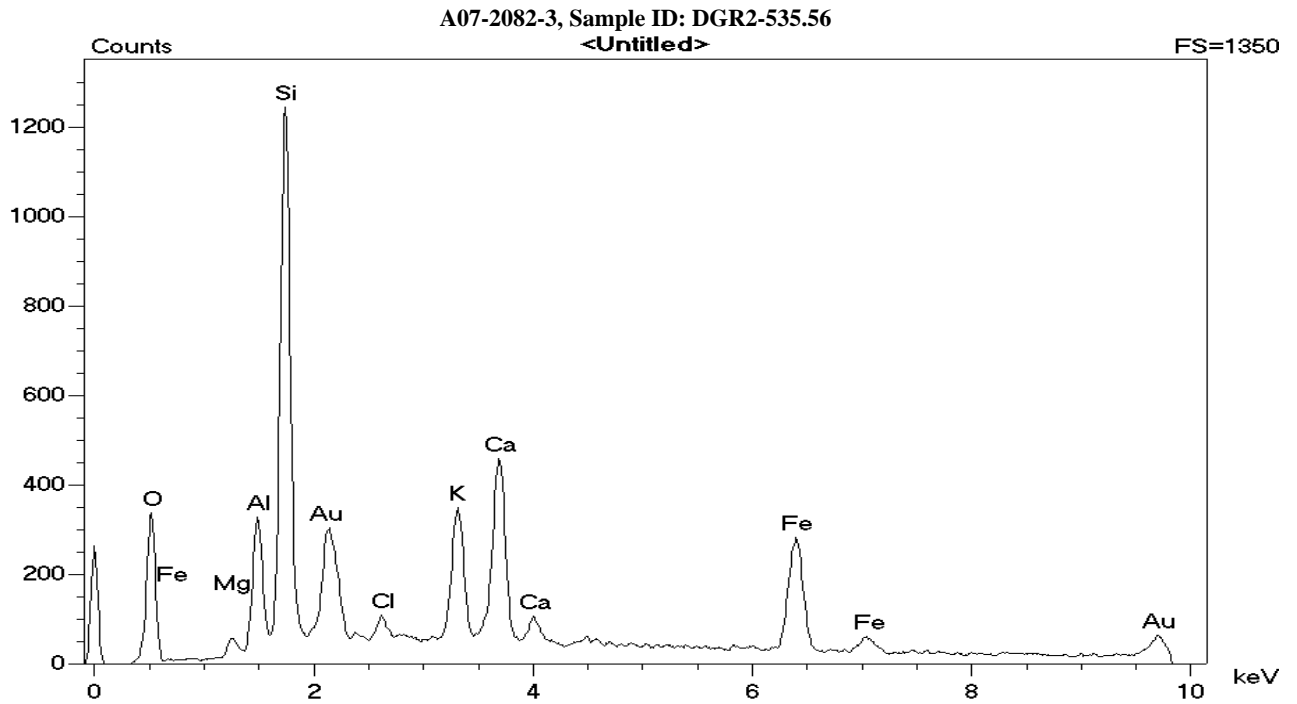


Figure 23, Elemental composition of the region above. Gold originates from sputtered coating.

Sample DGR2-570.73 (A07-2082-5)

A07-2082-5, Sample ID: DGR2-570.73

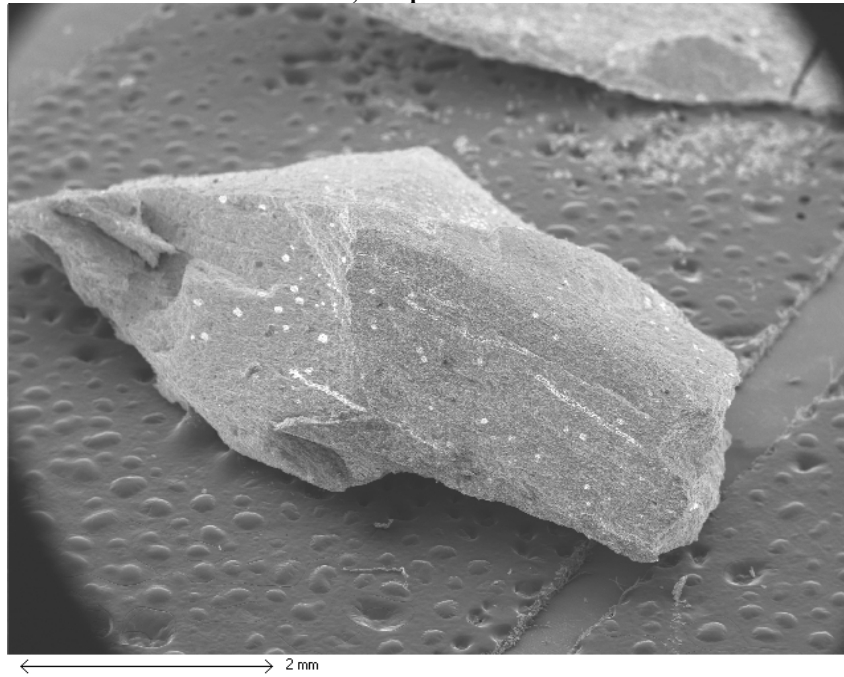


Figure 24 , Low magnification fragment of the DGR2-570.73 core showing two kinds of high Cl regions: spots and lines/layers in the general matrix, SEMx17.

A07-2082-5, Sample ID: DGR2-570.73

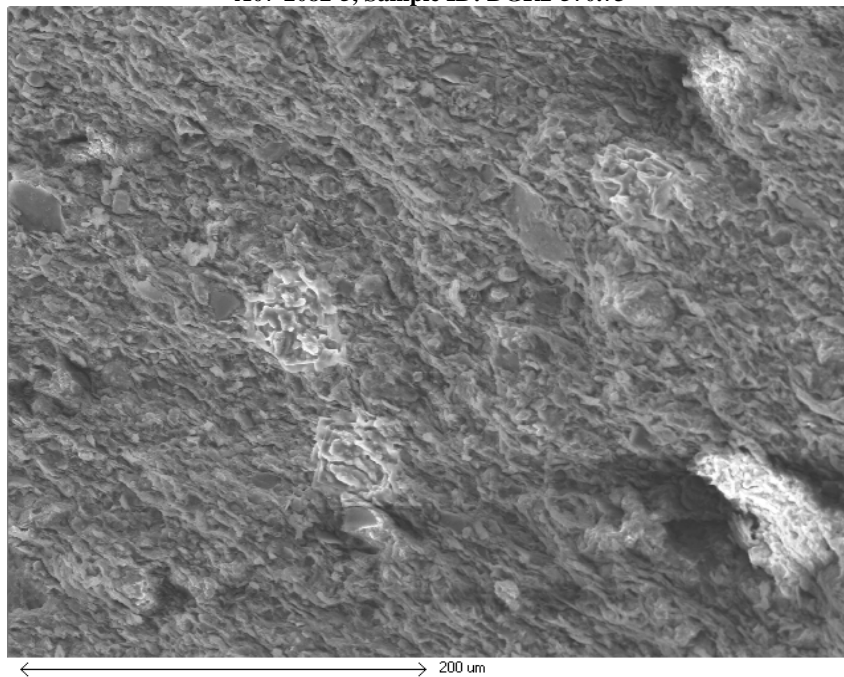


Figure 25, Details of the high Cl spots visible in Figure 24, SEMx274.

A07-2082-5, Sample ID: DGR2-570.73

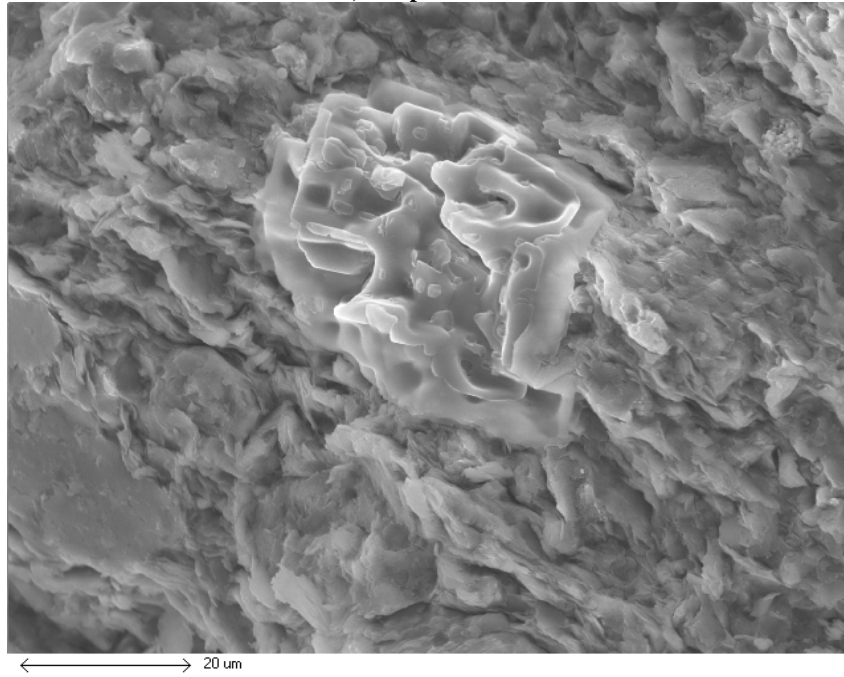


Figure 26, Details of the high Cl spots visible in Figure 24, SEMx274.

A07-2082-5, Sample ID: DGR2-570.73

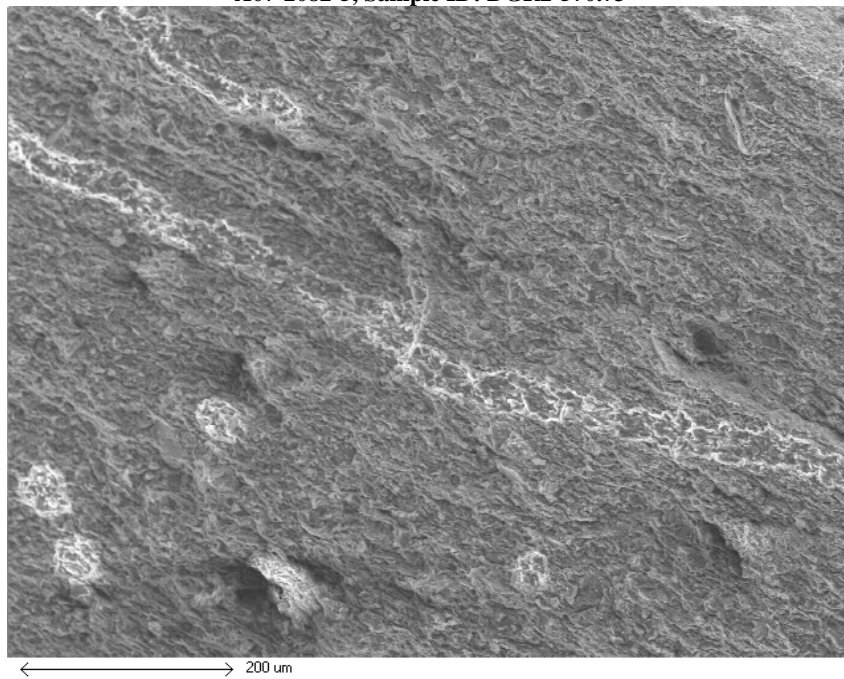


Figure 27, High Cl concentration line/layer, SEMx143.

A07-2082-5, Sample ID: DGR2-570.73

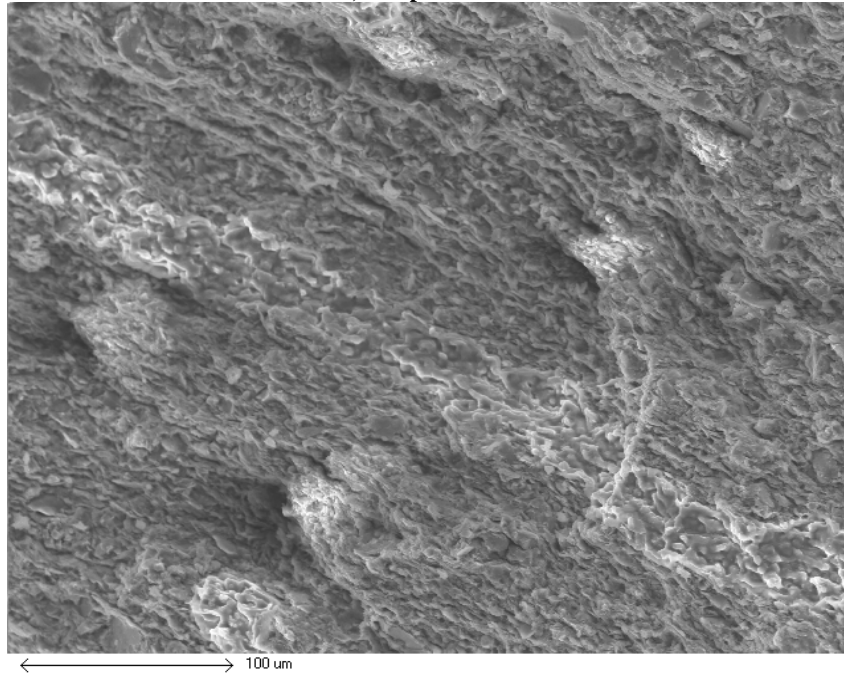


Figure 28, Detail of the high Cl line/layer, SEMx287.

A07-2082-5, Sample ID: DGR2-570.73

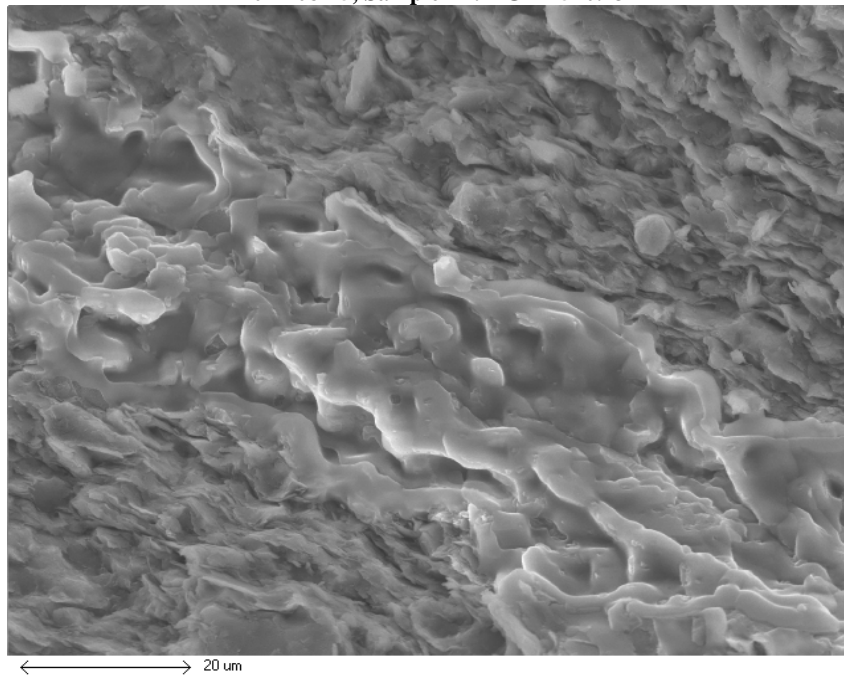


Figure 29, Detail of the high Cl line/layer, SEMx1150.

A07-2082-5, Sample ID: DGR2-570.73

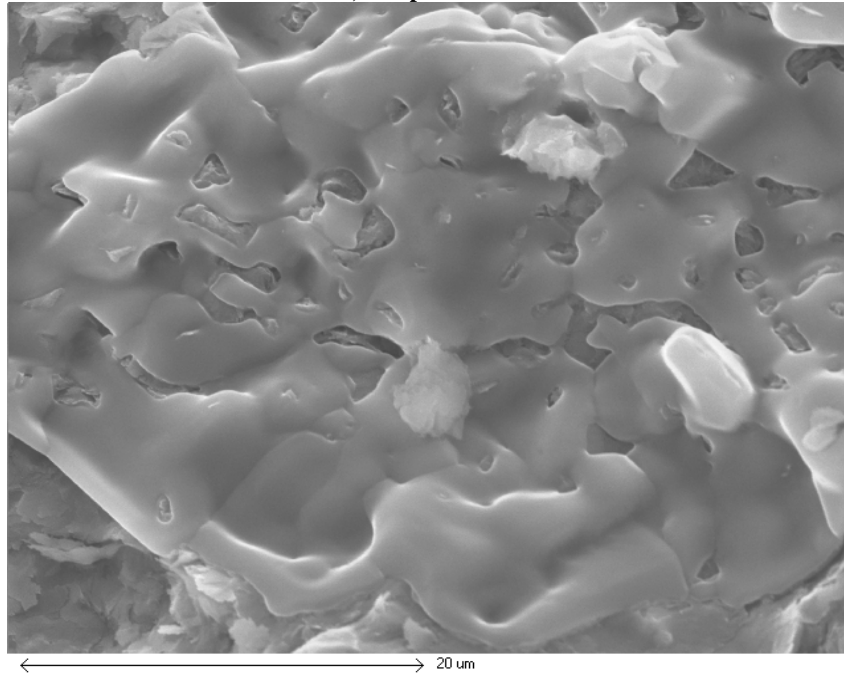


Figure 31, Detail of the high Cl concentration layer. SEMx2720,

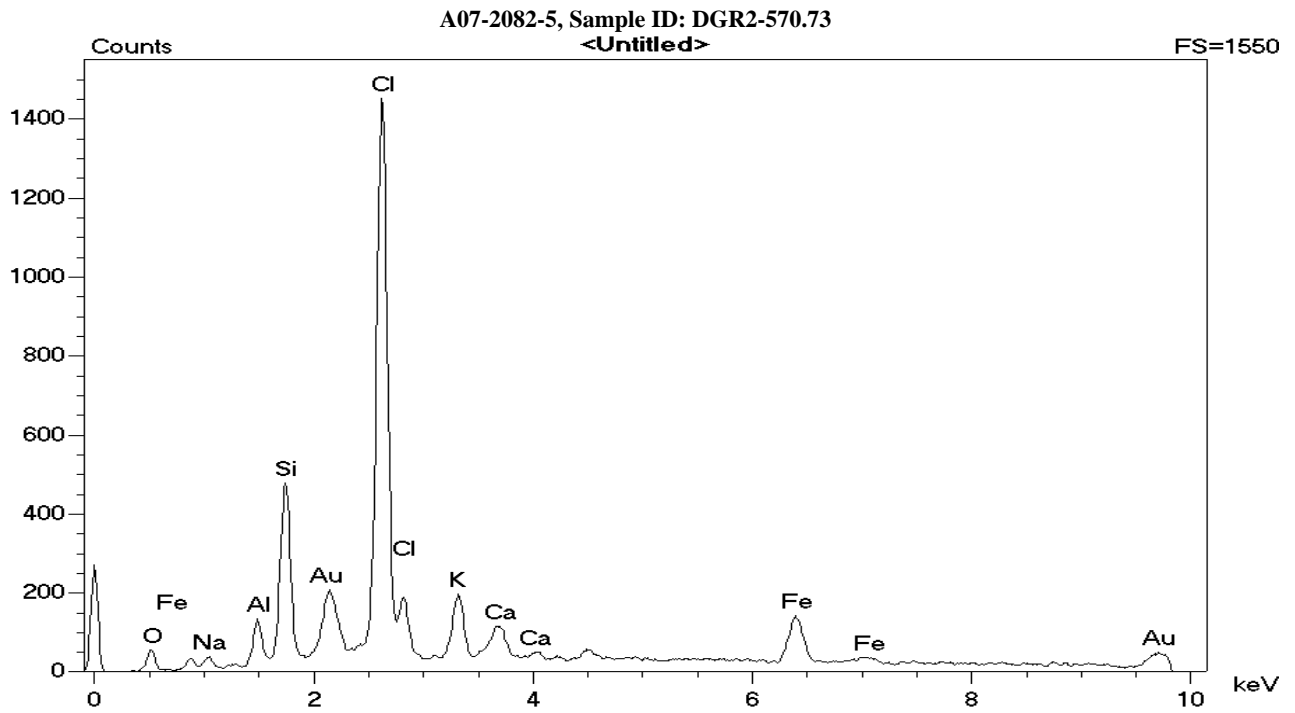


Figure 32, Elemental composition of the high Cl concentration region. Gold originates from sputtered coating.

A07-2082-5, Sample ID: DGR2-570.73

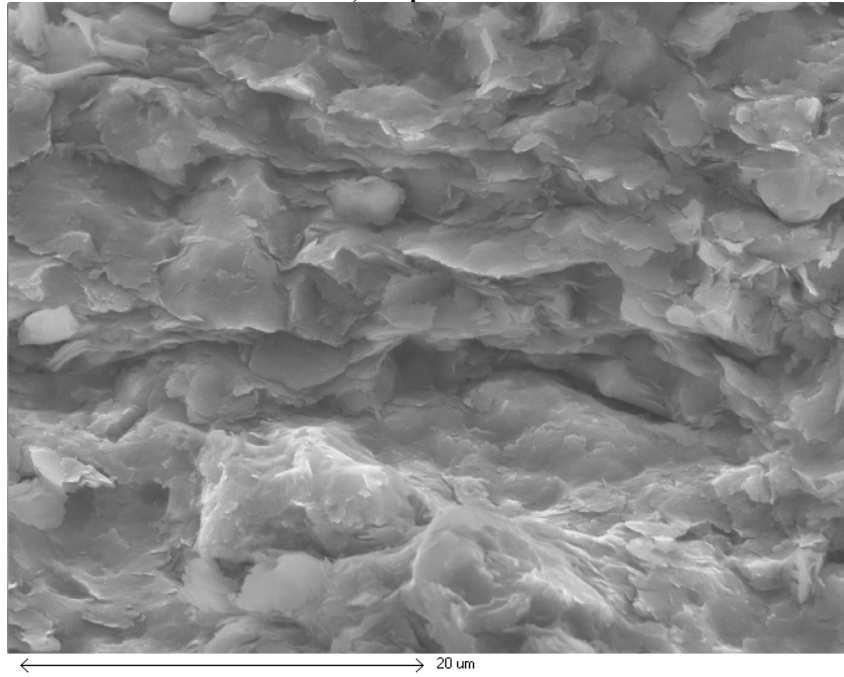


Figure 33, View of general matrix with low Cl concentration, SEMx2720.

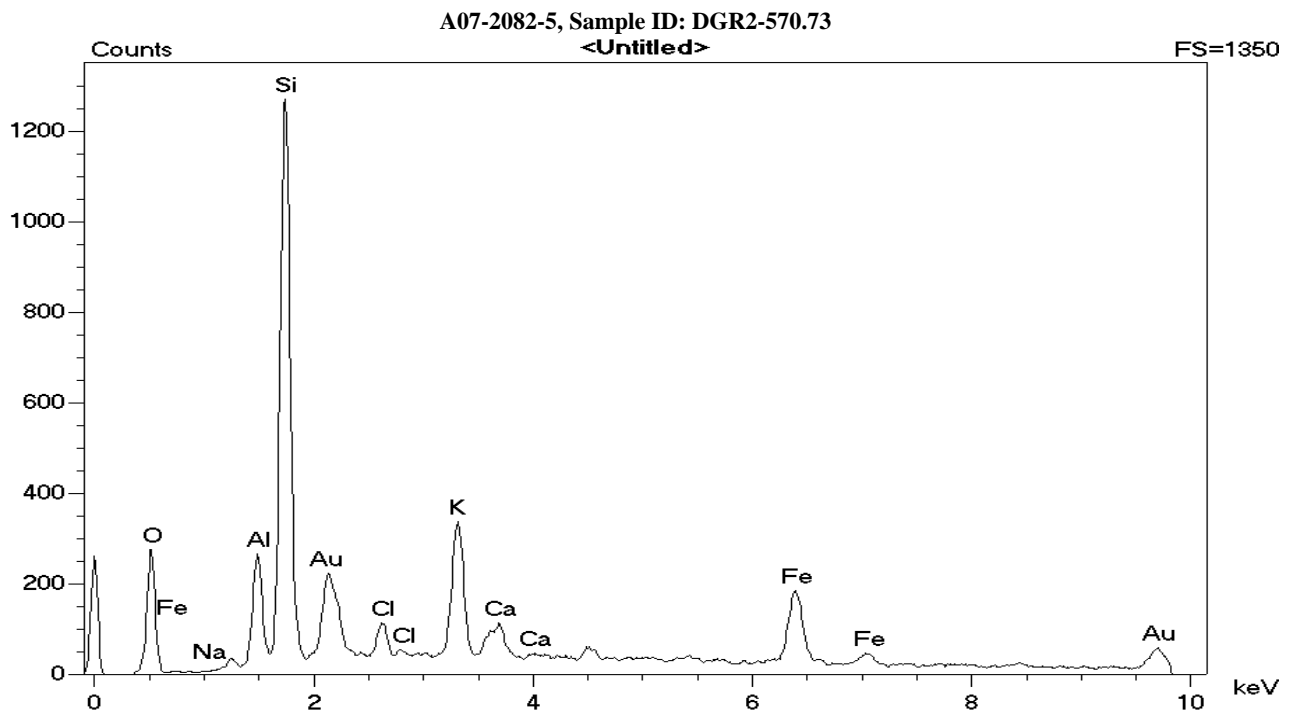


Figure 34, Elemental composition of the matrix. Gold originated from sputtered coating.

A07-2082-5, Sample ID: DGR2-570.73

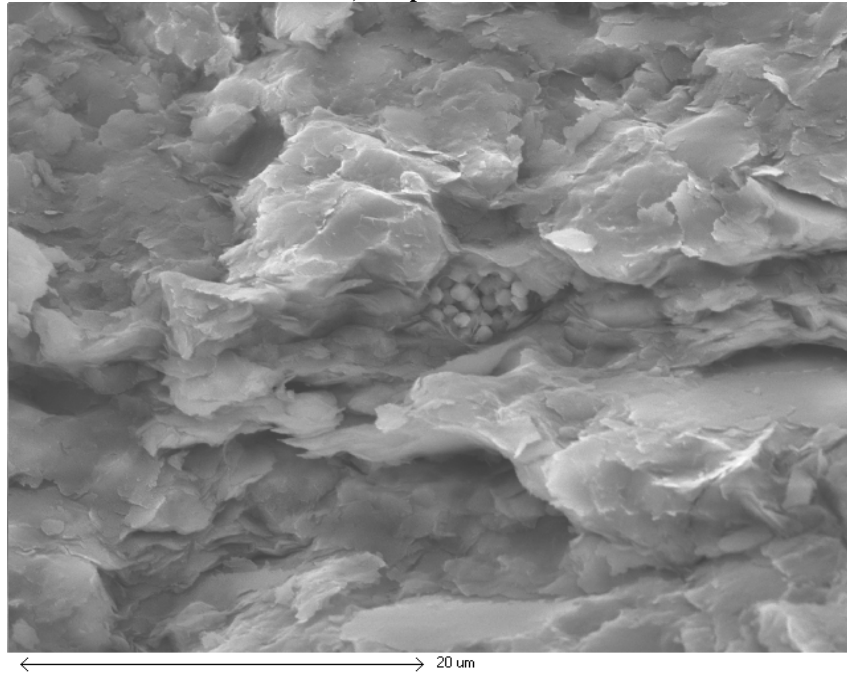


Figure 35, Matrix of the core with a pocket of framboidal FeS, SEMx2720.

Sample DGR2-606.62 (A07-2082-7)

A07-2082-7, Sample ID: DGR2-606.62

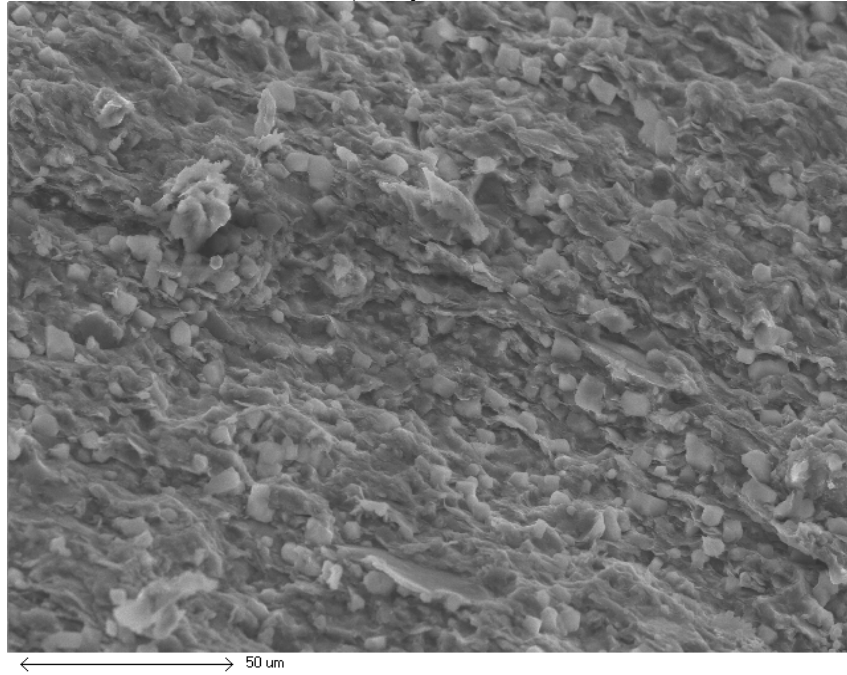


Figure 36, Region of the matrix with high density of cubical particles, see Figures 37, 38 for details. For comparison, see a region with low density of such particles in Figure 53, SEMx573.

A07-2082-7, Sample ID: DGR2-606.62

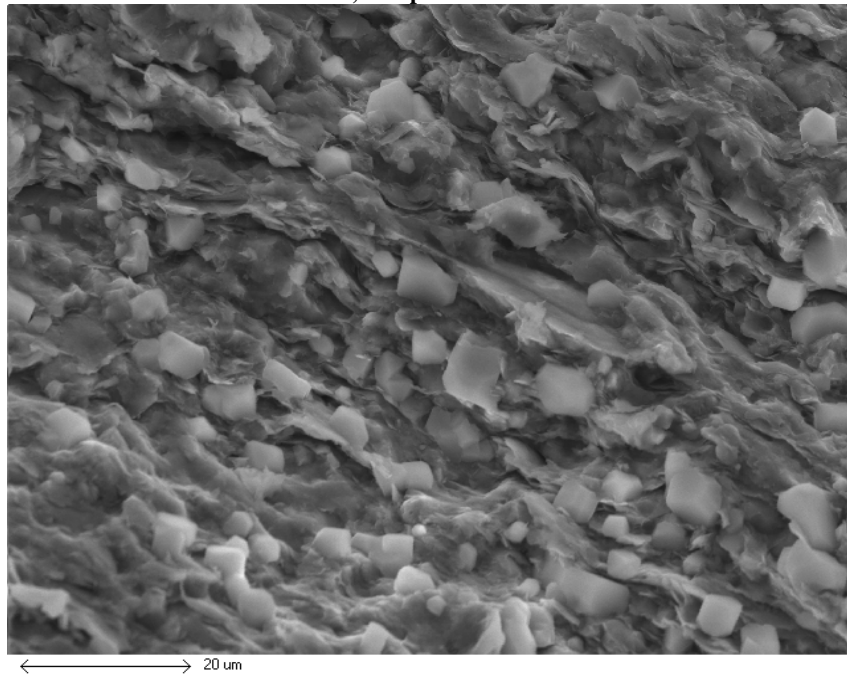


Figure 37, Details of the cubical particles, SEMx1150.

A07-2082-7, Sample ID: DGR2-606.62

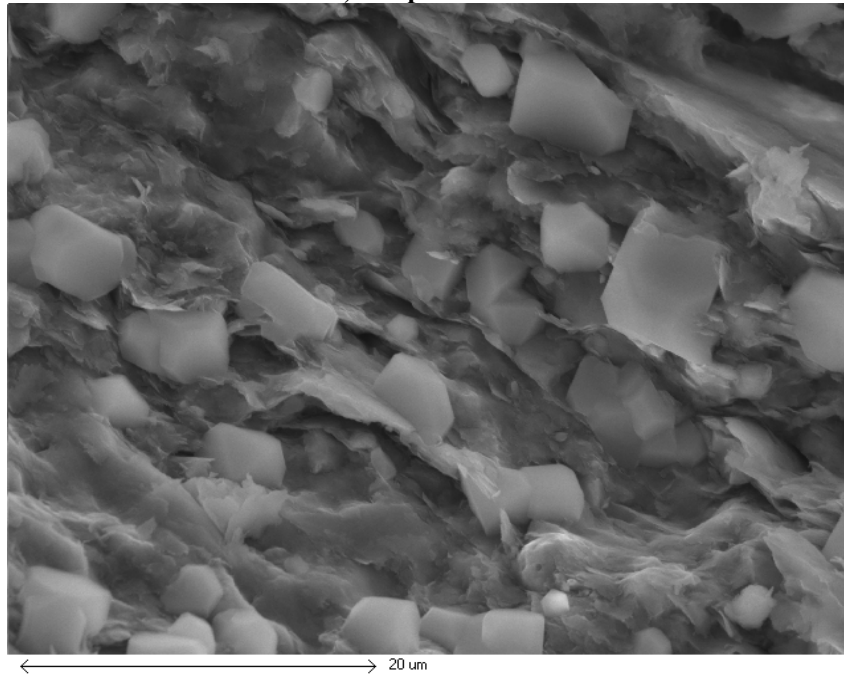


Figure 38, Details of the cubical particles, SEMx2400.

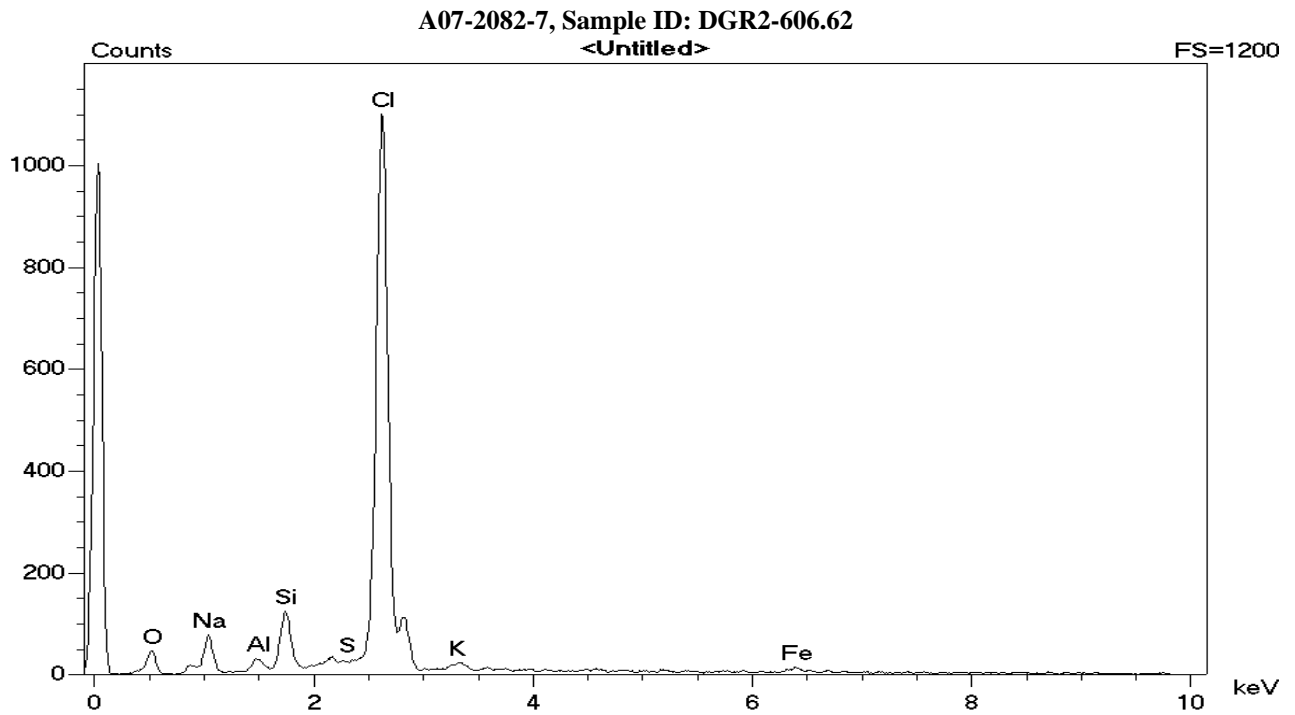


Figure 39, Elemental makeup at a cubical particle indicating high Cl content.

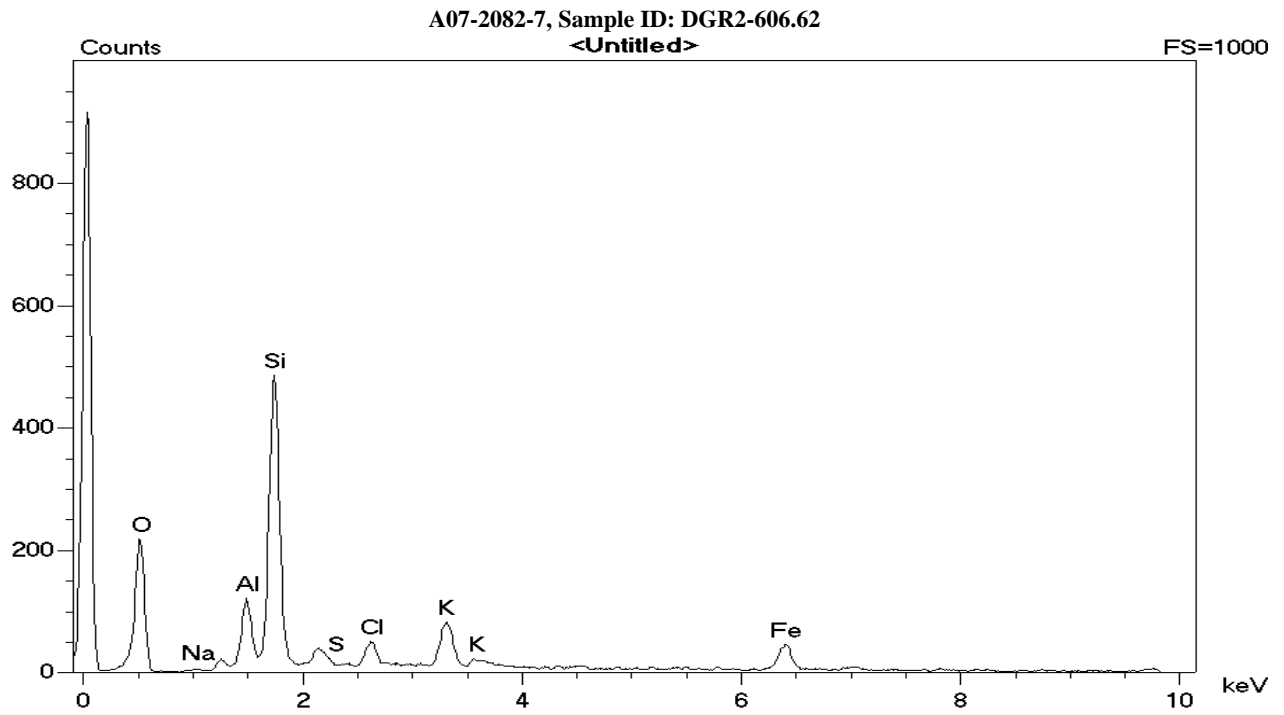


Figure 40, Elemental makeup nearby a cubical particle indicating low Cl and high Si and O content.

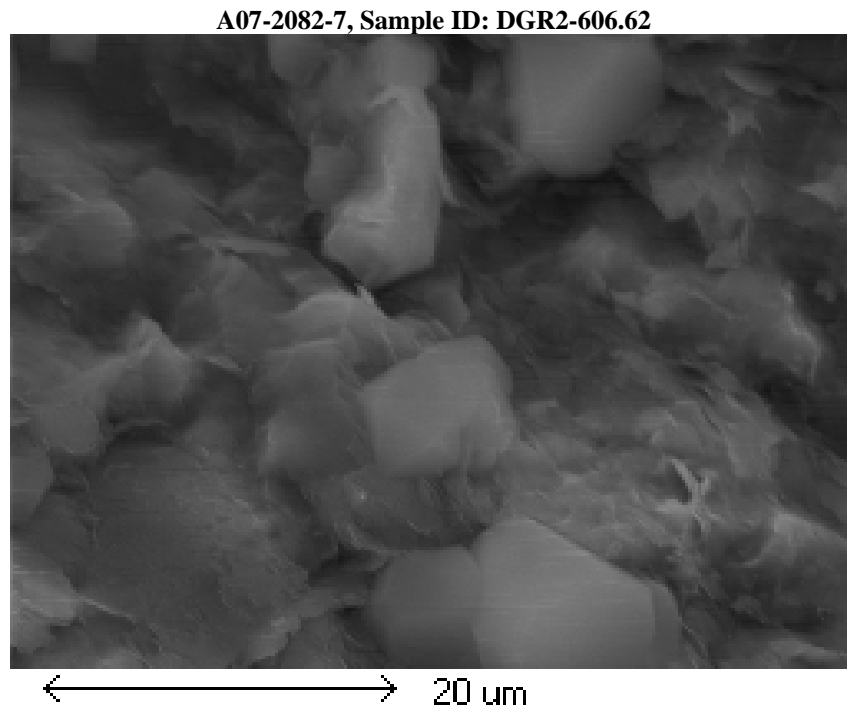


Figure 41, View of cubical particles embedded in the matrix. Elemental maps obtained from this region are shown below, Figures 42 to 45, SEMx4780.

A07-2082-7, Sample ID: DGR2-606.62

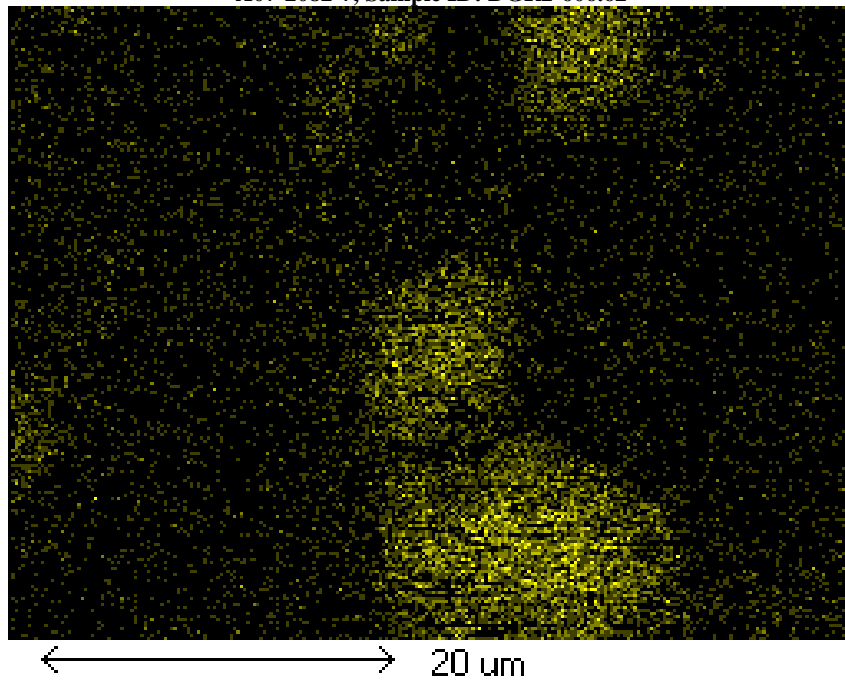


Figure 42, Chlorine map of the region shown in Figure 41.

A07-2082-7, Sample ID: DGR2-606.62

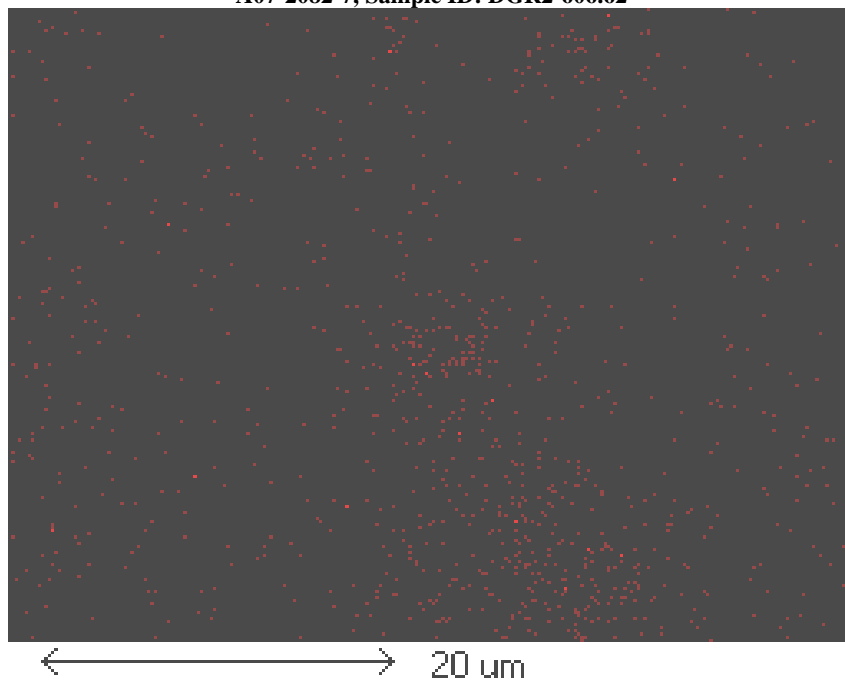


Figure 43, Sodium map of the region shown in Figure 41.

A07-2082-7, Sample ID: DGR2-606.62

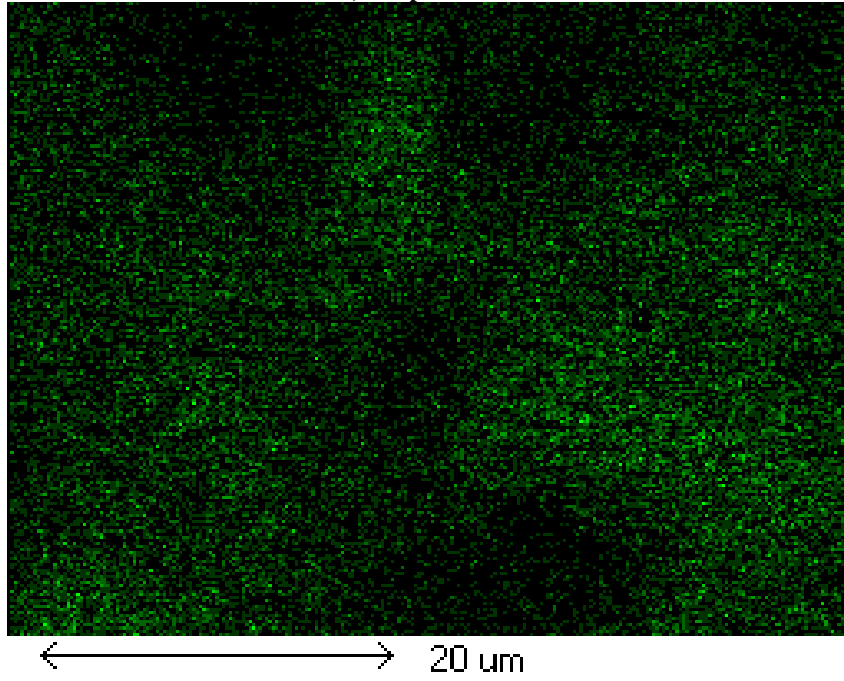


Figure 44, Silicon map of the region shown in Figure 41.

A07-2082-7, Sample ID: DGR2-606.62

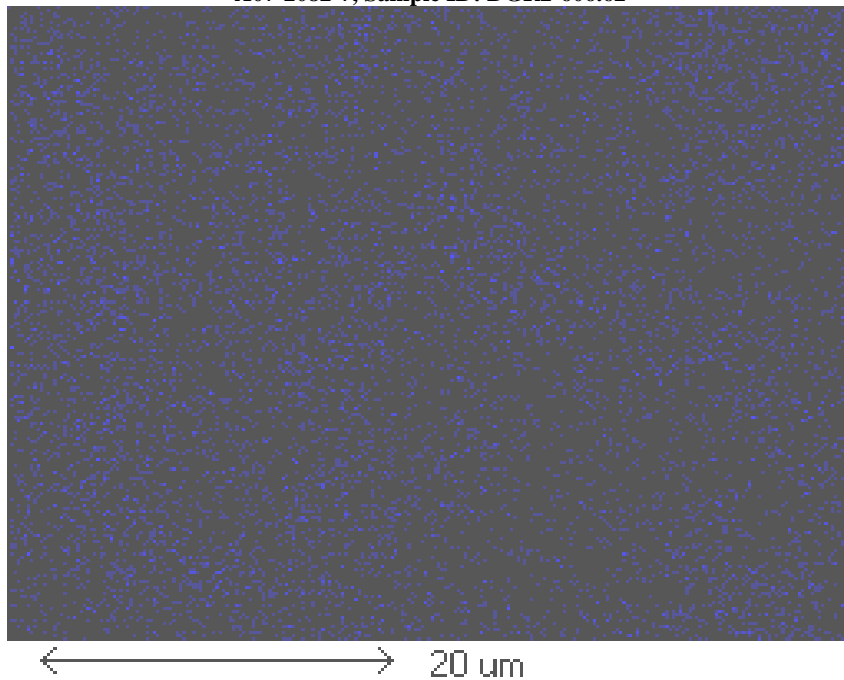


Figure 45, Potassium map of the region shown in Figure 41.

A07-2082-7, Sample ID: DGR2-606.62

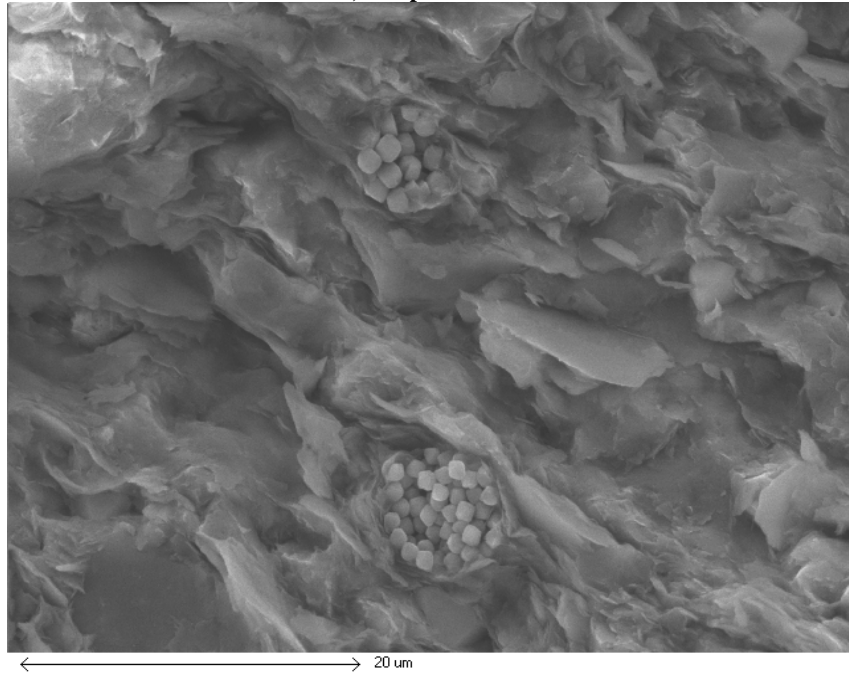


Figure 46, Framboidal FeS particles, SEMx2300.

A07-2082-7, Sample ID: DGR2-606.62

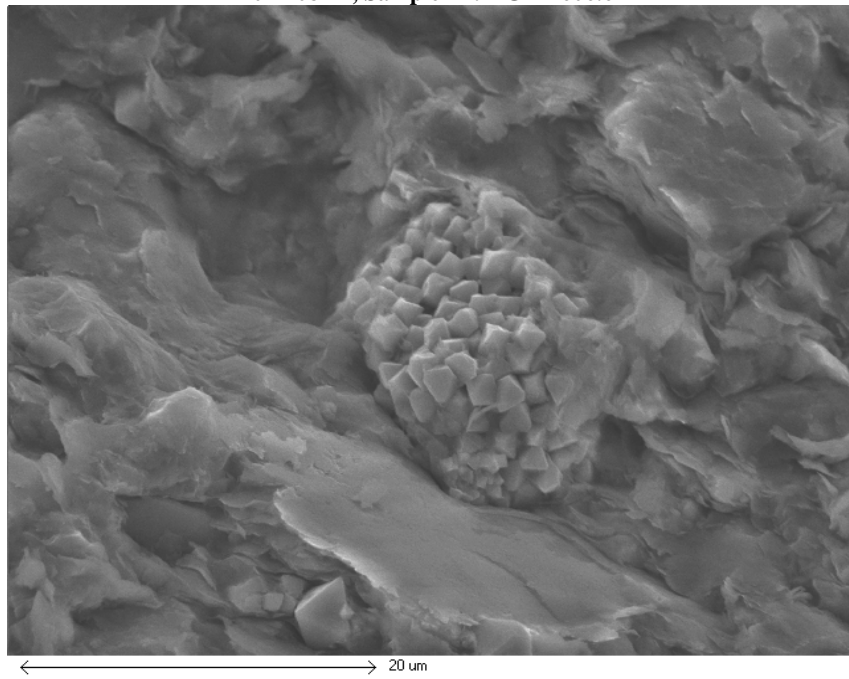


Figure 46, Framboidal FeS particles, SEMx2400.

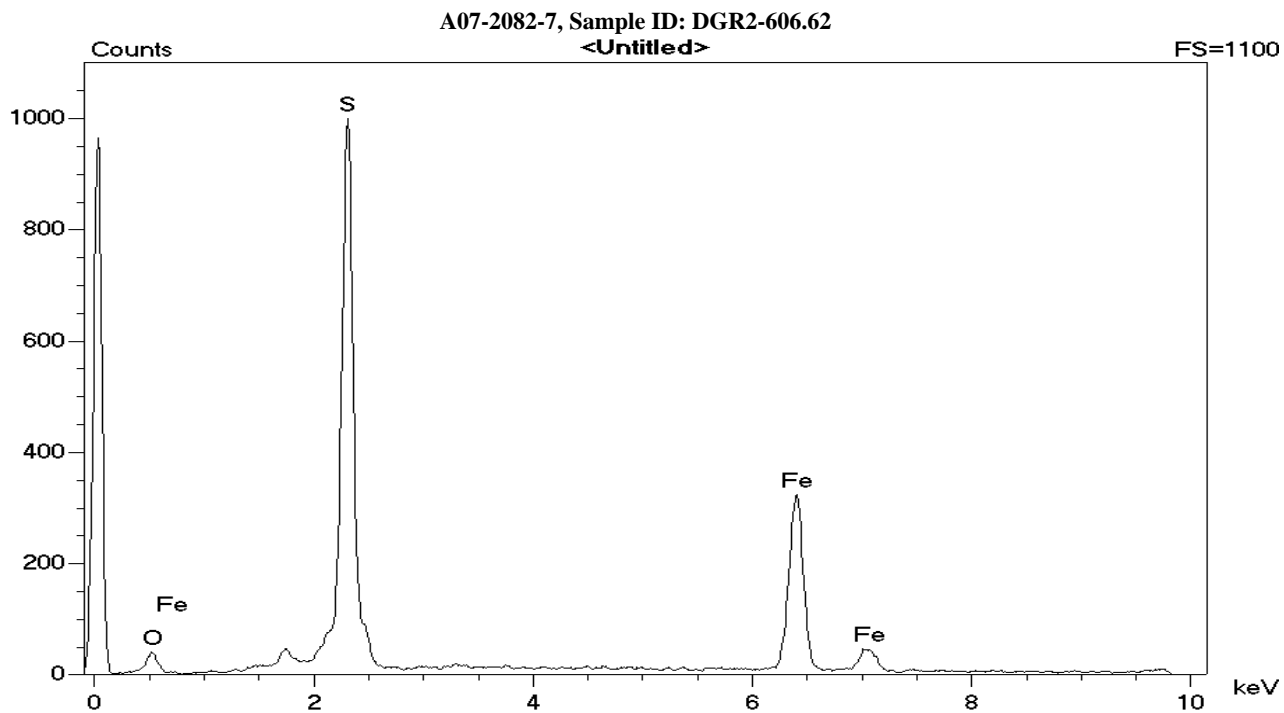


Figure 47, Elemental composition of the framboidal particles.

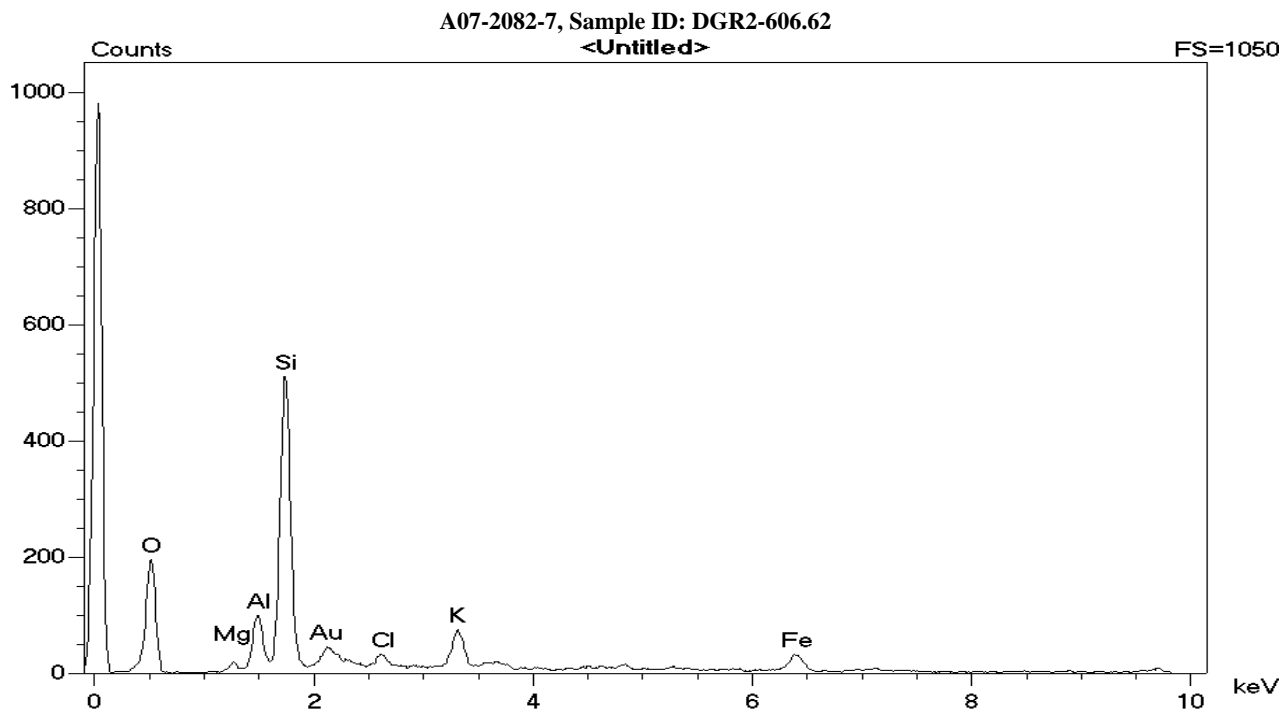


Figure 48, Elemental composition of the matrix around the framboidal FeS.

A07-2082-7, Sample ID: DGR2-606.62

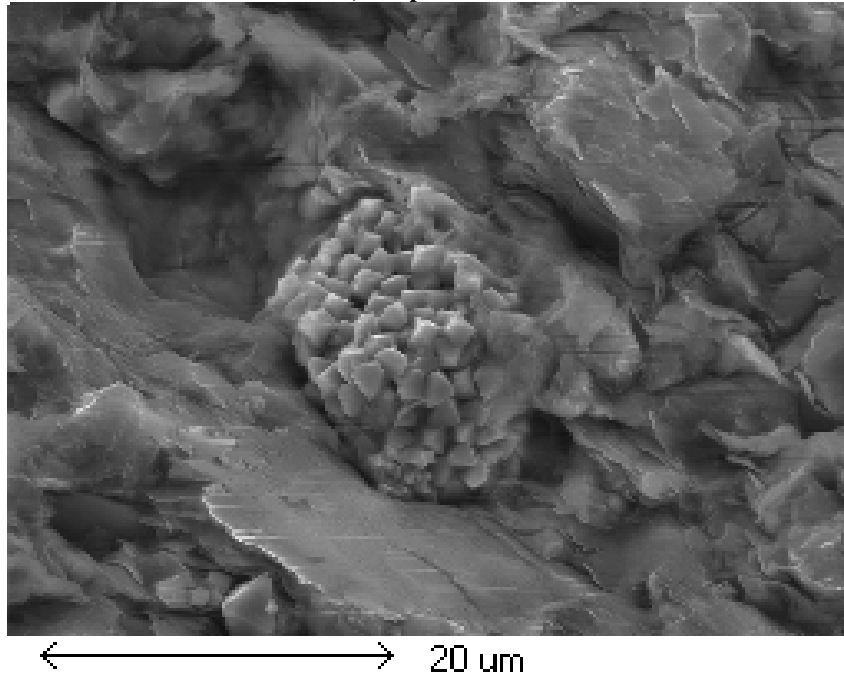


Figure 49, View of the framboidal particles embedded in the matrix. Elemental maps obtained from this region are shown below, Figures 50 to 54, SEMx2400.

A07-2082-7, Sample ID: DGR2-606.62

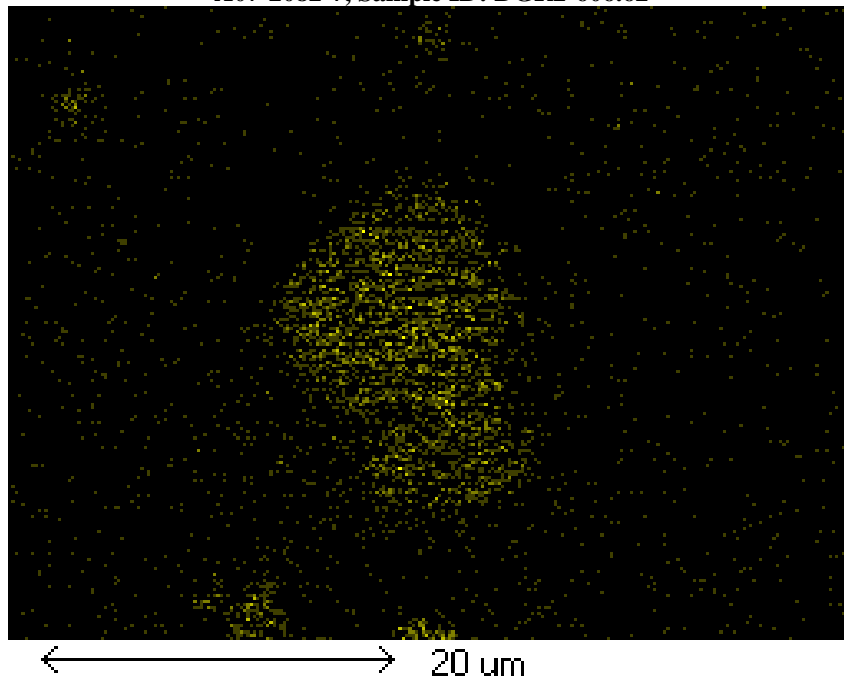


Figure 50, Sulphur map of the region shown in Figure 49.

A07-2082-7, Sample ID: DGR2-606.62

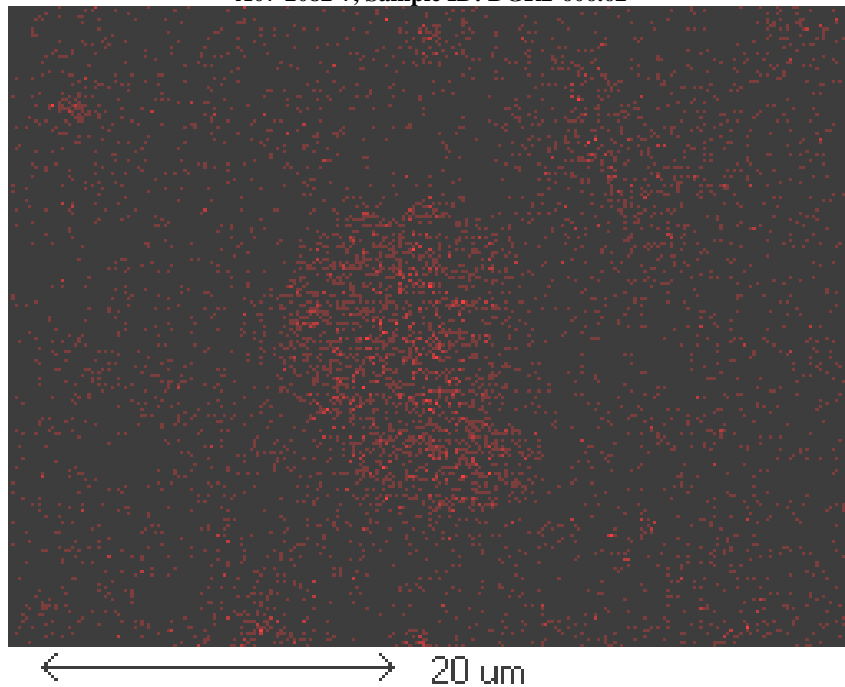


Figure 51, Iron map of the region shown in Figure 49.

A07-2082-7, Sample ID: DGR2-606.62

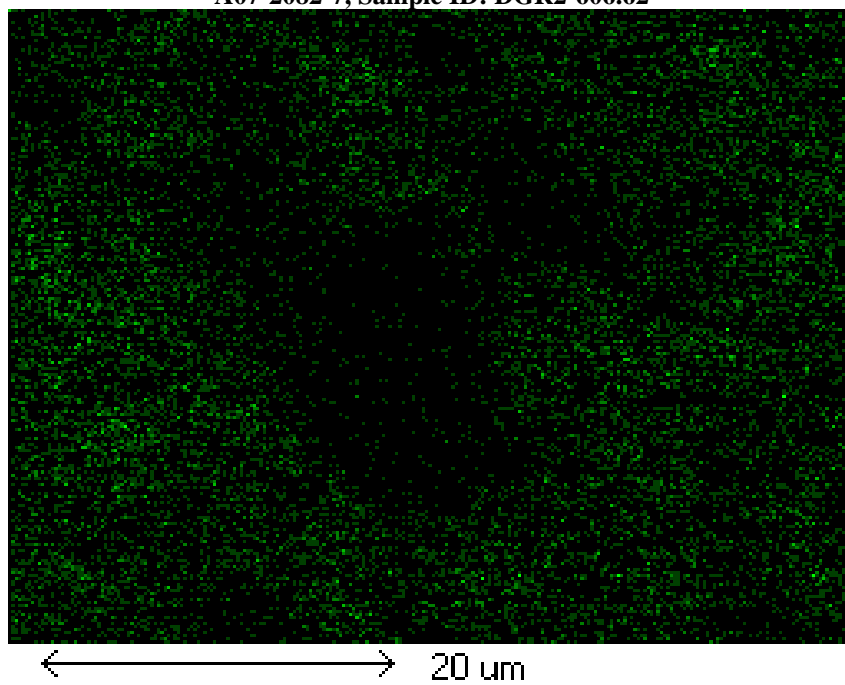


Figure 52, Silicon map of the region shown in Figure 49.

A07-2082-7, Sample ID: DGR2-606.62

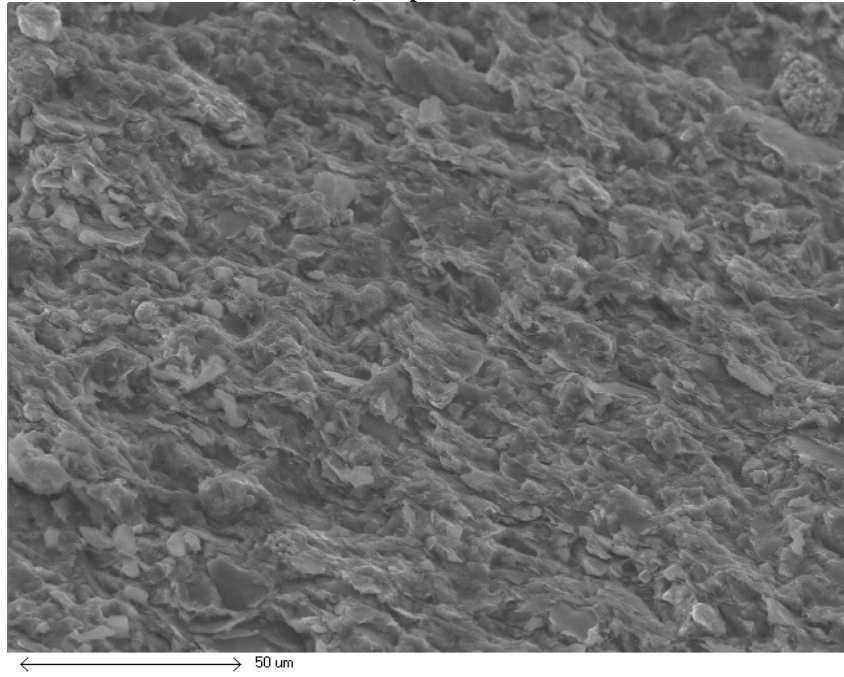


Figure 53, Region with low density of cubical particles, SEMx600

Sample DGR2-606.96 (A07-2082-8)

A07-2082-8, Sample ID: DGR2-606.96

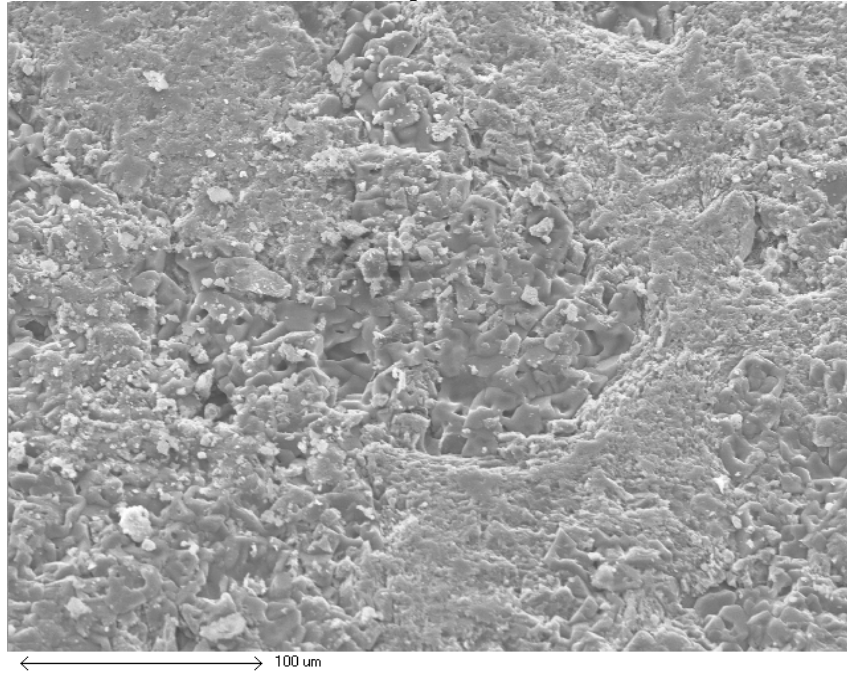


Figure 54, General view of the polished sample, high Cl concentration region is located at the centre and the surrounding matrix has low Cl concentration, SEMx326

A07-2082-8, Sample ID: DGR2-606.96

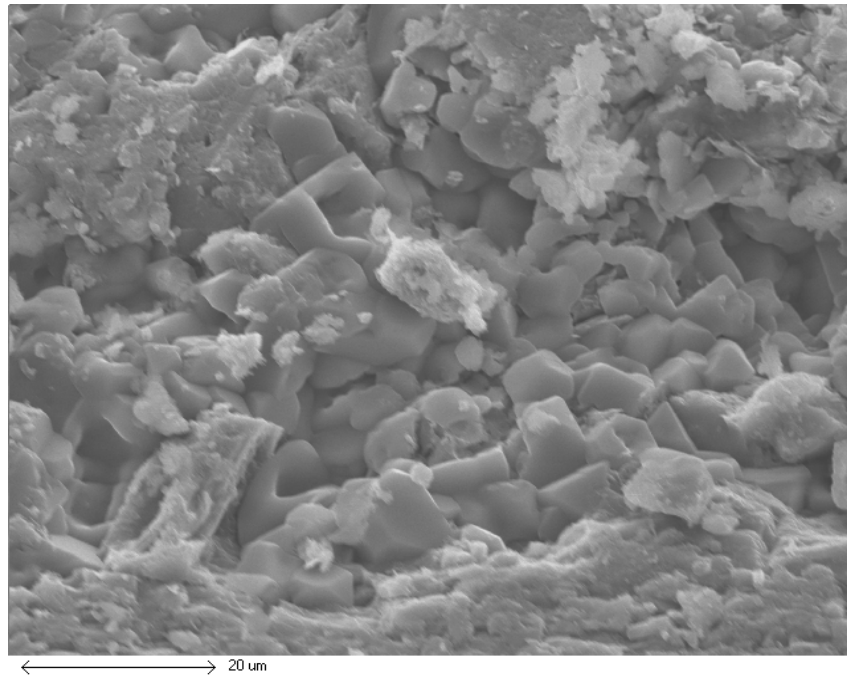


Figure 55, Detail of the high Cl region at the center of Figure 54, SEMx1310.

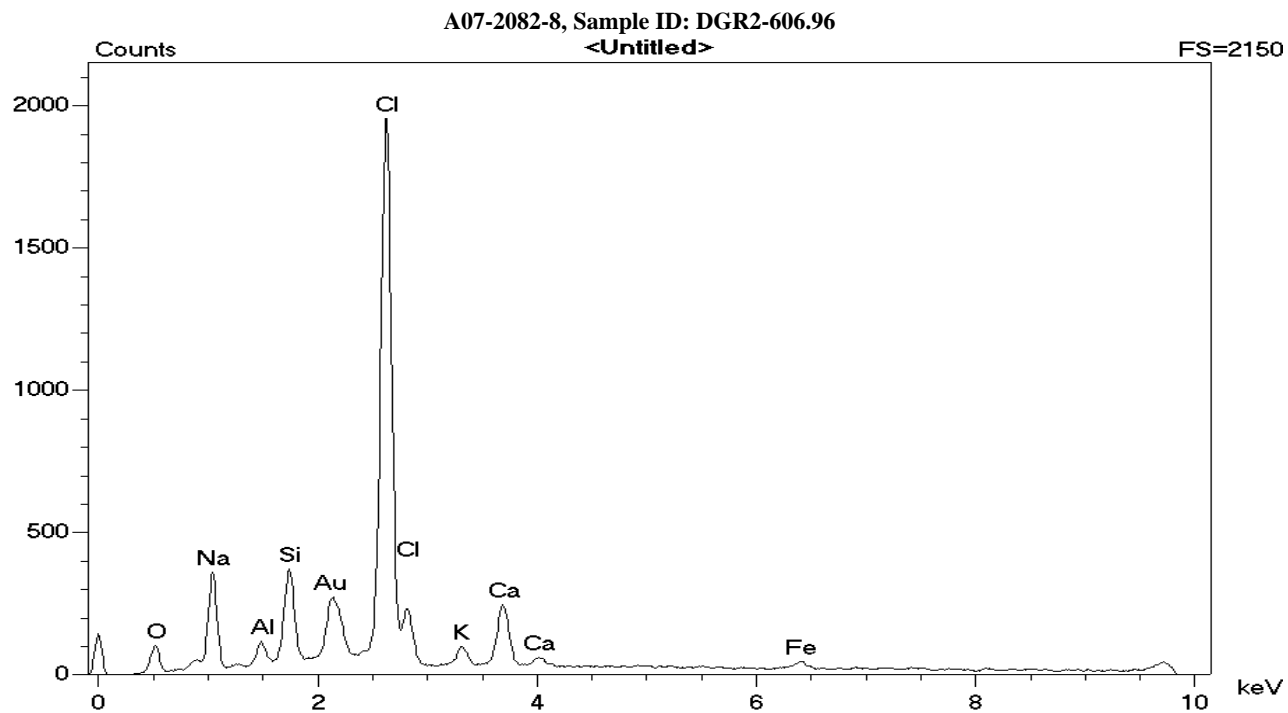


Figure 56, Elemental composition of the center region of Figure 54 and 55. Gold originated from sputtered coating.

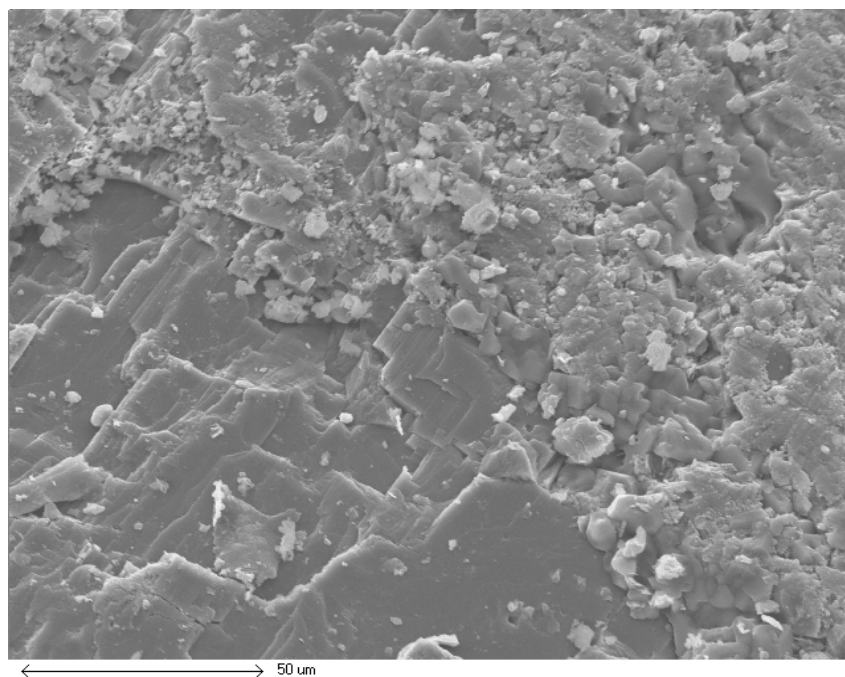


Figure 57, High S concentration region, SEMx655.

A07-2082-8, Sample ID: DGR2-606.96

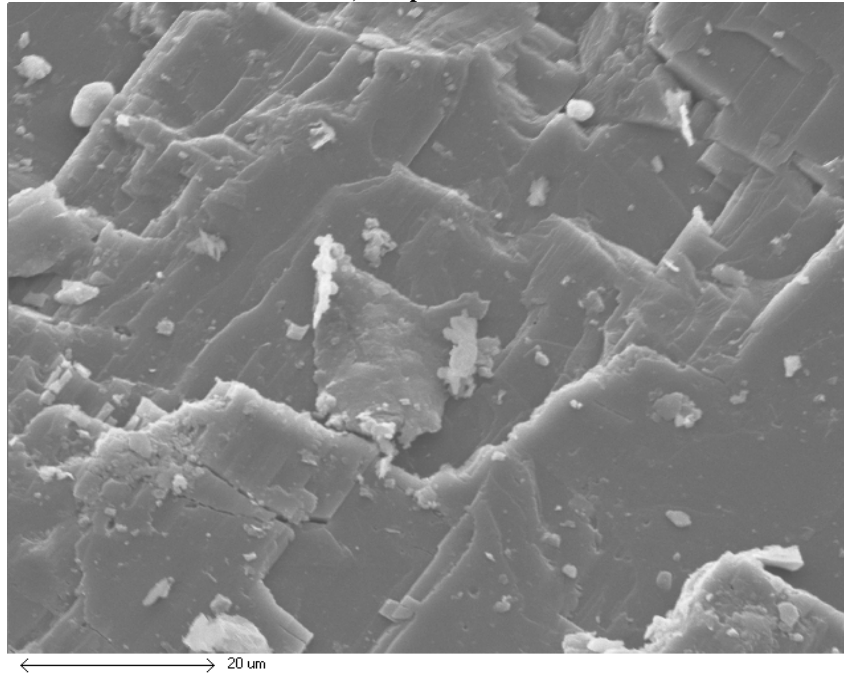


Figure 58, Detail of Figure 57, SEMx1310.

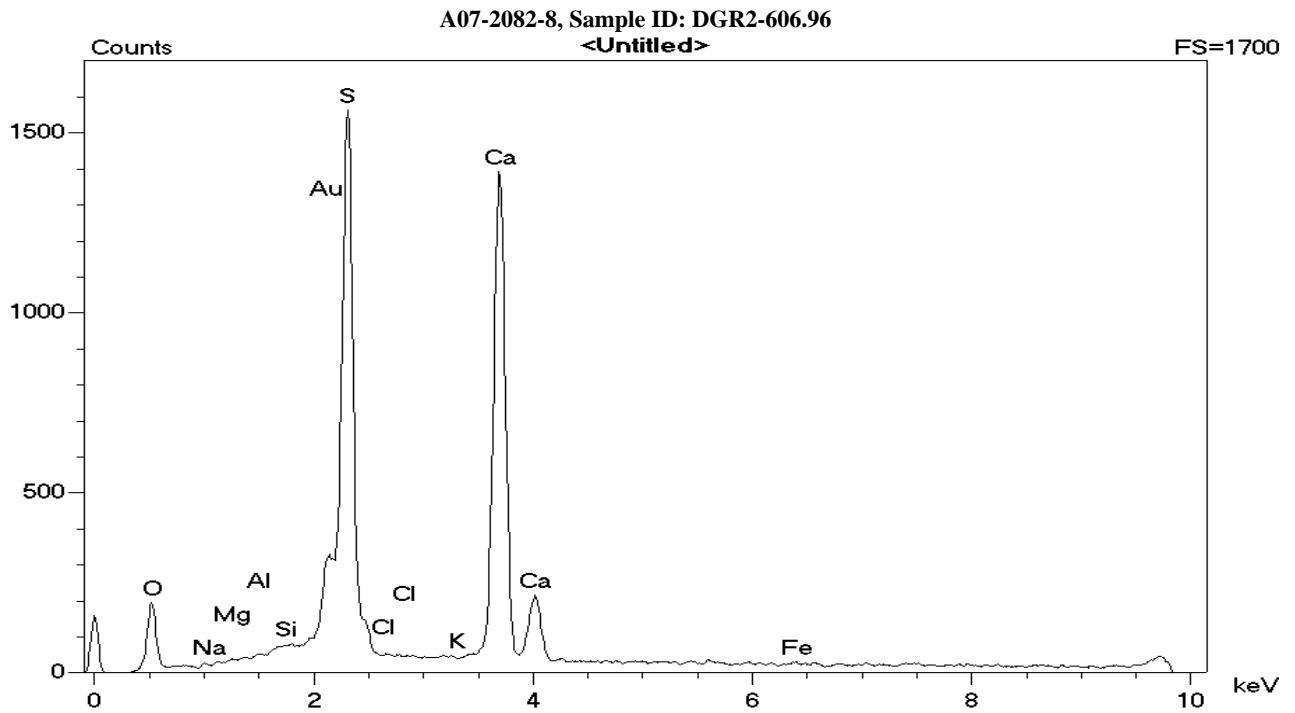


Figure 59, Elemental composition of the region shown in Figure 58. Gold originated from sputtered coating.

A07-2082-8, Sample ID: DGR2-606.96

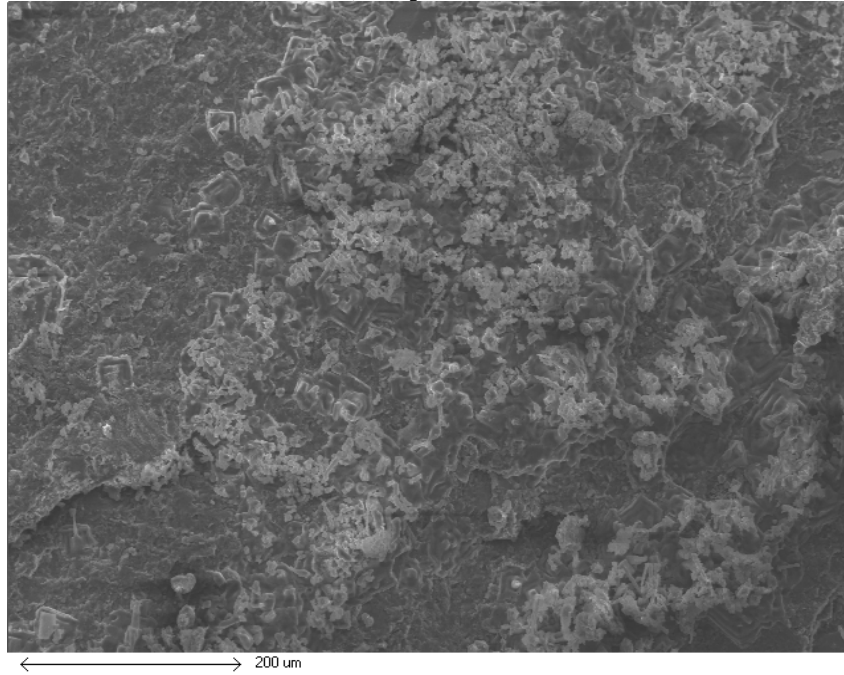


Figure 60, General view of a high Cl concentration region and the surrounding matrix, SEMx150.

A07-2082-8, Sample ID: DGR2-606.96

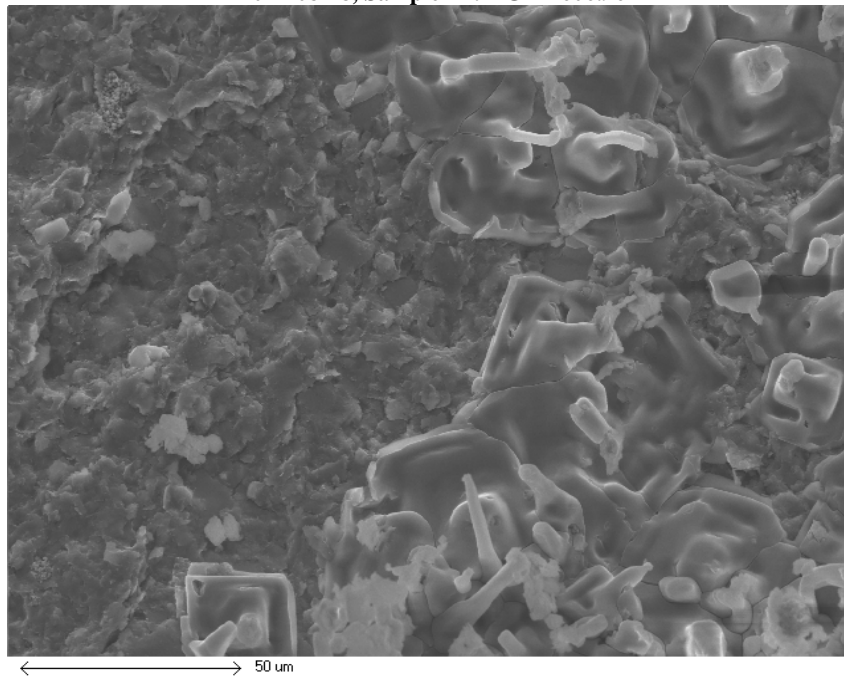


Figure 61, Details of the high Cl concentration region at right and the matrix at left, SEMx600.

A07-2082-8, Sample ID: DGR2-606.96

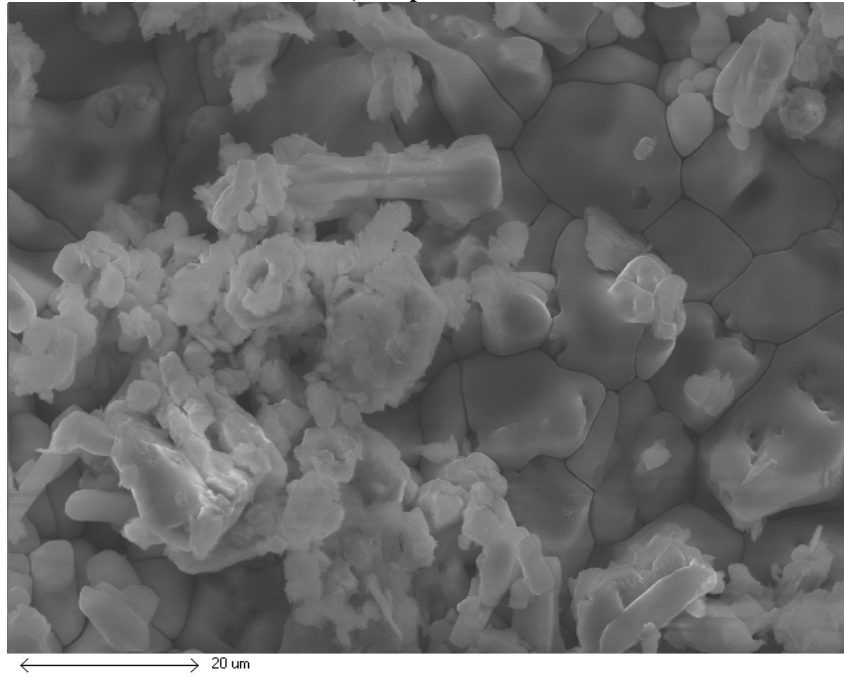


Figure 62, Detail of the high Cl concentration region, SEMx1200.

A07-2082-8, Sample ID: DGR2-606.96

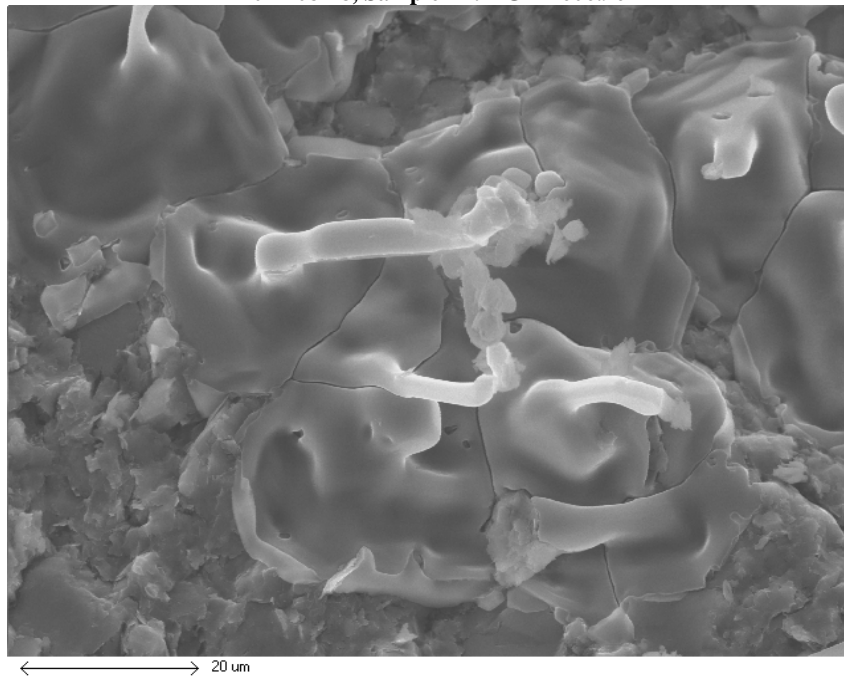


Figure 63, Detail of the high Cl concentration region, SEMx1200.

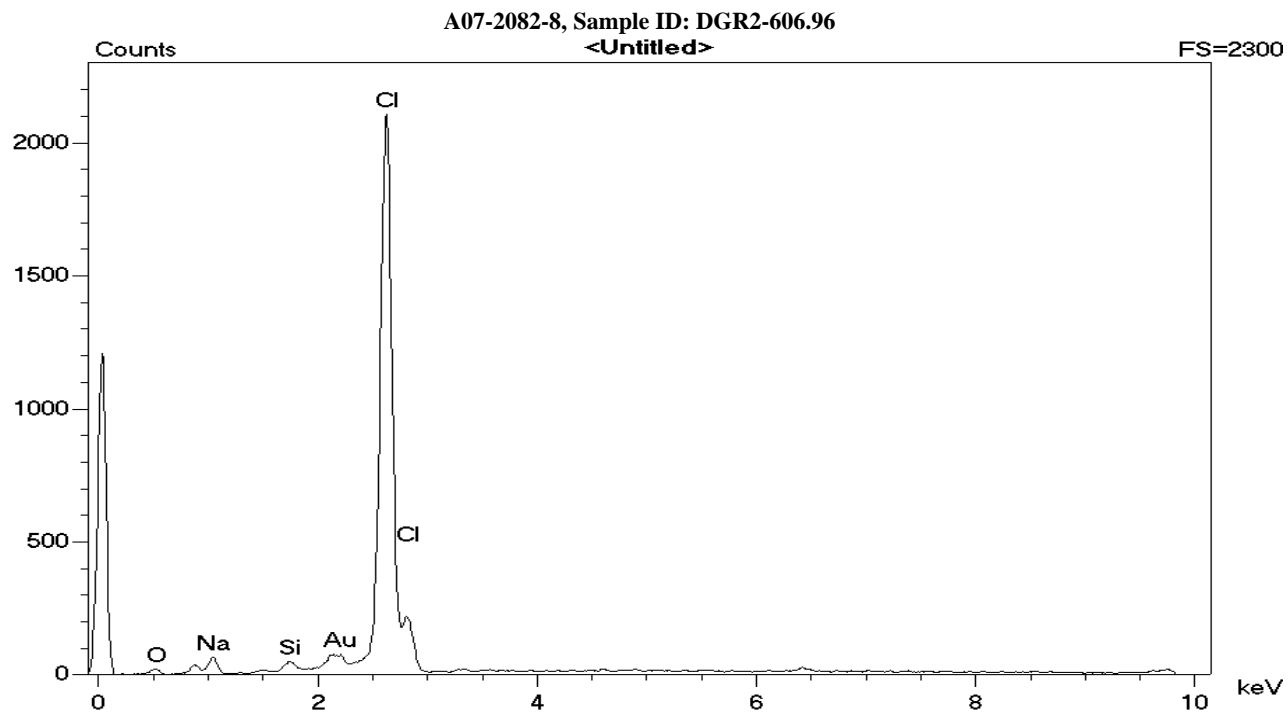


Figure 64, Elemental composition of the region shown in Figure 63. Gold originated from sputtered coating.

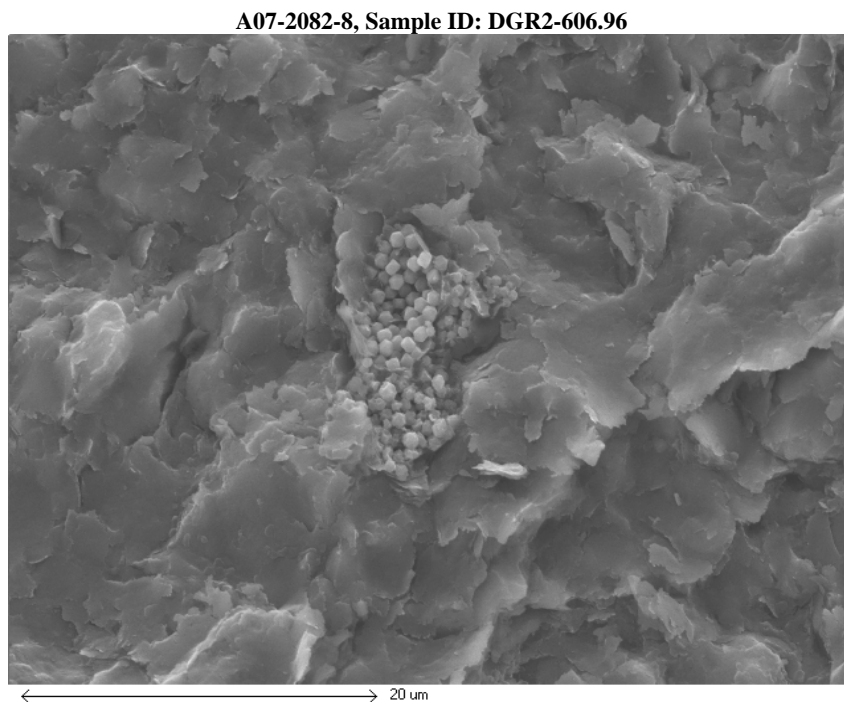


Figure 65, Framboidal FeS particles embedded in the matrix, SEMx2400.

A07-2082-8, Sample ID: DGR2-606.96

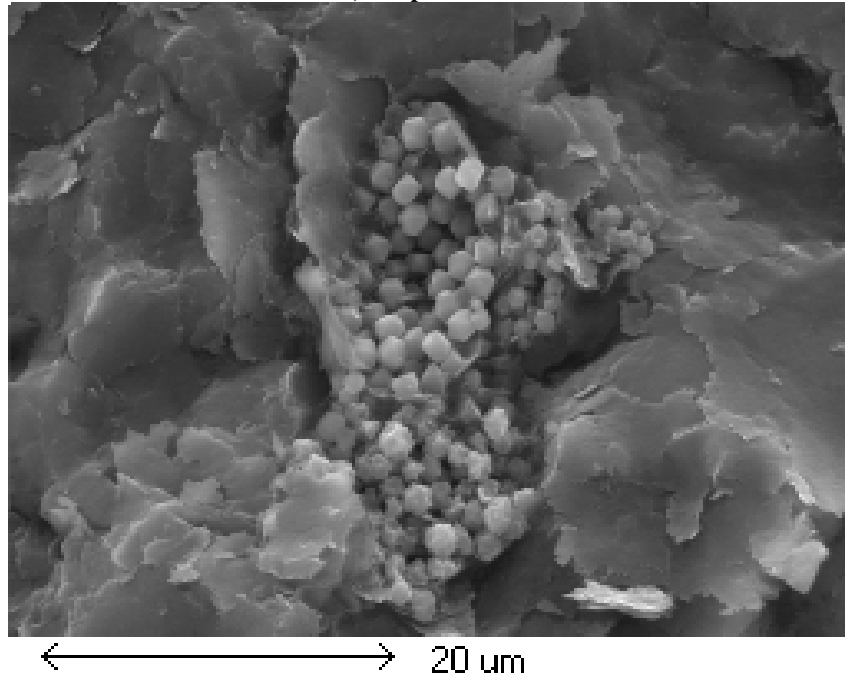


Figure 66, Details of the framboidal particles, SEMx4780.

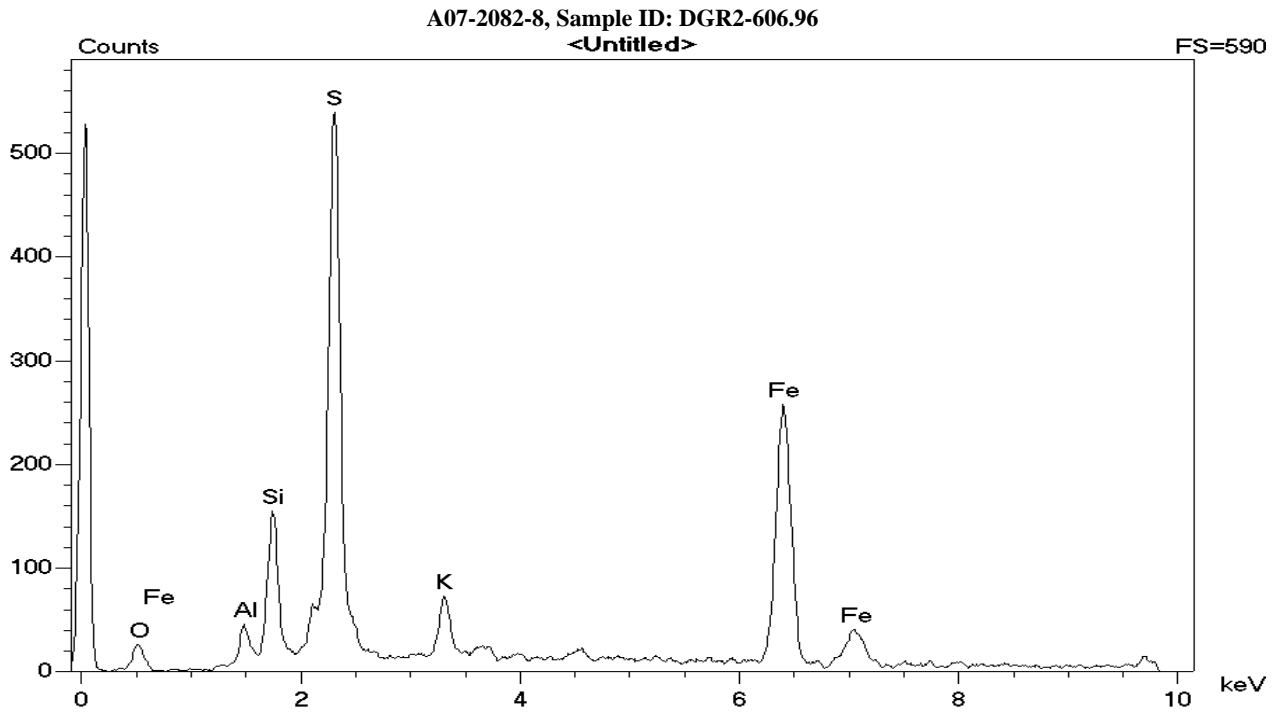


Figure 67, Elemental composition of the framboidal FeS particles. Gold originated from sputtered coating.

Sample DGR2-644.49 (A07-2082-10)

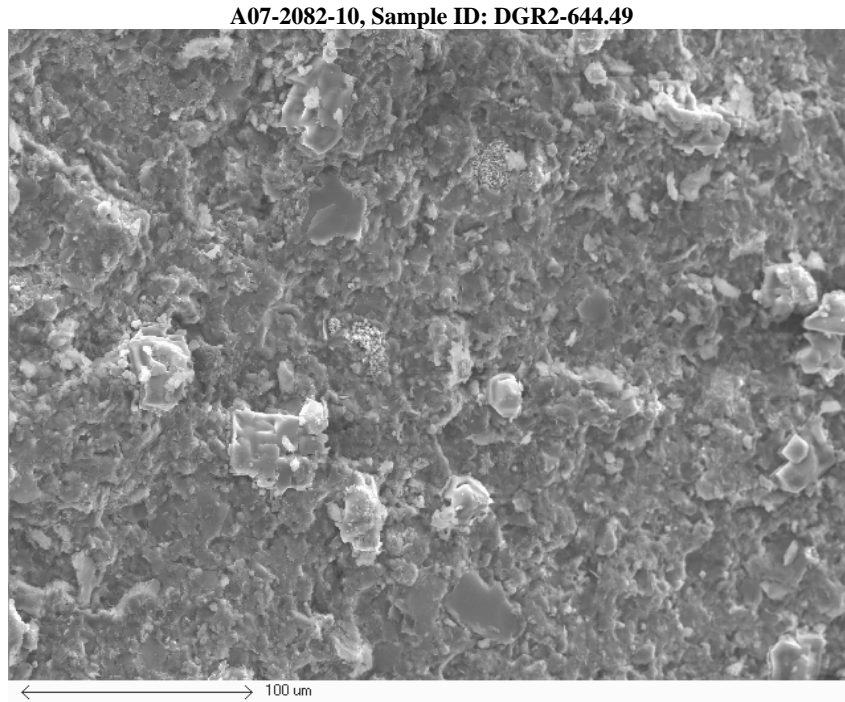


Figure 68, General view of the matrix with embedded high Cl concentration blocks and particles and with FeS particles, SEMx312.

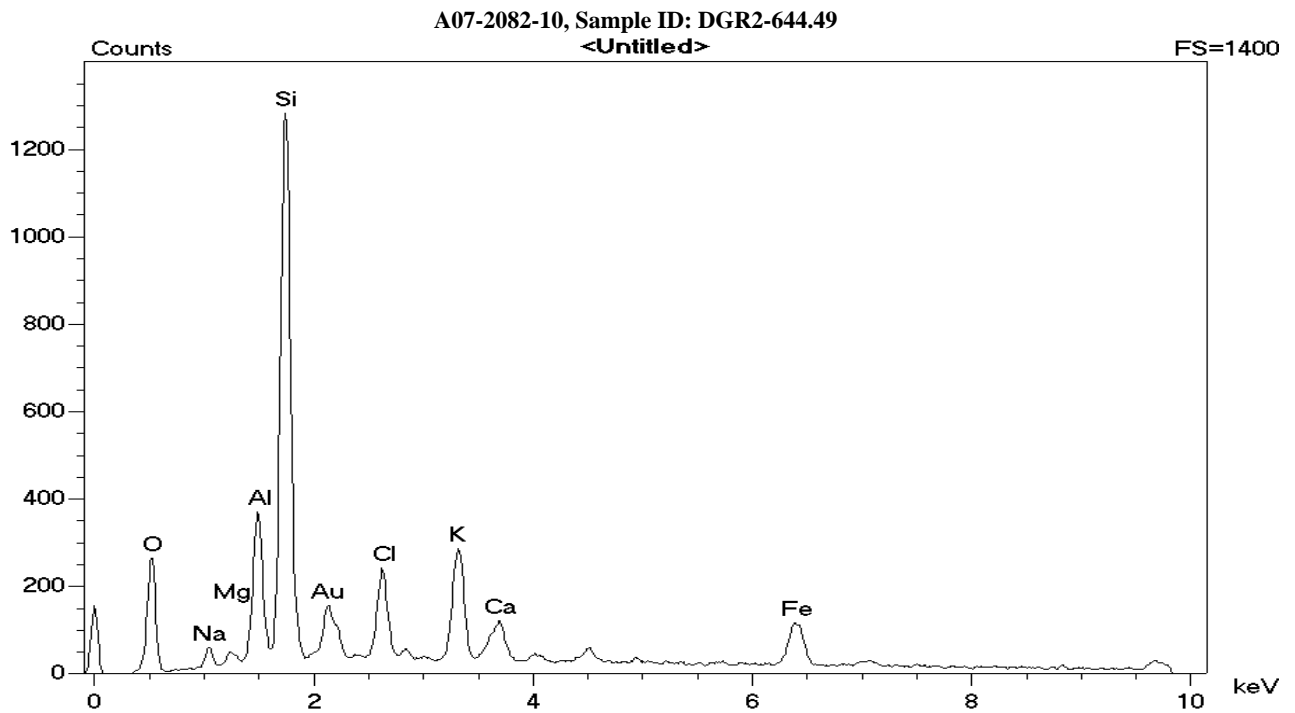


Figure 69, Elemental composition of the matrix from the region shown in Figure 68.

A07-2082-10, Sample ID: DGR2-644.49

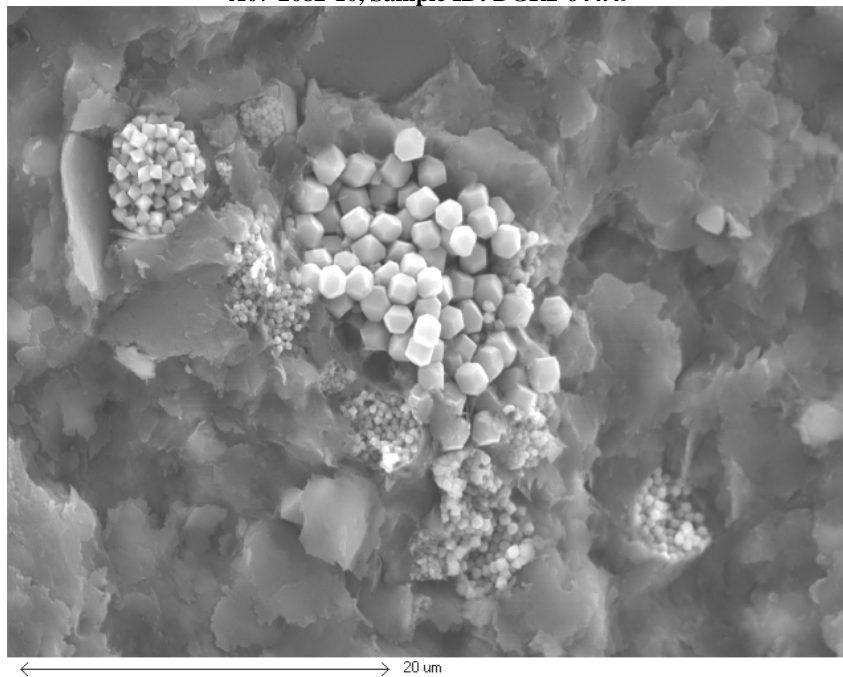


Figure 70, Details of the framboidal FeS particles embedded in the matrix, SEMx2500.

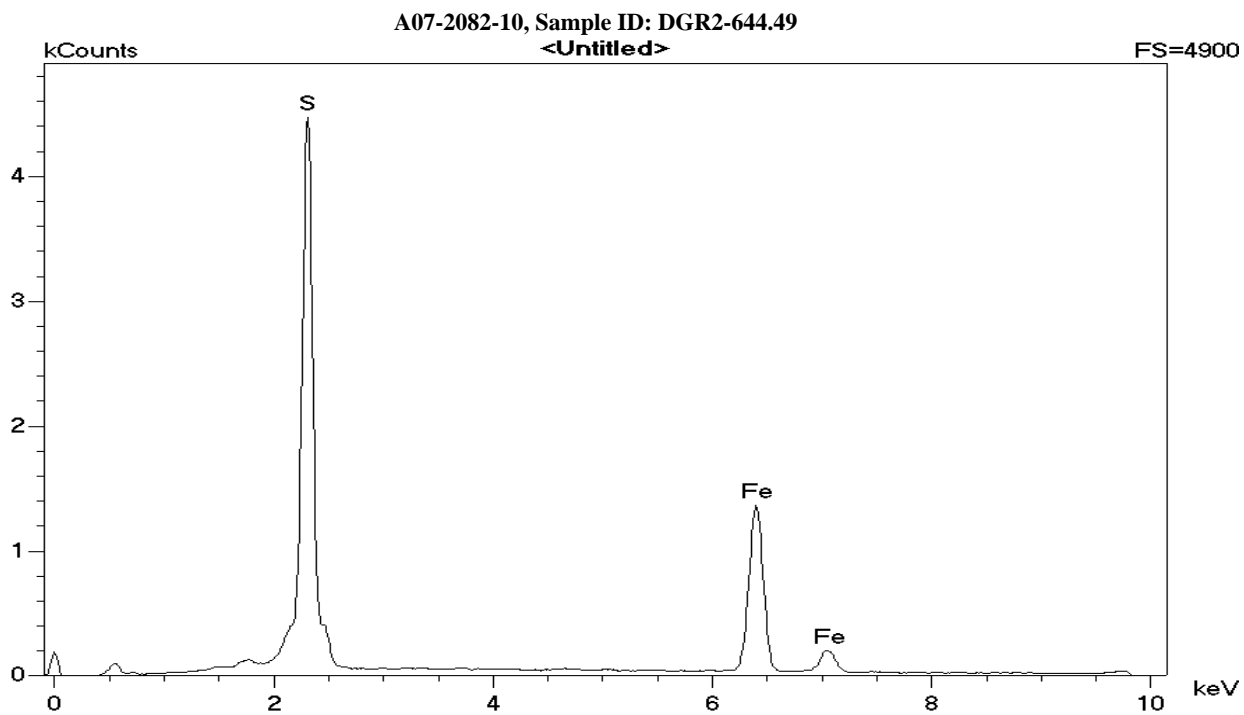


Figure 71, Elemental composition of the particles shown in Figure 70. Gold originated from sputtered coating.

A07-2082-10, Sample ID: DGR2-644.49

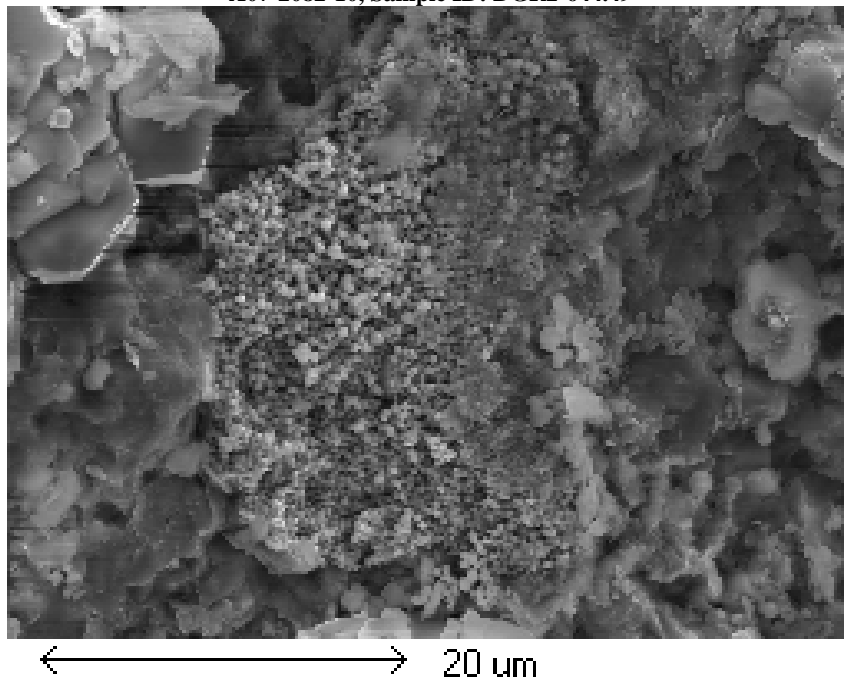


Figure 72, View of FeS particles at the center area of the micrograph, SEMx2082

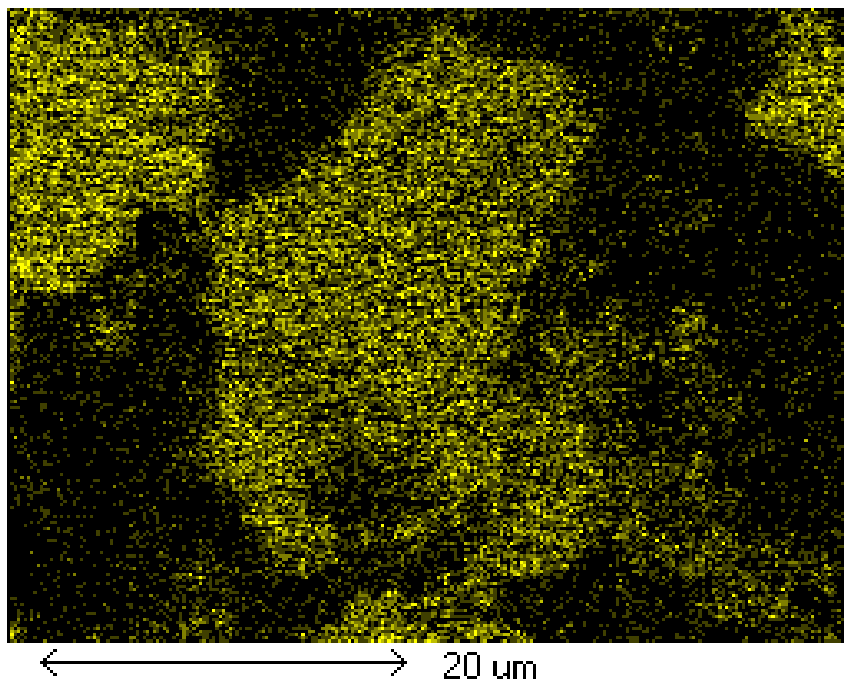


Figure 73, Iron map from the region shown in Figure 72. There are two regions of high Iron content, located at the right and left upper corners of the Figure, that do not have the framboidal morphology of the central particles.

A07-2082-10, Sample ID: DGR2-644.49

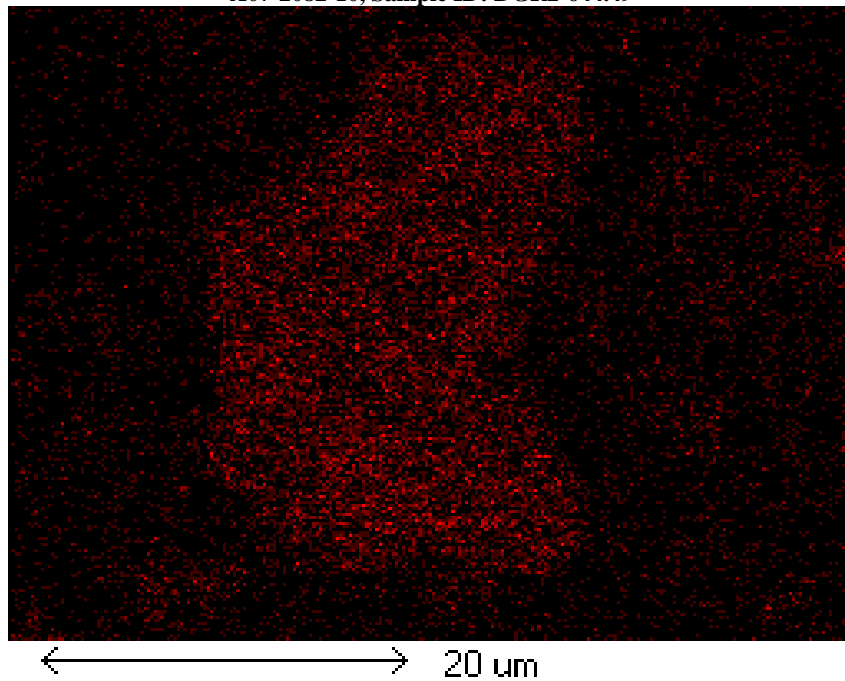


Figure 74, Sulphur map from the region shown in Figure 72. The two regions of high Iron content, located at the right and left upper corners of the Figure 73 do not show any substantial amount of sulphur concentration.

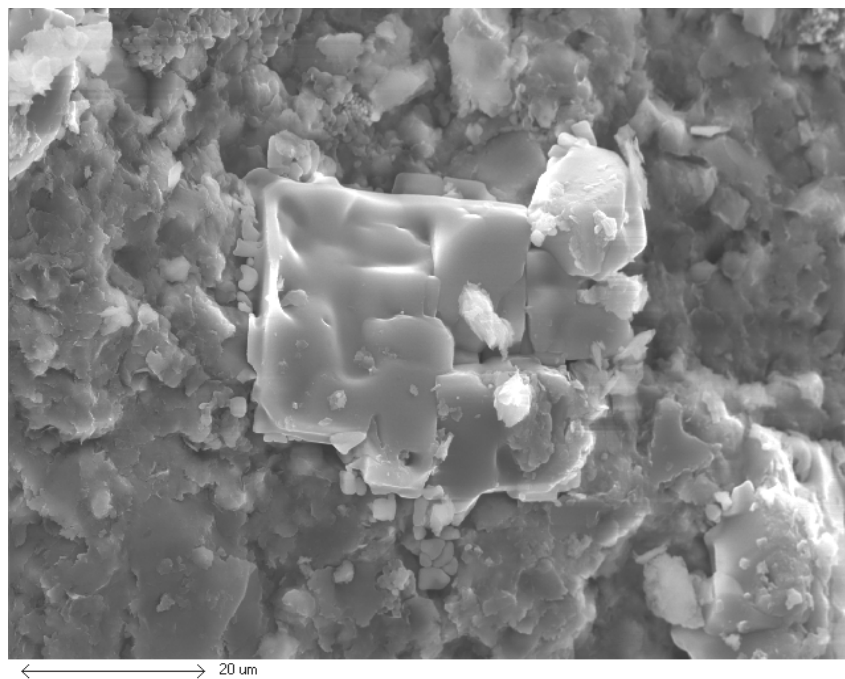


Figure 75, High Cl concentration particle, SEMx2082.

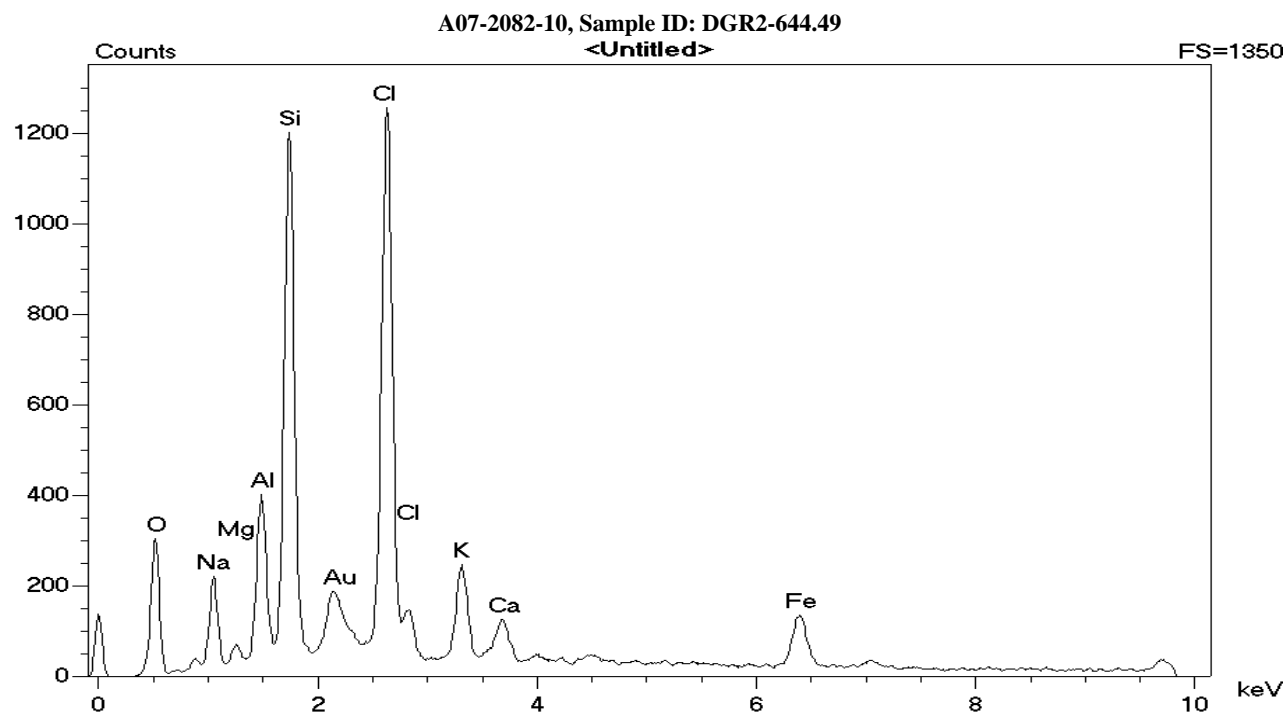


Figure 76, Elemental composition of particle shown in Figure 75. Gold originated from sputtered coating.

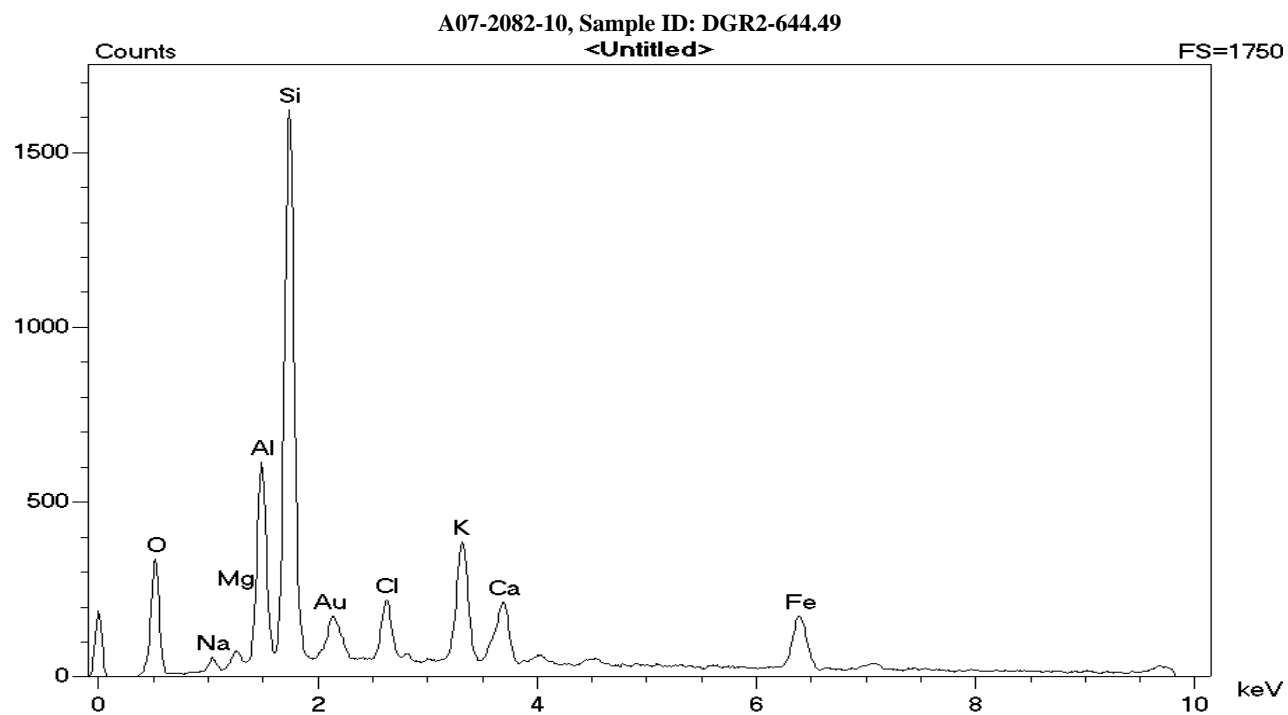


Figure 77, Elemental composition of matrix surrounding the particle shown in Figure 75. Gold originated from sputtered coating

A07-2338-2, Sample ID: DGR2-659.31

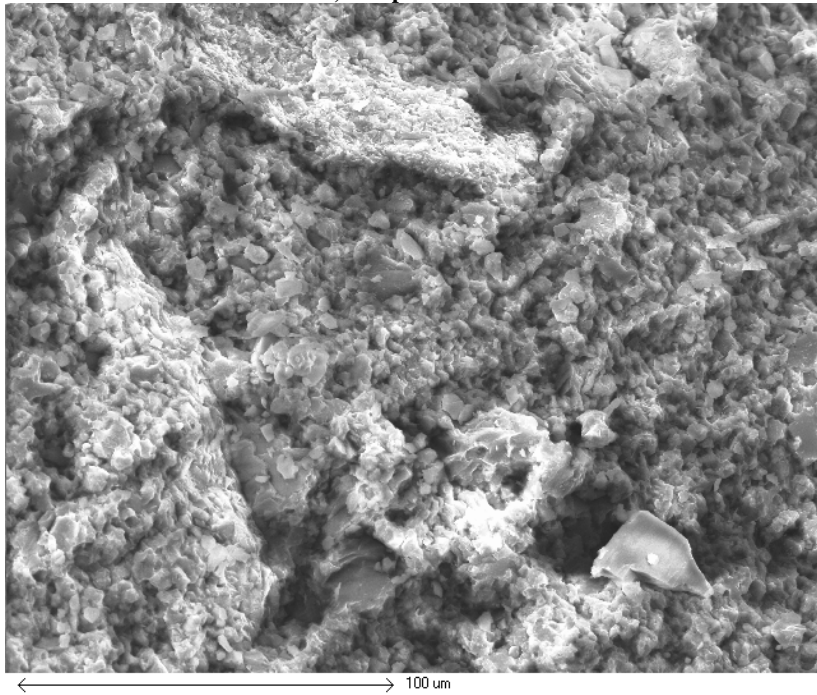


Figure 78. General view of the sample matrix, SEMx526. The corresponding elemental EDS spectrum is shown in Figure 79.

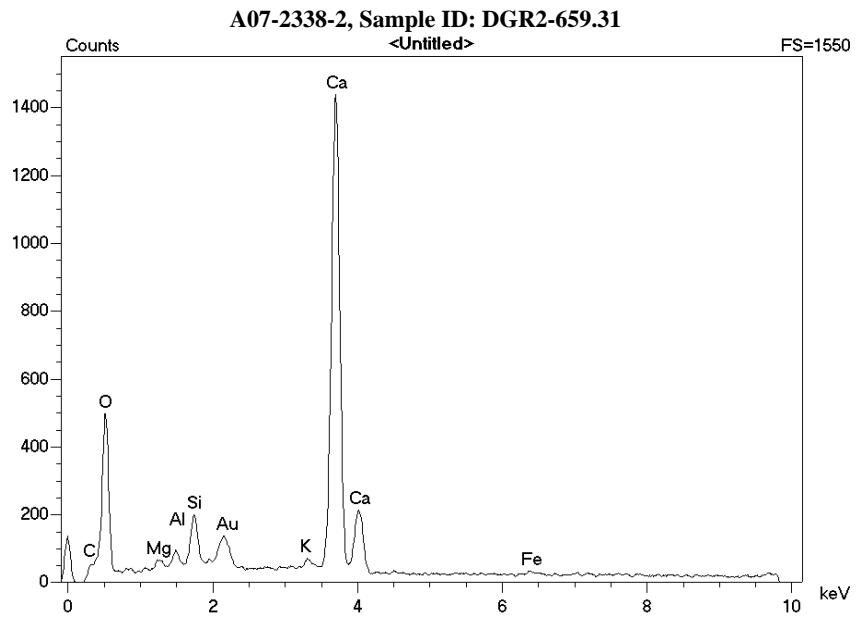


Figure 79. Elemental composition of the region shown in Figure 78. High concentration of Ca is evident. Gold originated from sputtered coating.

A07-2338-2, Sample ID: DGR2-659.31

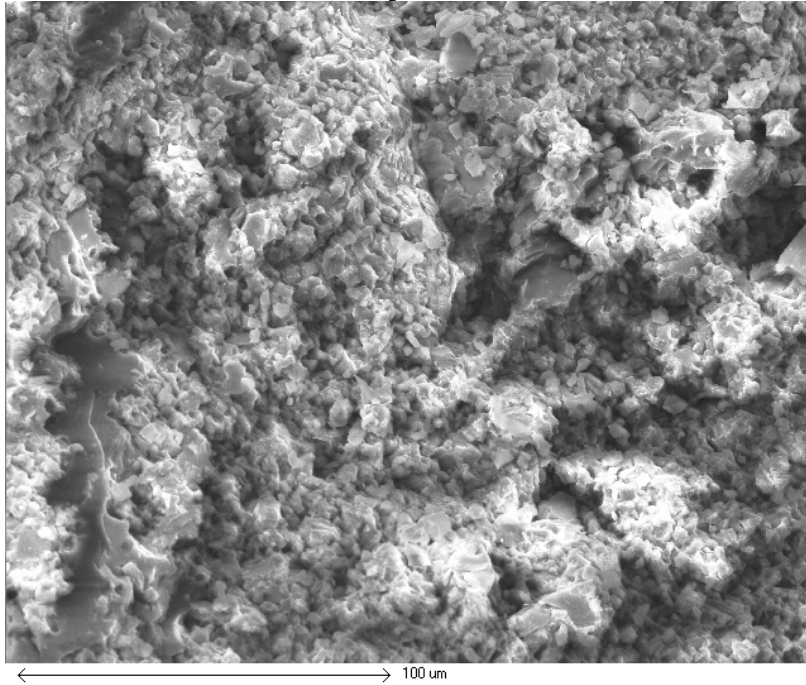


Figure 80. General view of the sample matrix at a different location, SEMx526. The corresponding elemental EDS spectrum is shown in Figure 81.

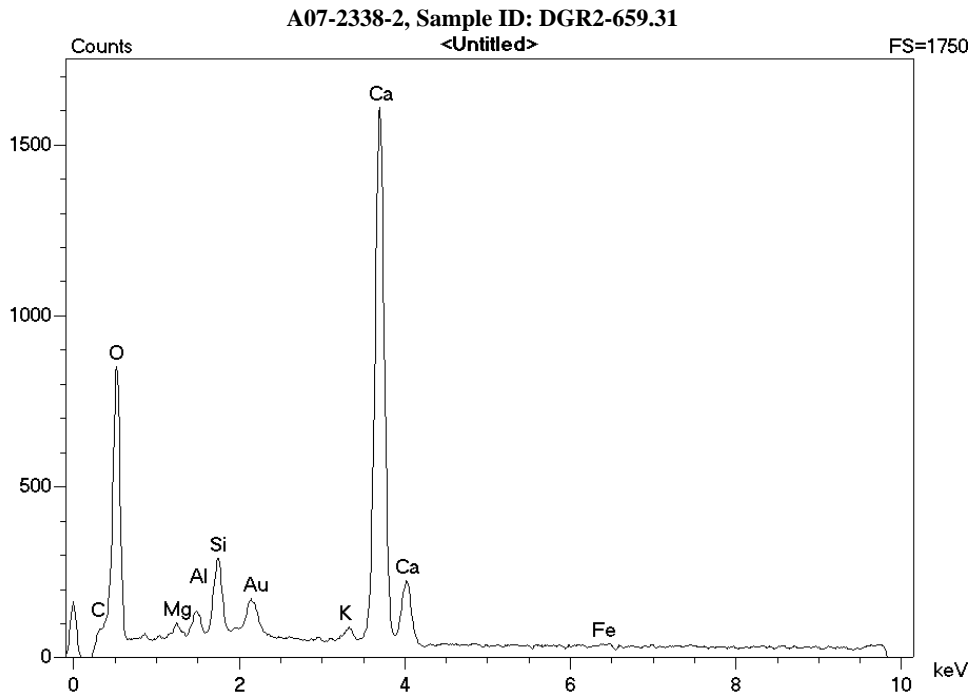


Figure 81. Elemental composition of the region shown in Figure 80. High concentration of Ca is evident. Gold originated from sputtered coating.

A07-2338-2, Sample ID: DGR2-659.31

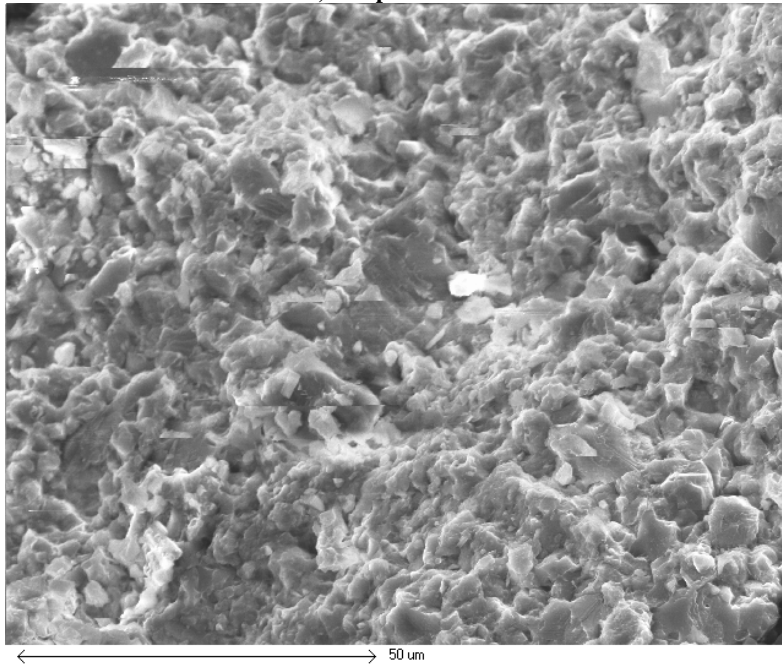


Figure 82. A region from Figure 80 shown in higher magnification, SEMx1050.

A07-2338-1, Sample ID: DGR2-704.87

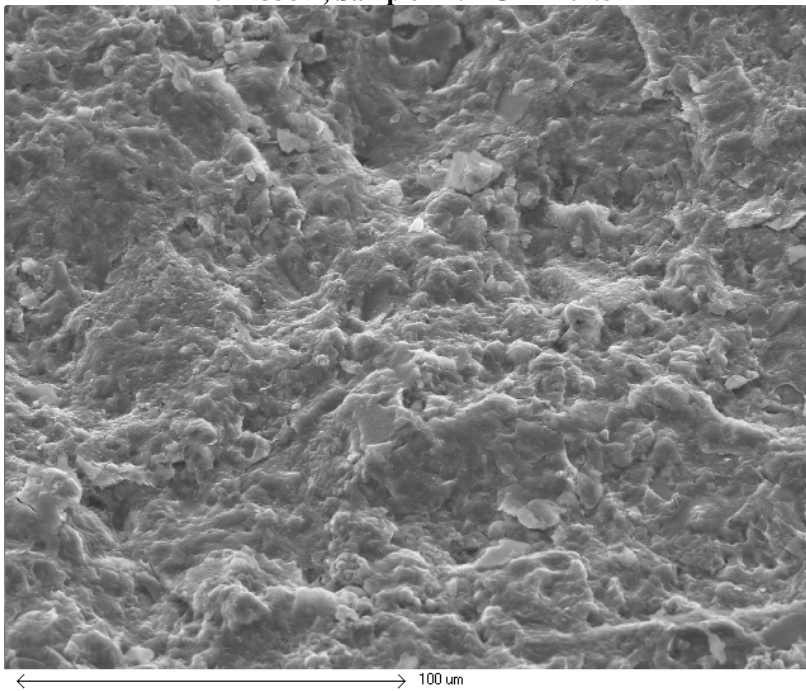


Figure 83. General view of the sample matrix, SEMx549

A07-2338-1, Sample ID: DGR2-704.87

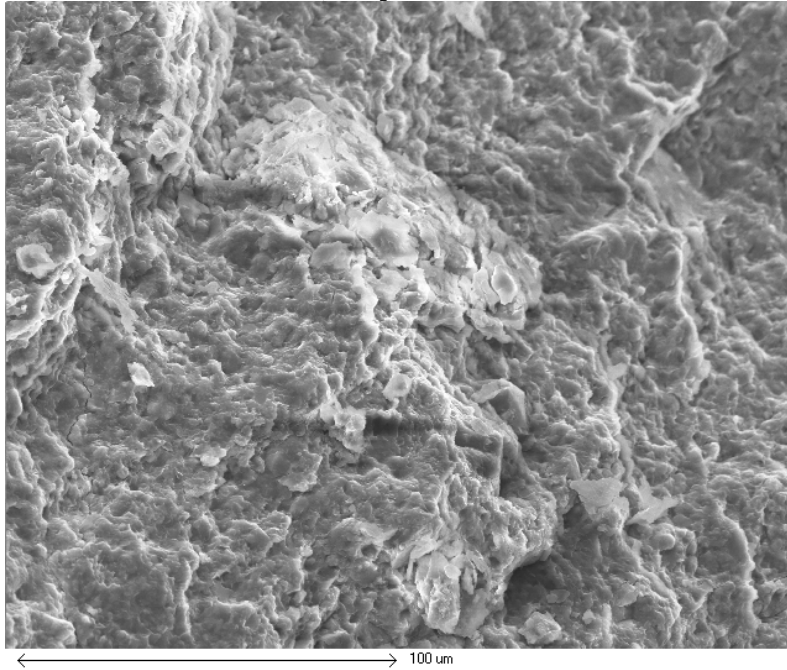


Figure 84. A region with high Na and Cl concentration, SEMx 549. Corresponding elemental composition spectrum is shown in Figure 85.

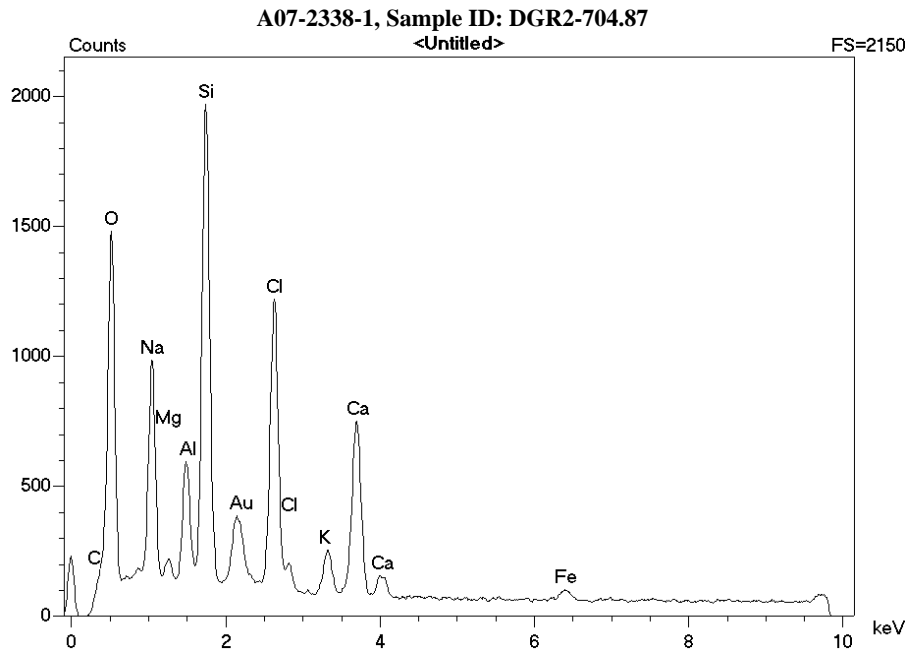


Figure 85. Elemental composition of the region shown in Figure 84. High concentration of Na and Cl is evident. Gold originated from sputtered coating.

A07-2338-1, Sample ID: DGR2-704.87

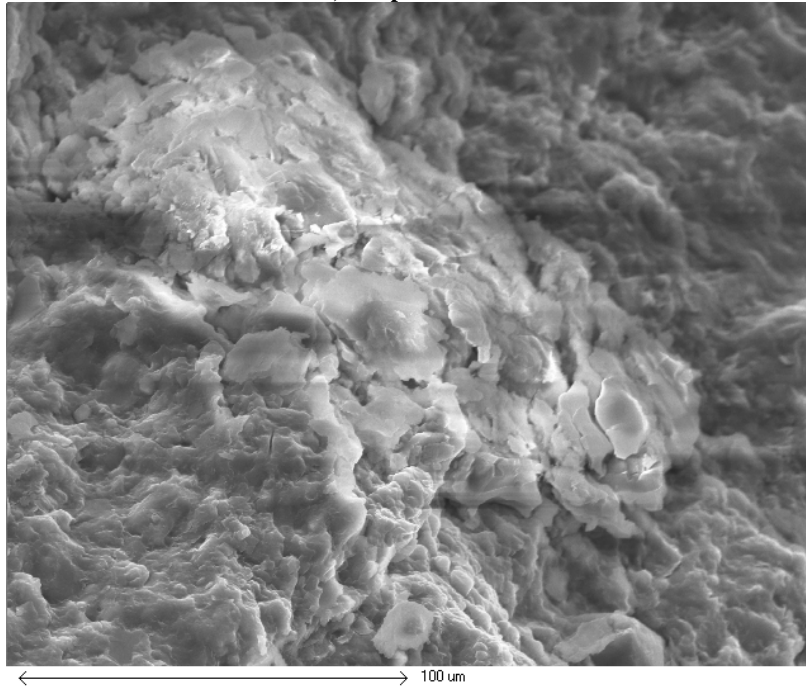


Figure 86. The central region from Figure 84 shown in higher magnification, SEMx1100.

A07-2338-1, Sample ID: DGR2-704.87

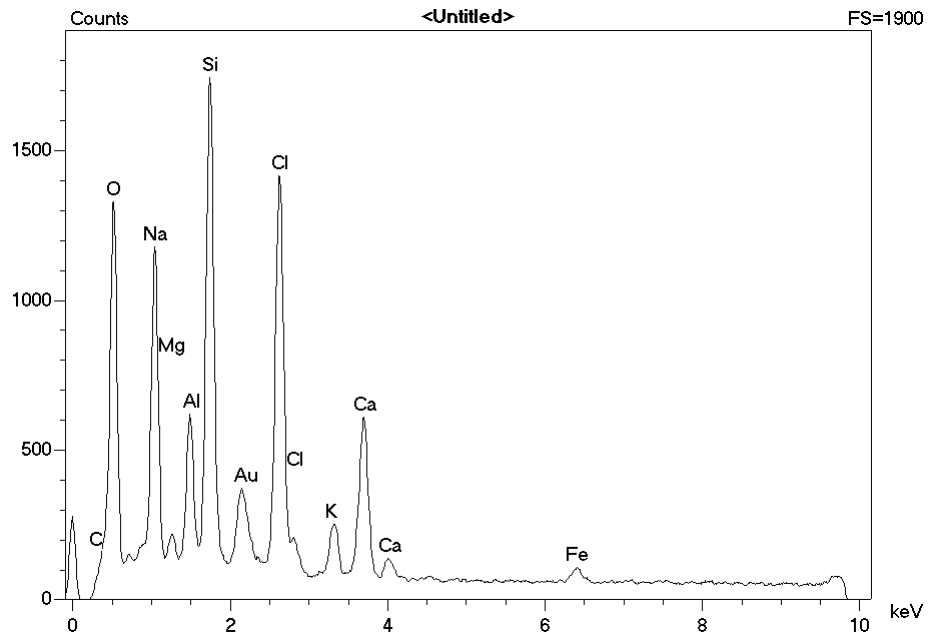


Figure 87. Elemental composition of the region shown in Figure 86. High concentration of Na and Cl is evident. Gold originated from sputtered coating.

A07-2338-1, Sample ID: DGR2-704.87

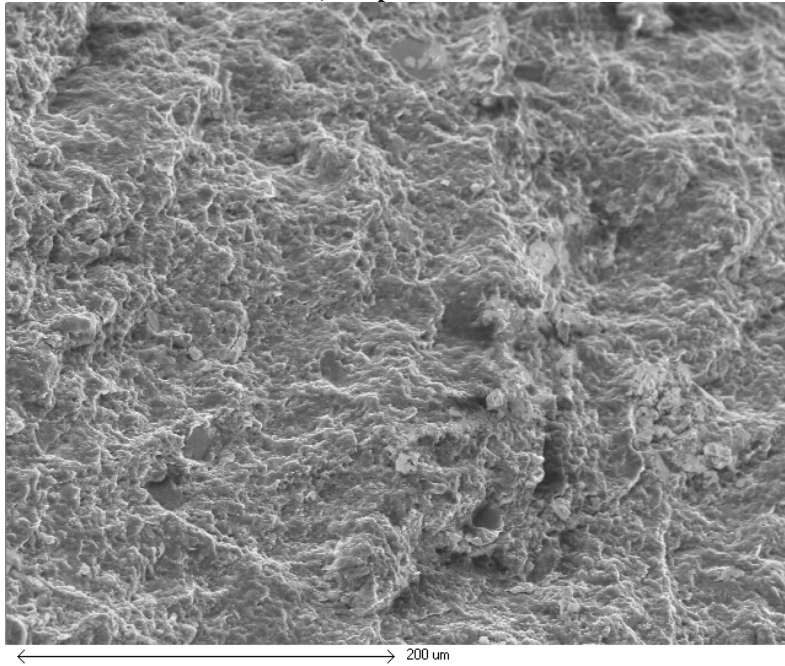


Figure 88. General view of the sample matrix at another location, SEMx274.

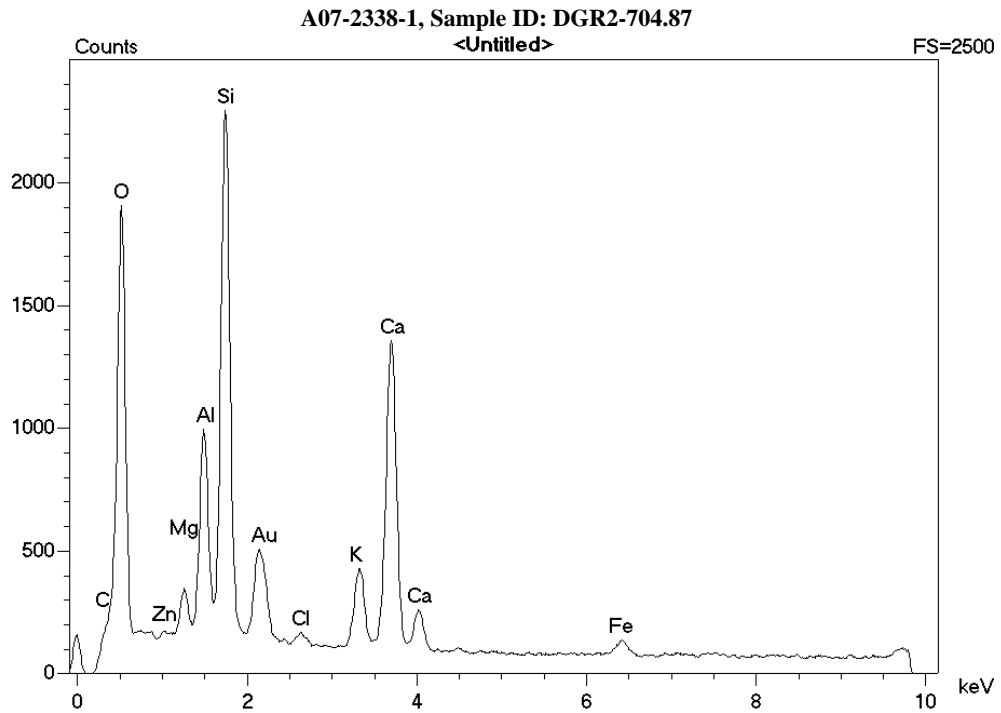


Figure 89. Elemental composition of the region shown in Figure 88. High concentration of Na and Cl is evident. Gold originated from sputtered coating.

A07-2338-1, Sample ID: DGR2-704.87

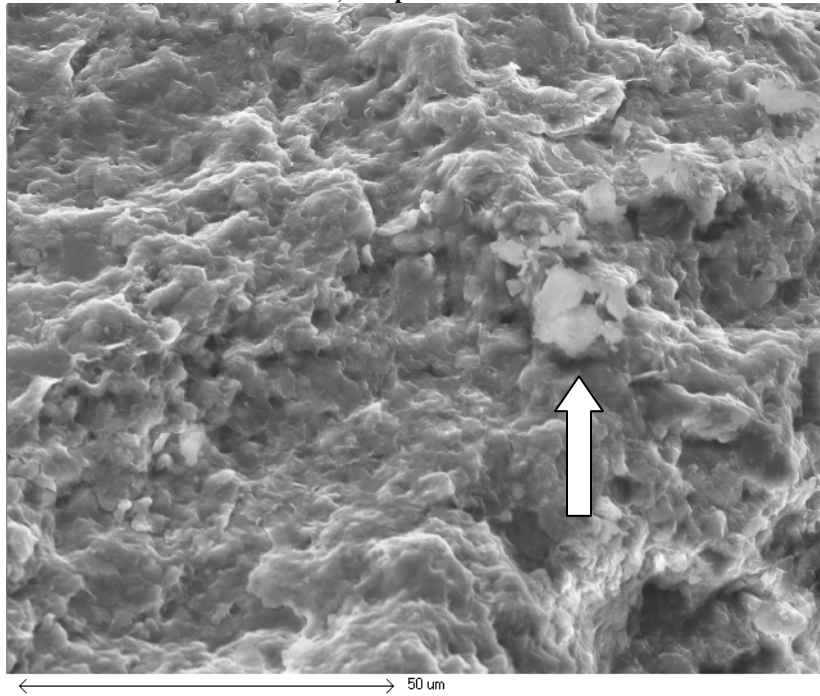


Figure 90. A region from Figure 88 shown in higher magnification, SEMx1050. Figure 91 shows the elemental composition of the region indicated by the arrow.

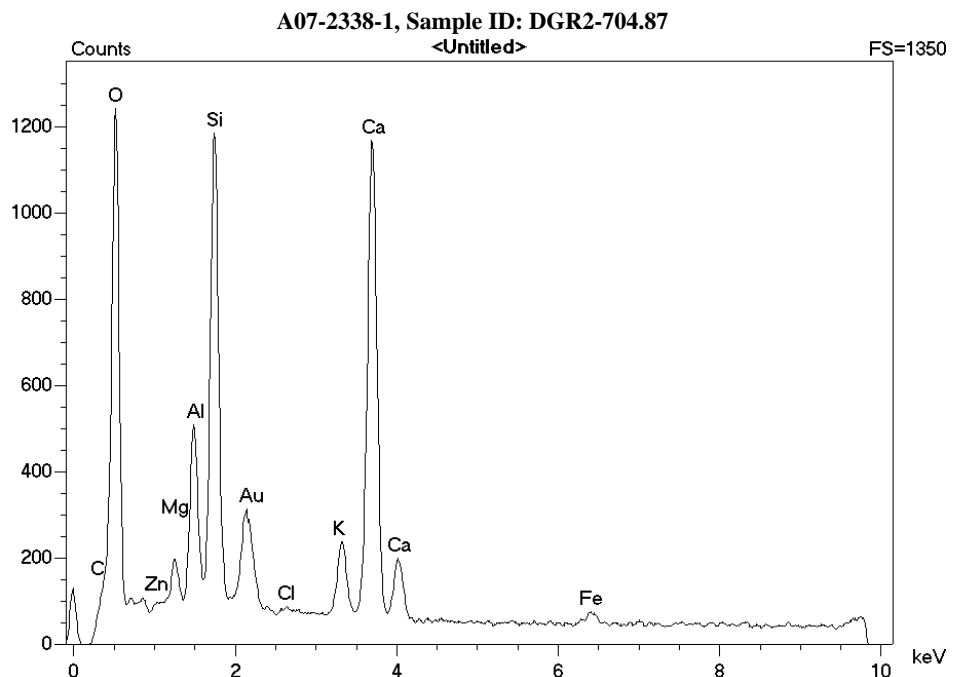


Figure 91. The elemental composition of the region indicated by the arrow in Figure 90.

DISCUSSION

Sodium Chloride appeared as cube-like crystallites with the majority of the EDS spectra showing high Cl content and appreciable Na content. The ratio of Cl to Na peak intensities in the EDS spectra was similar to that observed for the NaCl vein present in DGR1-456.01 sample, see Figure 3 p.7 report A07-1311-2.

Thin layers covering large area of the surface of cleaved samples, shown for example in Figure 20, were rich in Chlorine and had glassy, somewhat crusty appearance. Such layers, which seemed fairly abundant, were probably more brittle than the surrounding matrix as their glassy appearance would suggest. The concentration of Na appeared to be lower in the layers than it was for the cube-like crystallites, but this might be an artifact and needs some other confirmation.

It is possible that we overestimate the abundance and importance of the glassy layers. We might have observed them disproportionately frequently in the SEM study due to the fact that the layers were indeed more brittle than the surrounding matrix and cleaving the samples for the examination was preferentially exposing them.

One can pose the following questions for further consideration and examination:

Cl-rich glassy layers might be examined to confirm their identity. If they are composed of NaCl they should be water soluble – this might be confirmed by special sample preparation followed by SEM examination. It is not clear why these layers have such different appearance than the crystallites. Other than low concentration of Na, which was always present for the spectra taken from the layers, no other suitable metal seemed to accompany the high Cl concentration in the layers.

CONCLUSION

SEM/EDS examination of the selected samples from GDR2 cores revealed several minerals and among others Halite was present together with other, possibly related mineral with high Cl concentration and glassy appearance.

Full mineral identification and quantification by Rietveld refinement is in progress to further characterize the mineral make-up of the samples.

Please do not hesitate to contact us if you have any questions.

Reported by:

Reviewed by

Aniceta Skowron, Ph.D.
Senior Scientist

Activation Laboratories Ltd.

Eric Hoffman, Ph.D.
General Manager

Activation Laboratories Ltd.